

Functional analysis of the ubiquitously conserved protein
GCP1 from *Escherichia coli*

Dissertation

zur Erlangung des akademischen Grades des
Doktors der Naturwissenschaften (Dr. rer. nat.)

an der

Universität Konstanz
Fachbereich Biologie

vorgelegt von

Christian Weiß

Tag der mündlichen Prüfung: 11. Mai 2009

1. Referentin: Prof. Dr. Iwona Adamska
2. Referent: Prof. Dr. Winfried Boos

Summary

GCPs are described as putative glycoproteases that are ubiquitous in all living organisms with a sequenced genome. The amino acid sequence of the GCPs is highly conserved. It contains two histidines that presumably resemble the active center of the protease and an HSP70-actin like fold on the C-terminus.

Different experiments were performed during this study to solve the molecular function of GCP1 from *Escherichia coli*. Data from bioinformatical approaches on the amino acid sequence of the protein indicated, that GCP1 is an integral membrane protein located in the inner membrane of *E. coli*, spanning the membrane with two hydrophobic helices. An antibody against GCP1 was raised and it was demonstrated that GCP1 is regulated in a growth-phase dependent manner, accumulating during the logarithmic growth of *E. coli*. The protein locates soluble in the cytoplasm, as well as associated with the inner membrane. During early logarithmic growth, the majority of GCP1 locates at the membrane, while during other growth phases the majority of the protein is found in the cytoplasm. We used the HSP70-aktin domain for pull down experiments in order to identify potential protein-protein interactions of GCP1. It could be demonstrated that GCP1 directly interacts with the cell division protein FtsZ. A deletion mutant in *gcp1* was engineered and revealed that the deletion of *gcp1* led to cessation of growth. Thereupon a conditionally lethal *gcp1*-mutant was constructed and used to gather further information about the physiological function of the GCP1 protein. GCP1 is a low abundant but stable protein. Even after deleting *gcp1*, this concentration was sufficient to enable the cells to divide several times before they ceased growth. By combining an FtsZ-Gfp fusion with the conditionally lethal *gcp1*-mutant we could demonstrate that the depletion of GCP1 prevented the formation of the cell division apparatus, the so-called divisome of *E. coli*. A vital stain of GCP-depleted cells revealed that cells remained viable after the depletion, but cell division and growth were arrested. By comparing the proteome of depleted cells with control-cells, we demonstrated that despite the depletion of GCP1, protein biosynthesis and transcription still occurred. The results of this study suggest that GCP1 is involved in regulating cell division of *E. coli*.

Zusammenfassung

GCPs sind als vermeintliche Glykoproteasen, die in allen Lebewesen mit bekannter Genomsequenz vorkommen beschrieben. Dabei ist die Aminosäuresequenz der Proteine hoch konserviert. Sie beinhalten zwei Histidine, die das vermutliche aktive Zentrum der Protease darstellen, und eine C-terminale HSP70-aktin Domäne.

Während dieser Arbeit wurden verschiedene Experimente zur Aufklärung der molekularen Funktion von GCP1 in *Escherichia coli* durchgeführt. Daten aus einer Computeranalyse der Aminosäuresequenz zur Membrantopologie deuteten darauf hin, dass GCP1 über zwei transmembranäre Helices in die Cytoplasmamembran integriert ist. Unter Verwendung eines in dieser Arbeit erzeugten Antikörpers gegen GCP1 konnte gezeigt werden das GCP1 wachstumsphasenabhängig reguliert wird und während des logarithmischen Wachstums in der Zelle akkumuliert. Das Protein liegt dabei sowohl löslich im Cytoplasma, als auch mit der inneren Membran assoziiert vor. Im Gegensatz zu anderen Wachstumsphasen befindet sich der weitaus größte Teil des Proteins während der frühen logarithmischen Phase an der Membran. Die HSP70-aktin Domäne des Proteins wurde auf die Interaktion mit möglichen anderen Proteinen hin untersucht. Es konnte dabei gezeigt werden, dass GCP1 direkt mit dem Zellteilungsprotein FtsZ interagiert. Es wurde gezeigt, dass eine *gcp1* Deletion in *E. coli* zur Einstellung der Zellteilung und des Wachstums führt. Aus einer daraufhin konstruierten konditional letalen *gcp1*-Mutante wurden Hinweise auf die physiologische Funktion des GCP1 Proteins gewonnen. GCP1 liegt in der Zelle nur in geringer Konzentration vor. Selbst bei Deletion des *gcp1*-Gens ist diese Konzentration noch ausreichend, um einige weitere Teilungen der bakteriellen Zelle zu ermöglichen. Unter Verwendung einer FtsZ-Gfp Fusion, in Kombination mit der konditional letalen *gcp1*-Mutante, konnte gezeigt werden, dass die Depletion von GCP1 dazu führt, dass sich der Zellteilungsapparat nicht ausbilden kann. Ein spezifischer Nachweis von lebenden und toten Zellen zeigte, dass die Depletion von GCP1 die Zellen nicht tötet, sondern nur das Wachstum, bzw. die Zellteilung blockiert. Der Vergleich des Proteoms von GCP1-depletierten Zellen mit Kontroll-Zellen zeigte, dass trotz der Depletion von GCP1 weiterhin Proteinbiosynthese und Transkription abliefen. Die in dieser Arbeit erhaltenen Ergebnisse deuten darauf hin, dass GCP1 bei der Zellteilung von *E. coli* eine wichtige Rolle zukommt.

1	Introduction	5
1.1	GCPs are among the most conserved proteins and are ubiquitous in all living cells	5
1.2	Two homologues of GCPs exist in the three domains of life	7
1.3	A proposed function for GCP1 from the literature	8
1.4	Sequence analysis and a proposed secondary structure of GCP1 from <i>E. coli</i> suggest a membrane protein	8
1.5	GCP1 localizes in the mitochondria of the meristems of plants	11
1.6	Structural comparison of GCP1 from <i>E. coli</i> and <i>A. thaliana</i> with YeaZ from <i>Salmonella typhimurium</i> and GCP2 from different species	11
1.7	Cell division in <i>E. coli</i>	13
1.8	Aims of this work	14
2	Materials and Methods	15
2.1	Abbreviations	15
2.2	Bacterial strains	16
2.3	Primers	17
2.4	Plasmids	18
2.5	Media	19
2.5.1	Solid media	19
2.5.2	Additives	20
2.6	Microbiological methods	20
2.6.1	Storage of strains	20
2.6.2	Parameters of cultivation of <i>E. coli</i>	20
2.6.3	Counting cells in liquid media	21
2.6.4	Using the bacteriophage P1	21
2.7	Biomolecular methods	22
2.7.1	Preparation of plasmid DNA	22
2.7.2	Restriction digest of DNA	22
2.7.3	PCR	23
2.7.4	Ligation of DNA Fragments	24

2.7.5	Size dependent separation of DNA	24
2.7.6	Extraction of DNA from agarose gels	25
2.7.7	Cloning	25
2.7.8	TSS transformation	28
2.7.9	Chemical transformation (ultracompetent DH5 α cells)	29
2.7.10	Deletion of chromosomal genes by homologous recombination	29
2.7.11	Construction of strains	30
2.8	Biochemical methods	32
2.8.1	SDS PAGE	32
2.8.2	2D-PAGE (NEPHGE method)	33
2.8.3	Proteinidentification	34
2.9	Antibodies	35
2.9.1	Immunoblotting (Western blotting)	35
2.10	Overexpression of GCP1 and Protein purification	36
2.10.1	Test-expression of GCP1	36
2.10.2	Purification approaches	37
2.10.3	Refolding GCP1 from inclusion bodies	38
2.11	Comparison of growth of CWCM4 with and without arabinose	39
2.12	Localization of overexpressed GCP1	39
2.13	Expression studies in <i>E. coli</i> WT cells	40
2.13.1	Determination of the subcellular localization of GCP1 in WT <i>E. coli</i>	41
2.14	Microscopy	42
2.15	Effects of long time GCP1-depletion	43
2.16	Testing cell viability	42
2.17	Complementation studies	43
2.18	Pulldown experiments	43
2.19	YeaZ overexpression	44
2.20	YeaZ purification	44
2.21	Bioinformatics	45

3 Results	46
3.1 Overexpression and purification of GCP1 from <i>E. coli</i>	46
3.1.1 GCP1 is overexpressed in substantial amounts	46
3.1.2 Small amounts of overexpressed GCP1 co-sediment with the membrane fraction of an <i>E. coli</i> cell lysate	47
3.1.3 Purification of GCP1 from inclusion bodies	47
3.1.4 Refolded GCP1 from inclusion bodies remains soluble in distinct buffers	48
3.2 Characterization of the $\Delta gcp1$ mutant	49
3.2.1 GCP1 is essential for growth of <i>E. coli</i> on LB medium	49
3.2.2 A conditionally lethal mutant in <i>gcp1</i> was constructed using an arabinose-inducible plasmid system	50
3.3 Characterization of the conditionally lethal <i>gcp1</i> mutant	52
3.3.1 The conditionally lethal mutant reverts with high frequency	52
3.3.2 The reversion frequency of the conditionally lethal mutant can be reduced	53
3.3.3 Lack of the inducer arabinose leads to a growth deficit of the conditionally lethal <i>gcp1</i> mutant	54
3.3.4 2D-PAGE gel analysis of protein patterns from WT <i>E. coli</i> and the conditionally lethal <i>gcp1</i> mutant strain CWCM4	58
3.3.5 2D-PAGE gels of the conditionally lethal <i>gcp1</i> mutant CWCM4 show consistent and significant differences in protein patterns in comparison to the WT strain	59
3.3.6 Proteins affected by GCP1-depletion are related to protein biosynthesis and cell division	63
3.4 Characterization of <i>gcp1</i> expression in WT cells	65
3.4.1 GCP1 accumulates during the early logarithmic phase of <i>E. coli</i> growth	65
3.4.2 GCP1 is distributed between soluble and membrane fractions	66
3.4.3 GCP1 is recruited to the membrane during logarithmic growth	66
3.4.4 GCP1 is not detectable in the periplasm, nor is it secreted to the medium	66
3.5 Biochemical characterization of GCP1	68
3.5.1 GCP1 contains a C-terminal protease recognition sequence sharing similarity with the <i>ssrA</i> -tag	68
3.5.2 The evolutionary invariant histidines are essential for the function of GCP1	69
3.5.3 The HSP70-actin-fold of GCP1 is not essential for cell viability	69
3.5.4 The N-terminus of GCP1 is essential for cell viability	70
3.6 The HSP70-actin-fold domain interacts with FtsZ protein	73
3.6.1 Depletion of GCP1 is lethal due to impaired cell division	75
3.6.2 Depletion of GCP1 abolishes FtsZ ring formation	77
3.7 Characterization of YeaZ	79
3.7.1 YeaZ is easily overexpressed and purified	79
3.7.2 A polyclonal antibody against YeaZ was raised	80
3.7.3 YeaZ is a soluble protein	81

4 Discussion	82
4.1 Structural and functional conservation of GCPs across kingdoms	82
4.2 GCP1 localization in <i>E.coli</i>	82
4.3 Is GCP1 an active protease?	83
4.4 YeaZ in bacteria	83
4.5 Low amounts of GCP1 are sufficient to facilitate cellular growth	84
4.6 The reversion frequency of the conditionally lethal mutant suggest a “loss-of-function” mutation in a second gene	85
4.7 Cells remain viable after the depletion of <i>gcp1</i>	86
4.8 Correct divisome assembly is dependent on GCP1	87
4.9 2D-gel analysis of GCP1-depleted cells sustains the involvement of GCP1 in cell division	88
4.10 GCP1 could control the correct time point for initiation of cell division	90
5 Literature	92
6 Acknowledgements	99

1 Introduction

1.1 GCPs are among the most conserved proteins and are ubiquitous in all living cells

GCPs (Glycoproteases), also referred to as O-sialoglycoprotein endopeptidases, are ubiquitarily present in each living organism whose genome has been sequenced up to now. The amino acid sequences of GCPs are highly conserved throughout the genomes of species from all kingdoms of life (Figure 2, Page 6). It includes two invariant histidines in all cases (Figure 1, Page 5). These histidines are reported to coordinate a Zn^{2+} -ion in order to form a catalytic domain (Weart, Lee et al. 2007), thereby assigning the GCPs to the group of Zn^{2+} -metalloproteases of the M22 peptidase family (<http://merops.sanger.ac.uk>). These proteases also contain an HSP70-actin fold on the C-terminus of the polypeptide (Aravind and Koonin 1999). The HSP70-actin fold is a distinct domain in different proteins that is often involved in protein-protein interactions (Aravind and Koonin 1999). Among other proteins, the HSP70-actin fold is found in the chaperones of the heat shock response and in actin. The actin fold is a protein structural motif that binds ATP in the presence of Ca^{+2} or Mg^{+2} -ions and catalyses the transfer of a phosphate group from ATP to a hydroxyl group of proteins. This motif can be found in various sugar kinases, as well as prokaryotic phosphatases and cell cycle proteins, FtsA, MreB and StbA (Kabsch and Holmes 1995). It was further proposed that during the evolution GCP1 might have adapted the HSP70-actin fold to the protease function by grafting the metal-binding motif HXEXH onto its structural framework that created a protease active site (Aravind and Koonin 1999). Therefore, GCPs might represent an ATP-dependent Zn^{2+} -metallopeptidase with chaperone activity.

Figure 1: The invariant histidines within the amino acid sequence of GCPs from different organisms

<i>Arabidopsis thaliana</i>	VGVH H MEAHALV
<i>Escherichia coli</i>	IPVH H MEGHLLA
<i>Pasteurella haemolytica</i>	LGVH H MEGHLLA
<i>Synechocystis sp.</i>	LGVH H LEGHIYA
<i>Saccharomyces cerevisiae</i>	VGVN H CIGHIEM
<i>Drosophila melanogaster</i>	LPVH H MEAHALQ
<i>Mus musculus</i>	IPIH H MEAHALT
<i>Homo sapiens</i>	IPIH H MEAHALT

Figure 1 shows a sequence alignment of the invariant histidines within the GCP sequences from diverse species (as labeled).

Figure 2: A sequence alignment of GCP1 from *E. coli* with GCP1 and GCP2 from *Homo sapiens*

ref NP_071748.2	O-sialoglycoprotein endopeptidase-like 1	186
ref NP_060277.1	O-sialoglycoprotein endopeptidase	159
>ref NP_071748.2	 O-sialoglycoprotein endopeptidase-like 1	
Length=414		
Identities = 124/356 (34%), Positives = 177/356 (49%), Gaps = 29/356 (8%)		
Query 3	VLGIETSCDETGIAIYDDEKGLLANQLYSQVKLHADYGGVVPPELASRDHVRKTVPLIQAA	62
Sbjct 39	VLGIETSCDDTAAAVVDETGNVLEAIHSQTEVHLKTGGIVPPAAQQLHRENIQIRIVQEA	98
Query 63	LKESGLTAKDIDAVAYtagpglvlgallvgatvgrSLAFAWDVPaipVHHMEGHLAPMLE	122
Sbjct 99	LSASGVSPDLSAIATTIKPLGALSGLVLSFSLQLVGLKPPFIPHHMEAHALTIRL-	157
Query 123	DNPPEFPFVALLVSGGHTQLISVTGIGQYELLGESIDDAAGEAFDKTAKllgl-dyp---	178
Sbjct 158	TKNKEFPFLVLLISGGHCLLALVQGVSDFLLLGKSLDIAPGDMLDKVARRLSLIKHPCCS	217
Query 179	---ggp11SKMAAQGTAGRfVFPpMTDRPGLDFSFSGLKTFaANTIRdNGTDD-----	229
Sbjct 218	TMSGGAIEHLAKQGNRFHFDIKPPLHAKNCDFsFTGLQHVTDKIIMKKEKEEGIEKGQ	277
Query 230	--QTRADIARAFEDAVVDTLMIKCKRA-----LDQTGFKRLVMAGGVSANRTLRAK	278
Sbjct 278	ILSSAADIAATVQHTMACHLVKRTHRAILFCKQRDLLPQNN-AVLVASGGVASNFYIRRA	336
Query 279	LAEMMKRRGEVfYARPEFCTDNGAMIAyAGMVRfKA--GATADL-GVSVrPRWPL	331
Sbjct 337	LEILTNAQCTLLCPPRLCTDNGIMIAWNGIERLRAGLGILHDIEGIRYEPKCP	392
>ref NP_060277.1	 O-sialoglycoprotein endopeptidase	
Length=335		
Identities = 117/332 (35%), Positives = 178/332 (53%), Gaps = 16/332 (4%)		
Query 3	VLGIETSCDETGIAIYDDEKGLLANQLYSQVKLHADYGGVVPPELASRDHVRKTVPLIQAA	62
Sbjct 4	VLG E S ++ G+ + D K +LAN + V G +P +R H + L+Q A	60
Query 63	LKESGLTAKDIDAVAYtagpglvlgallvgatvgrSLAFAWDVPaipVHHMEGHLAPMLE	122
Sbjct 61	LTESGLTSQDIDCIAYTKGPGMGAPLVSVAVVARTVAQLWNKPLVGVNHCIGHIEMGRLI	120
Query 123	DNPPEFPFVALLVSGGHTQLISVTGIGQYELLGESIDDAAGEAFDKTAKllgl--dypgg	180
Sbjct 121	TGATS-PTV-LYVSGGNTQVIAYSE-HRYRIFGETIDIAVGNCLDRFARVLKISNDPSPG	177
Query 181	p11SKMAAQGTAGRfVFPpMTDRPGLDFSFSGLKTFaANTI-rdNGTDDQTRADIARAF	239
Sbjct 178	YNIEQMAKR---GKKLVELPYTVK-GMDVVSFGILSFIEDVAHRMLATGECTPEDLFCFSL	233
Query 240	EDAVVDTLMIKCKRALDQTGFKRLVMAGGVSANRTLRAKLAEMMKRRGEVfYARPEFCT	299
Sbjct 234	QETVFAMLVEITERAMAHCGSQEALIVGGVGCNVLQEMMATMCQERGARLFATDERFCI	293
Query 300	DNGAMIAyAGMVRfKAGAT---ADLGVSVrPR	328
Sbjct 294	DNGAMIAQAGWEMFRAGHRTPLSDSGVTQRYR	325

Figure 2 shows a sequence alignment of GCP1 from *E. coli* with GCP1 from *H. sapiens* (upper alignment) and with GCP2 from *H. sapiens* (lower alignment). In both alignments the upper row resembles the GCP1 sequence from *E. coli* while the lower row resembles the GCP1 or GCP2 sequence from *H. sapiens* respectively. The alignment was carried out using the webpage of the "National Centre for Biotechnological Information" <http://www.ncbi.nlm.nih.gov/>

1.2 Two homologues of GCPs exist in the three domains of life

Bacteria contain a different version of GCP than archaic. The bacterial version is GCP-type1 (GCP1), while the archaic version is called GCP-type2 (GCP2). In contrast to these prokaryotic organisms that possess only one of the homologues, all eukaryotic organisms contain both versions of the protein, GCP1 and GCP2. In average, the molecular mass of the bacterial GCP1 is about 35-36 kDa and the polypeptide contains approximately 320-340 amino acids. In eukaryotes, where the *gcp1* gene-product localizes inside the inner mitochondrial membrane (Chapter 1.5, Page 11,) and is carrying a transit peptide, the protein sequence of GCP1 consists of about 480 amino acids (GCP1 from *Arabidopsis thaliana*) of which 86 amino acids fall upon the transit peptide. The approximate molecular mass of GCP1_(processed) (lacking the leader peptide) in *A. thaliana* is 44 kDa. GCP2 from *A. thaliana*, which localizes within the cell membrane consists of 353 amino acids with a molecular mass (Butland, Peregrin-Alvarez et al. 2005) of about 39 kDa (*Homo sapiens*: GCP1_(processed) = 414 aa, 45 kDa; GCP2 = 335 aa, 36 kDa). In archaea, the length of the GCP2 varies greatly from species to species (from aa 314 in *Nanoarchaeum equitans* to aa 535 in *Methanocaldococcus jannaschii*). One additional ortholog of the GCPs is present in bacteria – YeaZ. This polypeptide is also assigned to the M22 peptidase family since it shares the structural characteristics of the GCPs described above; however, it lacks the invariant histidines. Thus, the protein is most likely not an active protease. While in gram-negative bacteria, each protein (GCP1 and YeaZ) is encoded by a single gene on an independent locus of the chromosome, in gram-positive bacteria the *gcp1* and *yeaZ* gene are organized as operon (Zalacain, Biswas et al. 2003). All members of the M22 peptidase family are essential for cell viability (GCP1, GCP2 and YeaZ), but only the molecular function of GCP2 (Kae1) from the archaeon *Pyrococcus abyssi* and the yeast *Saccharomyces cerevisiae* was identified up to date. The protein interacts with a kinase (Bud32) to form a complex that binds DNA and is involved in maintaining genome integrity, chromosome replication and transcription (Hecker, Graille et al. 2009) (Hecker, Lopreiato et al. 2008) (Hecker, Leulliot et al. 2007).

1.3 A proposed function for GCP1 from the literature

The first GCP1 to be characterized was prepared from *Mannheimia (Pasteurella) haemolytica* – a pathogen that resides in the respiratory tract of cattle and causes the “cattle shipping fever”. The protein is reported being secreted into the medium and when the purified protein was further investigated *in vitro* a proteolytical activity was observed. Namely peptides modified with a specific glycosylation (O-sialoglycosylation) were hydrolyzed (Sutherland, Abdullah et al. 1992) (Mellors and Lo 1995). When the sialyl residue was removed from the substrate, no more hydrolysis of the peptide was observed (Mellors and Sutherland 1994). Due to the observed narrow substrate specificity the GCPs obtained their name (O-sialoglycoprotease). However, a more recent publication suggested that during the preparation of the GCP1 from *M. haemolytica*, at least one additional protease was co-purified together with GCP1 and this protease might be responsible for the specific cleavage of the O-sialoglycosylated substrate (Jiang 2004), thus leaving the answer to the physiological function of GCP1 unsolved again.

1.4 Sequence analysis and a proposed secondary structure of GCP1 from *E. coli* suggest a membrane protein

GCP1 from *E. coli* is a protein consisting of 337 amino acids with a molecular mass of 35,85 kDa. The encoding gene *gcp1* is located at minute 69,13 on the chromosome of *E. coli* (bp 3207171 to bp 3208184) in between two operons with an opposed direction to the *gcp1*-transcription: A tartrate metabolism related operon (*ttdA-ttdB-ygjE*) upstream of *gcp1* and a σ^E -controlled macromolecular synthesis operon (*rpsU-dnaG-rpoD*) downstream of *gcp1* (Figure 3, Page 9).

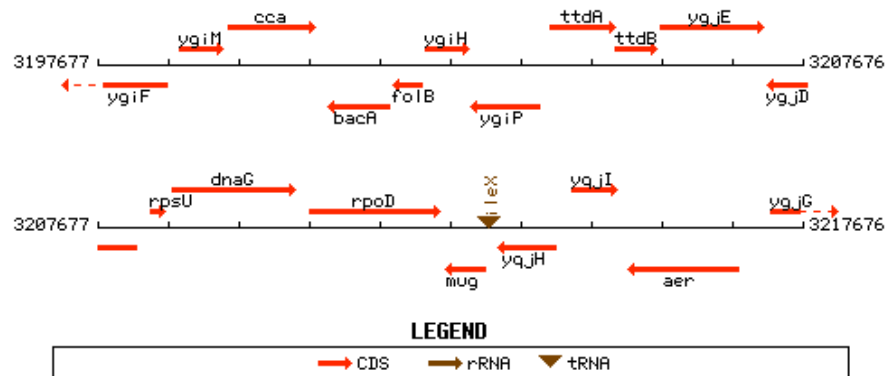
Figure 3: The *gcp1*-locus on the chromosome of *E. coli*

Figure 3 illustrates the localization of the *gcp1* ORF within the *E. coli* chromosome (bp 3197677 to bp 3217676). ORFs are marked by red arrows indicating direction of transcription and labeled with the encoded gene

A bioinformatic approach predicted two hydrophobic α -helices in the protein sequence of GCP1. The „DAS” transmembrane prediction server (**d**ense **a**lignment **s**urface **m**ethod <http://www.sbc.su.se/~miklos/DAS/maindas.html>) that was employed for this approach uses the amino acid sequence of a protein to predict hydrophobic stretches within the polypeptide that resemble α -helices. The DAS-server predicts the first α -helix between amino acids A₈₀ and F₁₀₂ and the second between amino acids P₁₂₉ and G₁₄₇. According to the prediction (see Figure 4, Page 10) GCP1 in *E. coli* is a membrane protein. This is supported by later findings in this study that suggest GCP1 being at least associated with the membrane (Chapter 2.13.1 Page 41).

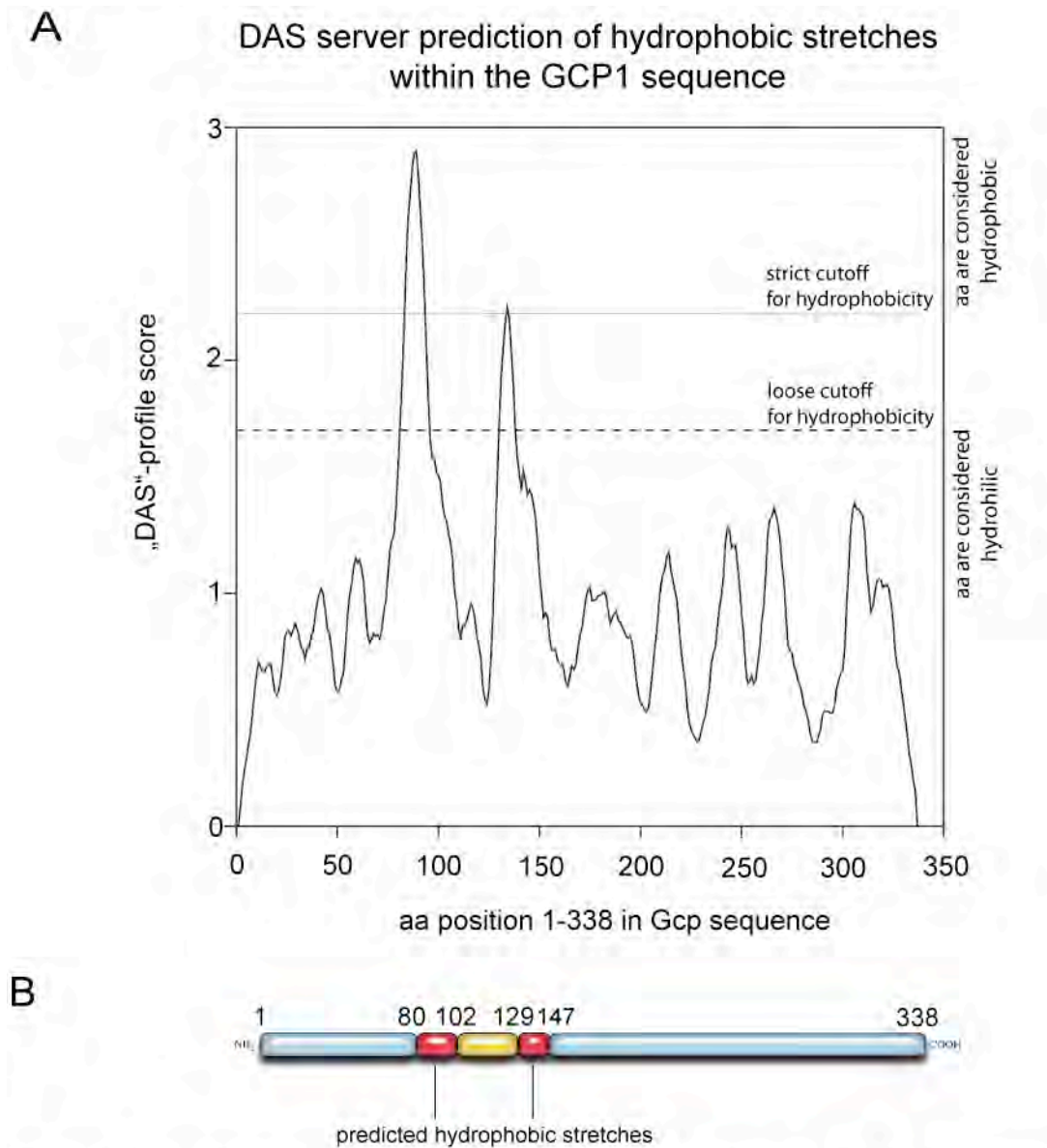
Figure 4: Hydrophobic α -helices predicted within the GCP1 sequence from *E. coli*

Figure 4: (A) Secondary structure prediction of GCP1 from *E. coli* by the „DAS transmembrane prediction“ server (<http://www.sbc.su.se/~miklos/DAS/maindas.html>). The hydrophobicity of adjacent aminoacids in the polypeptide chain is used for calculating the „DAS“-profile score. In the graph shown, the score is plotted against the aminoacid positions in the polypeptide sequence of GCP1. (B) The resulting model of GCP1 schematically represents hydrophilic stretches in blue (termini) or yellow (in between predicted helices). Predicted hydrophobic α -helices are marked in red. Numbers above the drafted model indicate the aminoacid position of each region in the GCP1 sequence.

1.5 GCP1 localizes in the mitochondria of the meristems of plants

It was demonstrated for *A. thaliana* that both genes, *gcp1* and *gcp2*, are expressed and not only pseudo genes. The gene product of *gcp1* inserts into the inner mitochondrial membrane and is detectable by immunoblot analysis only in the mitochondria of young developing organs. Young roots, stems, flowers, leaves and seeds showed significant amounts of GCP1. A strong accumulation of the protein was observed when leaves were injured or entered senescence. In contrast, GCP1 is almost not detectable in fully differentiated tissues. The highest expression level of GCP1 was demonstrated in shoot meristematic tissues, where undifferentiated cells divide. Interestingly only the lateral meristems contained GCP1 in contrast to the apical meristem. The reasons for this localization are unknown. Crossing heterozygous mutants of *A. thaliana* in which one allele of *gcp1* was deleted resulted in arrested seed development in ¼ of analyzed seeds in developing silicas (Huesgen 2007). The rate of ¼ of the seeds is consistent with the classical Mendel genetics that would predict ¼ of the seeds to be homozygous deleted in *gcp1*. No activity assay for GCP1 from plants is established yet. Therefore a possible function of *gcp1* in plants remains unclear.

1.6 Structural comparison of GCP1 from *E. coli* and *A. thaliana* with YeaZ from *Salmonella typhimurium* and GCP2 from different species

Recently the tertiary structure of YeaZ from *S. typhimurium* became accessible on <http://merops.sanger.ac.uk>. Comparing the GCP1 structure from *E. coli* with two predicted transmembrane α -helices and the integral membrane localization of the *A. thaliana* GCP1 with the solved structure of YeaZ from *Salmonella typhimurium*, confirmed the significance of the DAS prediction of α -helices within polypeptides (Chapter 1.4, Page 8). When the protein sequence of YeaZ from *S. typhimurium* was investigated for potential membrane spanning α -helices, no helix was predicted with a “strict cutoff”, but several with a “loose cutoff” (data not shown). This prediction is consistent with the soluble localization of YeaZ in the cytoplasm and with the several short helices present within the tertiary structure of the soluble protein. The structure of GCP2 in complex with Bud32 (Chapter 1.2, Page 7) was recently published (Mao, Neculai et al. 2008). For GCP2, also no transmembrane helices, but several short helices were predicted. This prediction is also consistent with the solved structure (data not shown).

Figure 5: Tertiary structure of YeaZ from *S. typhimurium*

Figure 5 shows the tertiary structure of YeaZ from *S. typhimurium* as displayed on <http://merops.sanger.ac.uk>. α -helices are drawn in red, β -sheets in green and loops between in turquoise. Residues replacing the predicted metal ligands are shown as ball-and-stick representation in purple: Leu94 and Ala98.

As mentioned before, sequence alignments between most different organisms revealed that GCPs are ubiquitary among all domains of life and that their amino acid sequence is extremely conserved. Even though the members of the M22 peptidase family (GCP1, GCP2 and YeaZ) share high sequence homologies, they obviously differ significantly in structure. Nevertheless, GCPs must be involved in conserved and elementary biological processes present in all living organisms. This study provides evidence that GCP1 from *E. coli* is involved in regulating cell division.

1.7 Cell division in *E. coli*

A septal apparatus that becomes organized at the division site of the bacterial cell accomplishes cell division in bacteria. The process of division in *E. coli* requires a concerted invagination of the multilayered cell envelope that consists of the cytoplasmic membrane, the peptidoglycane layer and the outer membrane. Division is thought to be initiated by the polymerization of FtsZ in a ring like structure, the so-called Z-ring, underneath the cytoplasmic membrane (Aarsman, Piette et al. 2005).

Over ten essential proteins gather together to form the divisome at midcell. Assembly might follow a strictly linear sequence (reviewed by (Buddelmeijer and Beckwith 2002; Buddelmeijer, Judson et al. 2002) (Errington, Daniel et al. 2003) or, as recently proposed (reviewed by (Vicente and Rico 2006)), might involve complexes in which assembly proceeds in a concerted way. In *E. coli* a formation of the Z-proto-ring is initiated by interaction between FtsZ, FtsA, ZipA and ZapA, whereby the cytoplasmic FtsA and the membrane-bound ZipA play a role in assembling the FtsZ ring on the cytoplasmic membrane. This early event is followed by the addition of FtsK to the cytoplasmic ring, a protein that coordinates septation with chromosomal segregation. At a later assembly stage, FtsQ, FtsB and FtsL form a periplasmic connector and proteins involved in synthesis of septal peptidoglycane cell wall, FtsW and FtsI, are added to the Z ring, followed by FtsN, as a ring protruding into the periplasm and connecting with the peptidoglycane layer. Finally, two murein hydrolases, AmiC and EnvC are recruited to the Z ring, where they play an important role in hydrolysis of peptidoglycane to separate daughter cells (reviewed by (Margolin 2000) (Wissel and Weiss 2004) (Vicente and Rico 2006) (Lutkenhaus 2007)). Spatial and temporal regulation of cell division is accomplished primarily at the level of Z ring assembly. Two mechanisms are important for this process: inhibition of Z ring assembly at the midcell by nucleoid occlusion and inhibition of Z ring assembly at the poles by Min proteins (reviewed by (Margolin 2000) (Wissel and Weiss 2004; Vicente and Rico 2006) (Lutkenhaus 2007)). Negative regulators of Z-ring assembly have been shown to interact with FtsZ directly, including *E. coli* Sula (Cordell, Robinson et al. 2003), MinC (de Boer, Crossley et al. 1990) (Hu, Mukherjee et al. 1999) reviewed by (Lutkenhaus 2007)) or SlmA (Bernhardt and de Boer 2005). This study delivers evidence that *E. coli* GCP1 interacts with FtsZ, a bacterial ancestor of eukaryotic tubulin, and that it is involved in cell division.

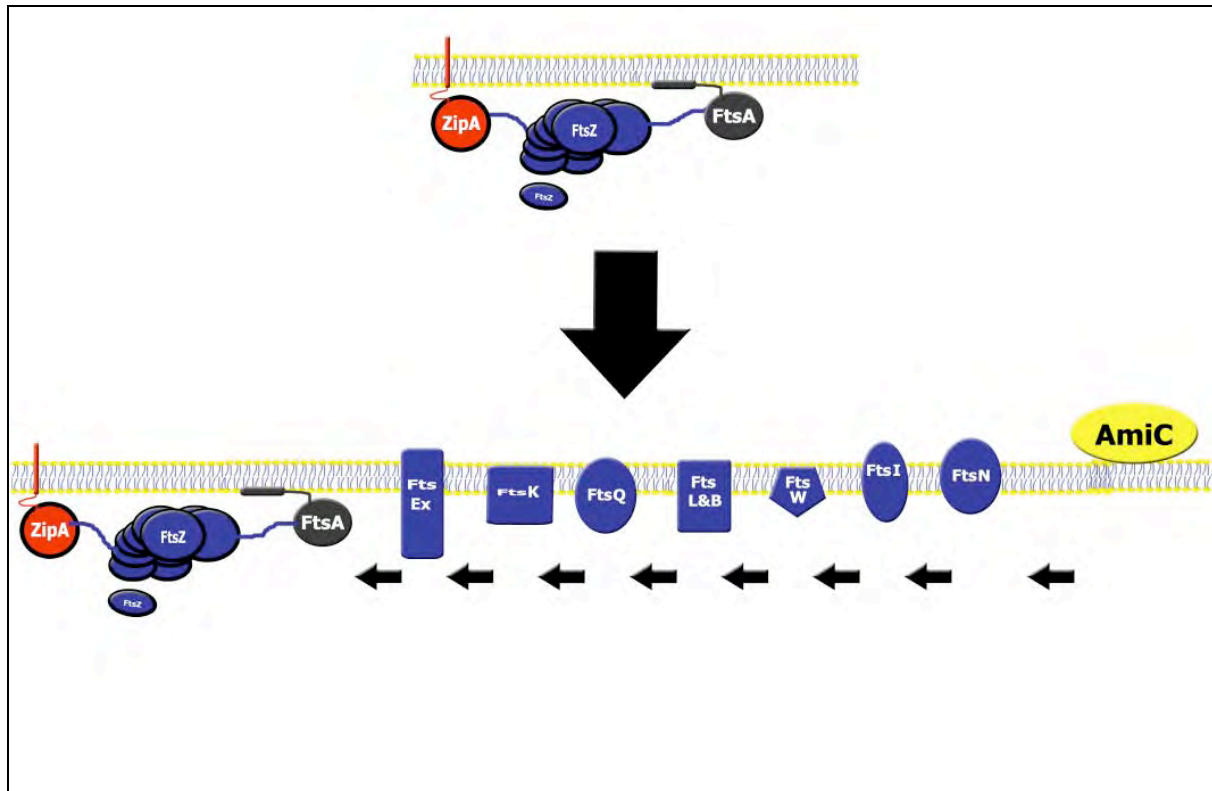
Figure 6: A schematic illustration of the chronology during divisome assembly in *E. coli*

Figure 6 schematically illustrates the chronology of the assembly of cell division proteins to the divisome of *E. coli*. In an initial step ZipA and FtsA assemble FtsZ on the membrane (on top of the scheme). Subsequently further cell division proteins assemble to the division site in order to first facilitate constriction, then chromosome segregation and finally cell division.

1.8 Aims of this work

The main aims of this study were:

- (a) The biochemical characterization of GCP1 from *E. coli* (the question whether GCP1 is an active protease should be tested by activity assays)
- (b) Determination of the subcellular localization (a secretion to the medium was reported for *M. haemolytica* GCP1) and expression studies (for this reason a polyclonal antibody should be raised against overexpressed and purified protein)
- (c) Functional analysis of GCP1 by investigating *gcp1* deletion mutants (identification of potential interaction partners by pull down experiments and investigation of the effects of GCP-depletion on the *E. coli* proteome by 2D-PAGE)

2 Materials and Methods

2.1 Abbreviations

aa	amino acids
amp	ampicillin
AP	alkaline phosphatase
APS	ammonium persulphate
BCIP	5-bromo-4-chloro-3-indolyl phosphate
bp	base pair
BSA	bovine serum albumine
Cam	chloramphenicol
DMF	dimethylformamide
DMSO	dimethyl sulfoxide
DTT	dithiothreitol
EtBr	ethidium bromide
IB	Inclusion Body
IB-buffer	Inclusion Body buffer
IB-buffer P	Inclusion Body buffer P
IB-buffer pH	Inclusion Body buffer pH
IPTG	IsoPropyl β -D-ThioGalactoside
Kan	kanamycin
LB	Luria broth
MCS	multiple cloning site
min	minutes
MMA	minimal medium A
mV	mill volt
NZA	NZ amine
NBT	nitroblue tetrazolium
OD _x	optical density at wavelength x nanometers
pfu	plaque forming units
Prep-buffer	preparation buffer
RT	room temperature
TBST	tris buffered saline, 0,1 % Tween 20
TBSTB	tris buffered saline, 0,1 % Tween 20, 2 % BSA
TCA	1,1,1-Trichloroethane
Temed	N,N,N',N'-Tetramethylethylenediamine
XP	5-bromo-4-chloro-3-indolyl phosphate

2.2 Bacterial strains

Strain	Relevant Genotype	Source
CW1	DY330, $\Delta gcp1::neo$	this study
CWCM1	MC1061, $\Delta gcp1::neo$	this study
CWCM2	MC1061 $\Delta gcp1$	this study
CWCM4	MG1655 $\Delta gcp1::neo$	this study
CWCM5	MG1655 $\Delta gcp1::neo \Delta(\lambda att-lom)::bla lacI^f P_{204}\text{-ftsZ-gfp}$	this study
MC1061	$\Delta araABC\text{-leu}$	(Meissner et al., 1987)
MG1655	WT <i>E. coli</i>	(Richmond et al., 1999)
BL21 λ DE3	<i>ompT gal dcm lon hsdS_B (r_B-m_B-)</i> λ DE3(<i>lacUV5-T7pol lacI^f</i>) <i>E. coli</i> B	(Lama et al., 1992)
DH5 α	F' <i>endA1 hsdR17 (r_K⁻m_K^{plus})</i> <i>glnV44 thi1 recA1 gyrA (Nal^r)</i> <i>relA1</i> $\Delta(\text{lacZYA-argF})$ U169 <i>deoR</i> $\emptyset 80dlac (\Delta lacZ M15)$	(Woodcock et al., 1989)
DY330	$\Delta lacU169 gal490 (\lambda c1 857 \Delta(\text{cro-broA}))$	(Yu et al., 2000)
JOE69	$\Delta(\lambda att-lom)::bla lacI^f P_{204}\text{-ftsZ-gfp}$	(Goehring, Robichon et al. 2007).

2.3 Primers

All primers used in this work were purchased from MWG (<http://www.mwg-biotech.com/>) and are listed below.

Primer	Sequence
GCP1_stop_Xho1	5'- CCG CTC GAG TTA CGC AGC CGG TAA CTC CG -3'
GCP1_5'_Bsa1	5'- ATC ATC GGT CTC TAA TGC GTG TAC TGG GTA TTG AAA C -3'
GCP1_Nco1	5'- CAT GCC ATG GGC CGT GTA CTG GGT ATT GAA ACT TCC TGC -3'
GCP1_Xho1_Histag	5'- CCG CTC GAG CGC AGC CGG TAA CTC CGC CAG -3'
EcoRI/GCP1	5'- GGA ATT CAT GCG TGT ACT GGG -3'
GCP1/XhoI	5'- CAA CTC GAG TTA TTA CGC AGC CGG -3'
ygjD_ko_3'	5'- AAC ATA TGG GTG CCG GAG AGC AAT TTC CGG CAC CGC ATA TGA ATA TCC TCC TTA - 3'
ygjD_ko_5'	5'- ACA CTG CGC GGT AAT AAA GCG AGG TAA AAC AAG TCT GTG TAG GCT GGA GCT GCT TC -3'
KanF	5'- GCT TCC TCG TGC TTT ACG GTA TCG -3'
KanR	5'- GGA GAA CCT GCG TGC AAT CCA TC -3'
rpsU_rev	5'- TCG CCA ACG ATG GTG ATG GTG -3'
NcoI-Gcp	5'- CATGCCATGGGCCGTGTAAGTGGGTATTGAAACTTCCTGC -3'
3'0,25gcp_XhoI	5'- CCGCTCGAGTTAAAAGCGCCCGGCAG-3'
3'0,5gcp_XhoI	5'- CCGCTCGAGTTACACCGCATCTTCAAAGGCG-3'
3'0,75gcp_XhoI	5'- CCGCTCGAGTTAGAACAACCTTCGCCGCGG-3'
5'EcoRI_gcp	5'- CGAATTCATGCGTGTACTGGGTATTGAAACTT-3'
Gcp_hsp70_3'	5'- CCCAAGCTTTTATAACTCCGCCAGCG-3'
Gcp_hsp70_3'-PAA	5'- CCCAAGCTTTTACGCAGCCGGTAACTC-3'
5'0,25gcpN_EcoRI	5'- CGAATTCATGGAAAAGGTTTGTAGCCAACCAATTGT-3'
5'0,5gcpN_EcoRI	5'- CGAATTCATGGGCGTCTGCCTGAACT-3'
5'0,75gcpN_EcoRI	5'- CGAATTCATGGCGGCGCTAAAGGAGTCT-3'
SiteDir1_5'	5'- CCCTGTACACTCCATGGAA-3'
SiteDir1_3'	5'- CGCTAACAGGGACCCTT-3'

2.4 Plasmids

Plasmid	Genotype	Resistance	Reference/ Source
pCW01	<i>gcp1</i> in pET24a	kan	this study
pCW02	<i>gcp1</i> with C-terminal His ₆ -tag in pET28a	kan	this study
pCW03	<i>gcp1</i> in pASKiBA3	amp	this study
pCW04	<i>gcp1</i> in pASKiBA3	amp	this study
pCW06	<i>gcp1</i> in in pBAD33 inducible by arabinose	cam	this study
pASKiBA3	expression plasmid , Anhydrotetracyclin-inducible	amp	{Sigma-Genosys, #1209}
pWR03	AraC expression plasmid	amp	{Reed, 1999 #1206}
pCP20	carries Flp-rekombinase	amp	{Datsenko, 2000 #1187}
pKD4	template for kan ^R -cassette	kan	{Datsenko, 2000 #1187}
pBAD33	expression plasmid , inducible by arabinose, T7 polymerase	cam	{Guzman, 1995 #713}
pET24a	expression plasmid, inducible by IPTG	kan	{Novagen, 2002 #1208}
pET28a	expression plasmid, inducible by IPTG	kan	{Novagen, 2002 #1208}
pCW10	<i>yeaZ</i> in pET24a	kan	this study
pCW11	<i>yeaZ-6_{his}</i> in pET28a	kan	this study
pCW50	<i>malE-hsp70_(GCP)</i> in pMalc2x inducible by IPTG	kan	this study
pCW51	<i>malE-hsp70_(GCP-PAA)</i> in pMalc2x inducible by IPTG	kan	this study
pMalc2x	MalE expression plasmid inducible by IPTG	kan	New England Biolabs
pGCP1 _{H111a/H115A}	pCW04 with <i>gcp1</i> H111/H115 changed against A	kan	this study
pGCP1N291 N243, N195,	pCW04 expressing truncated GCP1 (See Figure 16)	kan	this study
pGCP1N20-338, 40-338, 60-338	pCW04 expressing truncated GCP1 (See Figure 16)	kan	this study

2.5 Media

Media were prepared after Miller (Miller, 1972). The contents and a short description of the preparation are listed below.

Media for cultivating *E. coli*

LB-medium	10g Bacto Tryptone 5g Yeast extract 5g NaCl	H ₂ O to 1000ml, autoclaved
NAZ-medium	10g NAZ 5g Yeast extract 7,5g NaCl	H ₂ O to 1000ml, autoclaved
SOB- medium	0,5% Yeast extract 2% Tryptone 10mM NaCl 2,5mM KCl 10mM MgCl ₂ 10mM MgSO ₄	H ₂ O _{Millipore} to 1000ml, autoclaved
SOC-medium	10g Yeast extract 20g Bacto-Tryptone 5g NaCl 2,5g K ₂ HPO ₄ 1g MgSO ₄ x 7H ₂ O	H ₂ O _{Millipore} to 900ml, autoclaved, sterile glucose added to 20mM, final Volume 1000ml

2.5.1 Solid media

For preparing solid media plates, all described media were supplemented with 15 g agar (Bactoagar from Difco) per liter of medium. Approximately 25 ml of the media solution were applied per plate prior to hardening of the medium.

2.5.2 Additives

All additives that are listed below were used as concentrated stock-solution. Prior to addition to the medium the substances were sterilized.

Substance	Stock-solution	Solvent	Final concentration
Ampicillin	100 mg/ml	H ₂ O	100 µg/ml
Chloramphenicol	30 mg/ml	70 % Ethanol	30 µg/ml
Kanamycin	50 mg/ml	H ₂ O	50 µg/ml
Arabinose	20 %	H ₂ O	0,2% (w/v)
Na-Citrate	1 M	H ₂ O	20 mM
MgCl ₂	1 M	H ₂ O	50 mM

2.6 Microbiological methods

Media and solutions were sterilized at 121°C and a pressure of 1 bar in an autoclave. Temperature sensitive solutions were sterilized using a Millipore-filter with a cutoff of 0,2 µm. Glassware was sterilized by applying 180°C for at least 3 hours.

2.6.1 Storage of strains

Strains of *E. coli* that were to be stored viable for a prolonged period of time were cultivated over night in LB medium. The stationary culture was adjusted to 7% DMSO. Aliquots of 1ml were frozen in liquid nitrogen and stored at -80°C.

2.6.2 Parameters of cultivation of *E. coli*

Liquid cultures of *E. coli* were cultivated under aerobic conditions at 37°C. To ensure a steady stirring and ventilation of the culture, volumes of up to 5 ml were cultivated in a reaction-tube in a tube-roller, volumes > 10 ml in a conical flask on a shaker. Cultures in liquid media were also grown aerobically at 37°C. The strain DY330 and its derivatives were cultivated at identical conditions but at 28°C.

2.6.3 Counting cells in liquid media

For determining the cell density of liquid cultures, the photometrical OD (wavelength $\lambda = 578$ nm) of the cell suspension was determined in a cuvette of 1 cm light path (Amersham Biosciences Altospec 3100pm). A linear correlation of optical density to cell-number was assumed. An $OD_{578\text{nm}}$ of 1 equals $1,4 \times 10^9$ cells. (Miller, 1972). In order to avoid measurement errors, cell suspensions with a high optical density were diluted with the respective culture medium to an optical density below 0,5.

2.6.4 Using the bacteriophage P1

Genetic material can be transferred from one *E. coli* strain to another by making use of the bacteriophage P1 (Silhavy, 1984). For such means a phage-lysate is prepared from the donor strain and subsequently the recipient strain is infected with this. A portion of the phage particles in such a lysate is incorrectly assembled; such particles contain genetic material of the donor-strain instead of the phage-genome. When such an incorrectly assembled phage infects a cell of the recipient strain, the genetic material from the donor strain recombines with the DNA of the recipient – genetic information is transferred. In order to be able to isolate those individuals in whom the desired recombination occurred, a selectable marker (usually an antibiotic resistance) is necessary within the transduced DNA sequence.

2.6.4.1 Preparation of P1-lysates

A liquid culture of the donor strain is inoculated to a low $OD_{578\text{nm}}$ in 5 ml LB medium. When the culture reaches $OD_{578\text{nm}}$ 0,2 – 0,4 the culture is infected with 10 μl of a WT-P1-lysate ($\approx 10^6$ pfu $\cdot \text{ml}^{-1}$). Since P1-phages need Ca^{2+} ions to adhere on *E. coli* cells, the culture is adjusted to 10mM CaCl_2 . The infected cells are cultivated until lysis of all cells becomes apparent by clarification of the culture. A few drops of chloroform are intensively mixed with the culture, thereby killing residual living cells. Subsequently cellular debris is removed by centrifugation (2000 \cdot g). The resulting supernatant yields the final lysate. It is stored above chloroform in a glass-tube with screw top at 4°C.

2.6.4.2 P1-transduction

A liquid culture of the recipient strain is inoculated to a low OD_{578nm} in 5 ml LB medium. When the culture reaches OD_{578nm} = 1,0 – 1,5 the culture is adjusted to 10 mM CaCl₂ and split in aliquots of 1 ml. Different volumes (10 µl – 100 µl) of the donor-lysate are added to each aliquot. During the subsequent incubation of exactly 20 minutes at room temperature, the phages adhere to the cells of the recipient strain. Subsequently each aliquot is adjusted to 20 mM Na-citrate. This step results in the complexation of Ca²⁺ ions in the culture and thereby inhibits adhesion of further phages to the *E. coli* cells, thus preventing lysis of the culture. After phenotypic expression of the selectable marker (1 hour without selection pressure), cells are plated on the regarding selection plates (20 mM Na-citrate). Before the resulting colonies can further be used, each colony has to be streaked on plates containing 20 mM citrate in order to remove residual phages.

2.7 Biomolecular methods

2.7.1 Preparation of plasmid DNA

Plasmid DNA was extracted from DH5α cells using the “Quiaprep Spin Miniprep Kit” (Quiagen) according to the manufacturers manual.

2.7.2 Restriction digest of DNA

For cloning of genes and the first control of constructed plasmids, the plasmid DNA or PCR products were digested with a broad variety of endonucleases. The enzymes were purchased from New England Biolabs and Fermentas. For digestion, 1 µg of DNA (prepared plasmid or PCR-product) was digested using 1 µl of restriction enzyme. The reaction mixture was supplemented with the regarding buffer according to the manufacturers protocol resulting in a final volume of 20 µl. Each reaction was incubated at the advised temperature for at least 2,5 hours. In order to remove the active enzyme after digestion, the endonuclease was inactivated by incubating the reaction mix at 65°C for 15 minutes. Alternatively the digested DNA was purified using the “Quiaquick Gel Extraction Kit” (Quiagen) following the manufacturers protocol.

2.7.3 PCR

All PCR reactions were performed using the “KOD HiFi” DNA polymerase (Toibo). The annealing temperature for each reaction was determined using the website <http://alces.med.umn.edu/rawtm.html> (T_m determination of primers). PCR reactions were prepared on ice and in aliquots of 50 μ l as listed below following the manufacturers protocol. All reactions were performed in a “MyCycler” (BioRad)

Volume	PCR-reaction components
32,6 μ l	Nuclease free H ₂ O
5 μ l	10 x Puffer#1 for KOD HiFi DNA Polymerase
5 μ l	dNTPs (to 0,2 mM)
2 μ l	MgCl ₂ (to 1 mM)
1 μ l	template DNA
2 μ l	5' Primer (10 pMol· μ l ⁻¹)
2 μ l	3' Primer (10 pMol· μ l ⁻¹)
0,4 μ l	KOD HiFi DNA Polymerase

The conditions for performing PCR reactions using plasmid DNA or genomic DNA as template are listed below:

Template →	Plasmid-DNA (1-2 kbp target)	Genomic DNA (up to 2 kbp target)
Denaturation	15 seconds at 98°C	15 seconds at 95°C
Annealing	2 seconds at T_m of primer pair – 5°C	30 seconds at T_m of primer pair – 5°C
Elongation	25 seconds at 72°C	30-60 seconds at 72°C
Number of PCR cycles	25	30

For verification of each PCR reaction, 5 μ l of the reaction product were applied on an agarose gel in order to determine if a DNA band of the expected size was detectable. When verified, this

band was excised from the gel and purified by using the “Quiaquick Gel Extraction Kit” (Quiagen) following the manufacturers protocol.

2.7.4 Ligation of DNA Fragments

For the construction of all plasmid in this work, linear DNA (insert and vector) was ligated by using the T4-DNA ligase (USB). The ligase was applied following the manufacturers protocol. Instead of determining the DNA concentration prior to assembling the ligation reaction, the average DNA-concentration of vector DNA was assumed to be approximately $15\text{ng} \cdot \text{ml}^{-1}$. Because the “insert-DNA” passes diverse biochemical procedures prior to ligation and thereby was often low concentrated, following ratios of “insert-DNA” to “vector-DNA” were applied without determining the DNA-concentration.

Approach	Vector-DNA	Insert-DNA
1 - Ligation	2 μl	15 μl
2 - Ligation	2 μl	10 μl
3 - Ligation	2 μl	5 μl
4 – Religation-control	2 μl	-

Each reaction was placed in a water bath adjusted to 18°C . The water bath was placed in a Styrofoam box and the box was placed in a cold-room of 6°C , resulting in a water temperature of 6°C on the following day. Prior to transformation of chemically competent DH5 α -cells with the ligated plasmid (whole ligation reaction), the T4-DNA ligase was heat-inactivated by incubating the reaction mix at 65°C for 15 minutes.

2.7.5 Size dependent separation of DNA

This method makes use of the effect that the migration rate of DNA within an electrical field directly correlates with the size of the regarding DNA fragment. Small fragments migrate faster, large fragments slower towards the anode. DNA fragments were mixed with the according volume of 4x loading buffer and subsequently loaded on a 1 % agarose gel (1 % agarose (Roth), w/v in TAE). By applying a constant voltage of 100 mV the fragments were separated. Subsequently the DNA fragments were visualized by incubating the gel in a solution of $1\ \mu\text{g EtBr} \cdot \text{ml}^{-1}$ in 1 x TAE for 15 minutes. The EtBr molecules intercalate into the major groove of

the DNA. When the gel is illuminated using UV-light, fluorescing bands occur on the gel. Each band corresponds to a DNA fragment of a distinct size. In order to be able to assign a specific size in bp to each band, a marker mix was applied on one lane of each gel. If not noted otherwise, this marker mix was the peq GOLD Protein marker IV from PEQ-lab.

Buffer:	Components:
50 x TAE-buffer:	242 g Tris 100 ml 0,5 M EDTA 57 ml glacial acetic acid Total: 1 liter, pH 8,0
Loading buffer:	0,25 % Bromphenol-blue 0,25 % Xylencyanole 30 % Glycerine in H ₂ O

2.7.6 Extraction of DNA from agarose gels

DNA bands detected on agarose gels that were to be used further were excised from the gel with a clean scalpel. The DNA was extracted from the gel slice by using the „Qiaquick Gel Extraction Kit“ (Quiagen) following the manufacturers protocol.

2.7.7 Cloning

Details regarding the cloning of the plasmids listed below are listed in the chapters “PCR”, “Restriction digest of DNA” and “Ligation”. All cloned plasmids were transformed into chemically competent DH5 α -cells, which were subsequently plated on selection plates. The plasmid was the prepared from these cells and stored at -20°C.

pCW01/pCW02

For constructing pCW01, the *gcp1* ORF was amplified by PCR using chromosomal MG1655 DNA (kindly provided by Tina Jäger, Boos lab) as template and the primer pair EcoRI/GCP1 and GCP1/XhoI. The PCR product was purified from a TAE-agarose gel and subsequently digested with the restriction enzymes EcoRI and XhoI. The vector pET28a was digested using

the same enzymes and thereafter purified on a TAE-agarose gel. Subsequently vector and insert were ligated. The resulting plasmid pCW01 brings the *gcp1* ORF under the control of the T7-promotor yielding in an IPTG inducible *gcp1* expression plasmid. Cloning of pCW02 was carried out with the same parameters, but using the plasmid pET24a as vector instead of pET28a. Thereby GCP1 expressed from this plasmid carries an N-terminal His₆-tag.

pCW03

The *gcp1* ORF was excised from the plasmid pCW02 using the restriction enzymes EcoRI and XhoI and subsequently purified on a TAE-agarose gel. The same enzymes were used to open the vector pASKIBA3 and subsequently the linearized vector was also purified on a TAE-agarose gel. Subsequently vector and insert were ligated. The plasmid pCW03 is an anhydrotetracyclin inducible *gcp1* expression plasmid. The induction system features linear induction in dependence to the concentration of anhydrotetracyclin in the medium. The distributor of the vector pASKIBA3 declared that this induction system exhibits virtually no basal expression without the inducer. The vector expresses *gcp1* encoding for a few additional (recombinant) amino acids on the C-terminus of the protein.

pCW04

gcp1 was amplified by PCR as described for pCW01/pCW02. (Primer pair: GCP11_stop_Xho1 and GCP1_5'_BSA1). pASKIBA3 was linearized with the restriction enzymes XhoI and BsaI and purified on a TAE-agarose gel. The PCR product was digested with the same enzymes after it was purified. After repeated purification, insert and vector were ligated. The plasmid is almost identical to pCW03, but here GCP1 is expressed without any recombinant amino acids.

pCW06

The *gcp1* ORF was excised from pCW04 using the restriction enzymes XbaI and HindII and subsequently purified on a TAE-agarose gel. The vector pBAD33 was linearized using the same restriction enzymes and linearized pBAD33 was also purified on a TAE-agarose gel. Thereafter vector and insert were ligated. The resulting plasmid is an arabinose inducible GCP1 expression plasmid that exhibits no basal expression when arabinose is absent from the medium and glucose is present.

pCW10

For constructing pCW10, the *yeaZ* ORF was amplified by PCR using chromosomal MG1655 DNA (kindly provided by Tina Jäger, Boos lab) as template and the primer pair EcoRI/YeaZ and YeaZ/XhoI. The PCR product was purified from a TAE-agarose gel and subsequently digested with the restriction enzymes EcoRI and XhoI. The vector pET24a was digested using the same enzymes and thereafter purified on a TAE-agarose gel. Subsequently vector and insert were ligated. The resulting plasmid pCW10 brings the *yeaZ* ORF under the control of the T7-promotor yielding in an IPTG inducible *yeaZ* expression plasmid.

pCW11

Cloning of pCW11 was carried out as described for pCW10, but using the plasmid pET28a as vector instead of pET24a. Thereby YeaZ expressed from this plasmid carries an N-terminal His₆-tag.

pCW50/51

pMalc2x (from New England Biolabs) was linearized using EcoRI and HindIII. The hsp70-coding sequence of *gcpI* was amplified by PCR using pCW04 as template and the primer pair 5'EcoRI_gcp / Gcp_hsp70_3'. After purifying the PCR-product by a TAE-agarose gel, the insert was digested with the same enzymes as the vector and subsequently purified. Vector and insert were ligated as described before. pCW51 was engineered identically, but using Gcp_hsp70-PAA-3' as 3' primer.

pGCP1_{N291} pGCP1_{N243} and pGCP1_{N195},

These three plasmids were engineered identically to pCW10, with following exceptions: pCW04 as template for the PCR reaction and the following primer pairs for the regarding insert:

pGCP1₆₀₋₃₃₈: 5'EcoRI_gcp/3'0,25gcp_XhoI

pGCP1₂₀₋₃₃₈: 5'EcoRI_gcp /3'0,5gcp_XhoI

pGCP1₄₀₋₃₃₈: 5'EcoRI_gcp /3'0,75gcp_XhoI

all inserts were ligated into pET24d+.

pGCP1₆₀₋₃₃₈: pGCP1₂₀₋₃₃₈ and pGCP1₄₀₋₃₃₈:

These three plasmids were engineered identically to pCW10, with following exceptions: pCW04 as template for the PCR reaction and the following primer pairs for the regarding insert:

pGCP1₆₀₋₃₃₈: Gcp1_stop_Xho1/5'0,25gcpN_EcoRI

pGCP1₂₀₋₃₃₈: Gcp1_stop_Xho1/5'0,5gcpN_EcoRI

pGCP1₄₀₋₃₃₈: Gcp1_stop_Xho1/5'0,75gcpN_EcoRI

all inserts were ligated into pET24d+.

2.7.8 TSS transformation

This method (Hanahan, Jessee et al. 1991) was applied when no high transformation efficiency was required. 2ml of LB-medium were inoculated with the recipient strain from a single colony. When the culture reached an $OD_{578} = 0,2 - 0,3$ the cell suspension was cooled down in ice-slurry. 2 ml of 2 x TSS solution tempered to 4°C were added to the cell suspension and mixed. Cells acquire competence after a subsequent incubation on ice for 15 to 20 minutes. For the transformation, 1µl plasmid was mixed with an aliquot (1ml) of competent cells and incubated on ice for 30 minutes. When the transformation was performed with plasmids carrying any other antibiotic resistance than amp^R , a phenotypic expression of the antibiotic resistance genes was carried out (1h, 37°C in TSS). Subsequently cells were pelleted and plated on the regarding selection plates.

2 x TSS-solution: (= „transformation and storage solution“)

(Total volume 100 ml)

0,8 g Tryptone

0,5 g Yeast-extract

0,5 g NaCl

20 g PEG 8000 (6000)

10 % DMSO

100 mM MgSO₄

All components except DMSO and MgSO₄ were dissolved in water and autoclaved. DMSO and MgSO₄ were added from a sterile stock solution.

2.7.9 Chemical transformation (ultra competent DH5 α cells)

Chemical transformation of ligations was performed according to Inoue et al. (Inoue et al., 1990). Competent cells were obtained by inoculation of an 1/100 dilution of an DH5 α overnight culture in 250 ml SOB medium up to an OD_{578nm} = 0,5. The culture was rapidly cooled to 0°C and incubated on ice for another 15 min before cells were pelleted (10 min, 3000g, 4°C). Cell pellets were washed twice in ice-cold TB buffer, and subsequently resuspended in 20 ml ice-cold TB buffer supplemented with 7% DMSO. Cells were shock frozen in liquid nitrogen and stored in 1 ml aliquots at -80°C. If not exceptionally mentioned, further steps were carried out on ice. A volume of 1 ml of competent cells was used for 4 transformations, each with 20 μ l of the respective ligation (1 h, 4°C). Phenotypic expression was allowed in 1 ml LB for one hour at 37°C. Finally cells were plated on the regarding selection plates. All substances were dissolved in Millipore water with pH adjusted to 6.7 (using KOH or HCl), supplemented with 55 mM MnCl₂, filter sterilized, and stored at 4°C.

2.7.10 Deletion of chromosomal genes by homologous recombination

The chromosomal gene of interest was deleted by the replacement of its open reading frame by a kanamycin resistance cassette (Datsenko und Wanner, 2000). This cassette was amplified by PCR using pKD4 as template. By the using of the primers *ygjD_ko_3'* and *ygjD_ko_5'* the PCR products were elongated on each end by 35 bps., which represent the flanking regions of the chromosomal *gcp1*. DY330 was cultured in 10 ml at 28°C to a final OD_{578 nm} = 0.5 – 0.8. Following incubation for 15 min at 42°C (λ -red induction) the culture was rapidly cooled to 0°C, pelleted by centrifugation (5500g, 8 min, 4°C), three times washed in ice-cold water and finally resuspended in 100 μ l ice-cold sterile water. According to the manufacturers protocol competent cells were transformed with the PCR products by electro-transformation using a BioRad Gene Pulser (Ausubel, 1987). Following transformation of the PCR products into DY330 homologous recombination occurs between the overhangs of the PCR product and its chromosomal analogs. GCP1 is replaced by the kanamycin resistance cassette (kan^R) and so deleted. The strain DY330 was chosen due to the integration of a defective prophage, which codes for the λ -RED recombinase system (Murphy, 1998) into its chromosome. On the one hand DY330 obtains a recombination efficiency that is elevated by the factor 103 and which qualifies this method for experiments where a high probability of homologous recombination events is

required. On the other hand DY330 can only be cultured at temperatures till 28°C as higher temperatures would induce λ Red expression. Gene deletions by double homologous recombination could be controlled by PCR. For DNA amplification cells with the corresponding deletion were used as template. Primer pairs were characterized by the forward primer annealing within the integrating sequence and the reverse primer binding outside, in the flanking region of the recombination event. By this approach a PCR product is only generated in the case of a successful recombination event. For the transfer of the *gcp1* deletion into other strains, the P1-Transduction method was performed.

2.7.11 Construction of strains

The following sections briefly describe the construction of each strain used in this work.

CW1 and CWCM1:

The plasmid pCW06 was transformed in DY330 (Δ *lacU169 gal490* (λ *c1* 857 Δ (*cro-broA*)) and *gcp1* was deleted from the chromosome as described in Chapter 3.2.1. The resulting strain is CW1 (DY330- Δ *gcp1::neo*) harboring pCW06. In order to be able to transduce the Δ *gcp1::neo* genotype into other strains, a P1 lysate was prepared using the strain CW1 as donor. Subsequently, a conditionally lethal *gcp1* mutant was constructed in the strain MC1061 (Δ *araABC-leu*), a strain accumulating arabinose with high affinity but not utilizing it: MC1061 was transformed with pCW06. Chromosomal *gcp1* was deleted via P1-transduction under inducing conditions for plasmid-encoded *gcp1* (0,2 % w/v arabinose) using the P1 lysate prepared from CW1. The resulting strain from this transduction is CWCM1 (MC1061, Δ *gcp1::neo*) harboring plasmid pCW06 (pBAD33, *araC*⁺, P_{BAD}-*gcp1*).

CWCM2

CWCM1 harboring pCW06 was transformed with pCP20 using TSS transformation. Positive clones were incubated at 42°C. This temperature shift resulted in induction of expression of the Flp-recombinase. This recombinase recognizes the Frt-sites that are flanking the *neo* gene within the kanamycin resistance cassette, thus recombining *neo* out of the chromosome. Second, the origin of replication of the plasmid pCP20 is temperature sensitive, leading to no more replication of the plasmid. Subsequent testing for the loss of ampicillin resistance (pCP20) and kanamycin resistance (*neo*) during arabinose dependent growth led to CWCM2 clones.

CWCM4

MG1655 (WT *E. coli*) was transformed with pCW06 using TSS transformation. Subsequently the chromosomal *gcp1* deletion was transduced into the cells via P1 transduction using CWCM1 as donor.

CWCM5

CWCM4 harboring pCW06 was transduced with a P1 lysate prepared from JOE69 selecting for ampicillin resistance after transduction. The resulting strain resembles CWCM4 harboring pCW06 harboring an IPTG-inducible FtsZ-Gfp Fusion in the λ -attachment site.

2.8 Biochemical methods

2.8.1 SDS PAGE

For separating proteins by size, SDS-polyacrylamide-gel-electrophoresis (SDS-PAGE) after Laemmli was deployed (Laemmli 1970). Polyacrylamide gels were prepared in “Biorad Minicell Apparatuses” (Biorad) according to the manufacturer's protocol. All required solutions and buffers are listed in the table below among other solutions needed for carrying out SDS-PAGE. Gels were placed in a “Biorad Electrophoresis Chamber” (Biorad) filled with SDS running buffer. A constant current of 20mA per gel was applied for approximately 2 hours until the front end of separated proteins reached the bottom of the gel. If gels were not subsequently subjected to western blotting, the proteins on the gel were visualized by coomassie staining.

Buffer	Components
4 x Resolving gel	in H ₂ O: 1,5 M Tris 0,4 % SDS pH 8,8
4 x Stacking gel	in H ₂ O: 500 mM Tris 0,4 % SDS pH 6,8
10 x SDS-Running buffer	in H ₂ O: 250 mM Tris 1,9 M Glycine 1 % SDS
6 x Sample buffer	in H ₂ O: 60 mM Tris HCl, pH 6,8 2 % SDS 10 % Glycerine 4 % DTT 0,1% Bromphenol blue

Gel preparation:

Stacking gel (for 2 Gels)	2,5 ml 4 x Stacking gel buffer 4 ml Acrylamide-Stock 50 µl APS (10%) 5 µl Temed 3,45 ml H ₂ O
Resolving gel (for 2 Gels, 10 %)	1,25 ml 4 x Resolving buffer 0,65 ml Acrylamide-Stock 50 µl APS 5 µl Temed 3,07 ml H ₂ O

2.8.2 2D-PAGE (NEPHGE method)**Short description including solution composition and preparation:**

For two-dimensional gel electrophoresis cell pellets were agitated at 28°C in NEPHGE sample buffer (9.5 M urea, 2% Nonidet P-40, 5% ampholines, pH 3–10, (Servalyt, Serva), 0.3% SDS, 5% β-mercaptoethanol). Gel rods were poured as described (O'Farrell, Goodman et al. 1977) by addition of 27 µl of 10% ammoniumpersulfate and 19 µl of TEMED to a filtered and degassed solution of 5.5 g urea in 1.32 ml of acrylamide stock (28.38% acrylamide, 1.62% bisacrylamide), 4 ml 5% Nonidet P-40, and 0.5 ml Servalyte 3–10. The gel was topped up with overlay solution (8 M urea, 2,5% Servalyt 3–10) and polymerized for 1 h. The sample was applied to the gel, topped with 20 µl of overlay solution, and run for 4 h at 400 V from acidic (0.01 M H₃PO₄, plus pole) to the basic side (0.02 M NaOH, minus pole). The rod was equilibrated twice in 25 ml of equilibration buffer (10% glycerol, 10% β-mercaptoethanol, 2.3% SDS, 90 mM Tris-HCl, pH 6.8) for 20 min each and fixed to the top of a 15% SDS-PAGE with Laemmli SDS sample buffer +1% agarose. The gels were run for 1050 V/h and stained with Coomassie stain.

1st dimension gel preparation

2D-gels were prepared using the NEPHGE method. All buffers used for preparing the first and second dimension gel-matrix are listed above. The first dimension gel matrix was prepared in glass tubes of 10 cm length and a diameter of 2,5 mm. 6 tubes were prepared at a time. The components of the first dimension gel matrix were mixed as described above and sterile filtered using a filter of 0,2 µm cutoff. The glass tubes were closed with parafilm on one end, filled to 9

cm with the acrylamide mix and covered with 20 µl of overlay solution. After polymerization at room temperature, the parafilm (lower end) was removed from the glass tubes and the tubes placed in a 1st dimension gel apparatus (BioRad) so that the lower end of the tube was located in the anode buffer and the upper end covered by the cathode buffer. Samples were filled on top of the tube and covered with overlay solution. A constant voltage of 400 V was applied for 4 hours. Subsequently the first dimension gel was carefully released from the glass tube by using permanent ejection of water from a syringe with a very fine cannula. Finally incubating it twice in 25 ml of equilibration buffer for 20 minutes equilibrated the gel-stick.

2nd dimension gel preparation

SDS-PAGE gels (12 % acrylamide) were prepared as described above with the exception that larger glass-plates were used (20 cm x 15 cm). These glass plates contain a groove at their upper end in order to be able to place the first dimension gel on top of the second dimension. After polymerization of the stacking gel, the first dimension gel was placed on top of the second dimension and sealed with agarose buffer. Finally the gel was placed in the running chamber and a voltage of 75 Volts was applied for 9 hours (over night).

Sample preparation

The conditionally lethal *gcp1* mutant CWCM4 (MG1655 $\Delta gcp1::neo$) harboring pCW06 (pBAD33, *araC*⁺, *P_{BAD}-gcp1*) was cultured in 200 ml LB-medium (0,2% arabinose) to a low OD_{578nm}, washed with LB medium and the culture split into GCP1 induced (+ 0,2 % arabinose) and non-induced + 0,2 % glucose) subcultures. Samples were prepared when the growth deficit became apparent in the growth curve. In order to load equal amounts of cells onto the gels, the cells from each culture were pelleted in a 1.5 ml reaction tube until the pellet equaled the volume of 50 µl. Cells were then disrupted by the freeze-thaw method (freezing in liquid nitrogen and thawing again for 4 times). Subsequently the disrupted cells were resuspended in 150 µl of NEPHGE buffer and incubated at 27°C over night.

2.8.3 Protein identification

The identification of proteins of interest was carried out by “Proteome Factory” (Berlin). Protein spots (or bands) were excised with a clean scalpel and shipped to “Proteome Factory” (Berlin, <http://www.proteomefactory.com/>) from where the protein identification was delivered.

2.9 Antibodies

α -GCP1 antibodies

A band corresponding to GCP1 was excised from a SDS-PAGE from overexpressing GCP1 and send to Agrisera (Sweden) where polyclonal antibodies against GCP1 were prepared (rabbit α -GCP1).

α -YeaZ antibodies

Purified YeaZ protein was delivered to the TFA (Tierforschungsanstalt, University of Konstanz) where polyclonal antibodies against YeaZ were prepared (rabbit α -GCP1).

Other antibodies

All other antibodies used in this study were obtained from different laboratories or commercial suppliers. They are listed in the table below:

Antigen	Organism raised in	Applied dilution	Source
Gcp1	rabbit	1:5000	Agrisera (Sweden)
YeaZ	rabbit	1:10000	TFA (Konstanz)
His-Tag	mouse	1:15000	Quiagen
MalE	rabbit	1:15000	NEB
rabbit	goat	1:10000	NEB
mouse	goat	1:10000	NEB
FtsZ	rabbit	1:10000	John Beckwith (USA)
Omp	rabbit	1:10000	Winfried Boos (Konstanz)

2.9.1 Immunoblotting (western blotting)

The method of western blotting allows the immunohistological staining of specific proteins by an according antibody against this protein. In this study western blots were prepared in a “Semi-Dry” blotting device from BioRad according to the manufacturers protocol. Proteins from an SDS-PAGE were transferred to a PVDF membrane in transfer-buffer (1 hour transfer at 15 mV per gel). Subsequently the blot was developed by the use of the buffers listed below this chapter.

For blocking membrane surfaces that contained no protein, the blot was incubated for 2 hours in 100 ml TBSTB at room temperature. Subsequently the primary antibody was applied at the according dilution in TBSTB. After 2 - 4 hour incubation at room temperature with the primary antibody, the blot was washed three times for 10 minutes in 50ml TBST. The secondary antibody was applied in a 2-hour incubation step (antibody „goat- α -rabbit“, HRP conjugate 1 : 10000 in 10 ml TBSTB), followed by 2 washing steps of 10 minutes in 10 ml TBST. Finally the blot was washed for 10 minutes in AP and subsequently developed in 10 ml of fresh staining solution. Rinsing the blot with water terminated the staining reaction.

TBST	20 mM Tris, pH 7,5 150 mM NaCl 0,05 % Tween 20
TBSTB	TBST 2% BSA
AP	100 mM Tris, pH 9,5 100 mM NaCl 5 mM MgCl ₂
Staining solution	10 ml AP 66 μ l NBT (50 mg/ml in 70% DMF) 42 μ l XP (50 mg/ml in 70 % DMF)

2.10 Overexpression of GCP1 and Protein purification

2.10.1 Test-expression of GCP1

The strain BL21(DE3) was transformed with the plasmids pCW01 and pCW02. GCP1-expression was carried out in 250 ml of NZA medium (100 μ g kanamycin \cdot ml⁻¹) at 37°C with a rotation of 150 rpm in a 2 liter conical flask. Expression was induced by IPTG (final concentration 400 μ g \cdot ml⁻¹). Induction was tested during different growth phases of the culture ($OD_{578nm} = 0,3$ and $OD_{578nm} = 1,0$) in order to identify the ideal time point of induction. Expression was carried out over night. For testing the expression, 20 μ l of concentrated cell suspension ($OD_{578nm} = 5$) before and after induction respectively, were applied on an SDS-PAGE.

2.10.2 Purification approaches

All buffers used for the purification of GCP1 are listed below in this chapter. In all cases GCP1 carrying an N-terminal his₆-tag was expressed from pCW02 in the strain BL21(DE3). 250 ml NZA medium inoculated to OD_{578nm} = 0,2 and the cells were cultivated at 37°C with a rotation of 150 rpm in a 2 liter conical flask. Expression was induced when the culture reached an OD_{578nm} = 1,0 by adjusting the medium to 0,4 mM IPTG. After 4 hours of expression cells were pelleted by applying 6000 x g at 4°C. In order to prepare inclusion bodies from the cells, the pellet was resuspended in 10 ml prep-buffer and cells were disrupted in a “French Pressure Cell” (Aminco) by applying 1200 psi according to the manufacturers protocol. Disrupted cells were centrifuged at 1000 x g for 15 minutes in an SS34 rotor. Pelleted inclusion bodies were solubilized in 15 ml of IB-buffer and the solution was centrifuged for 30 minutes at 27000 x g. The resulting supernatant was applied on a NiNTA-agarose column in a FPLC (BioRad, “Bio-Logic Workstation”). During all purification approaches, protein was loaded on the column in IB-buffer and the column was subsequently washed with IB-buffer until no more protein was detectable in the washing buffer that passed through the column. Three different approaches were undertaken:

1. Washing the column with rising imidazole concentrations and elution with 200 mM imidazole. (Imidazole concentrations during the washes: 20 mM, 40 mM, 60 mM, 80 mM, 100 mM, 150 mM)
2. As 1., instead of IB-buffer, IB-buffer-P was used (also during preparation of inclusion bodies and when loading the column)
3. Washing and eluting by pH-shifts: Inclusion Bodies were resuspended in IB-buffer-pH (pH 7,5) and loaded to the column. The first wash was performed using 100% IB-Puffer pH (pH=7,5), subsequently the concentration of IB-Puffer-pH (pH=4,5) was raised in steps (10%, 20%, 30%, 40%, 50%, 60%, 70%, 80%, 100%).

Buffer	Components in H ₂ O:
Prep-buffer	100 mM NaCl 20 mM Tris 0,5 mM DTT pH 7,5
IB-buffer:	6 M Guanidiniumhydrochloride 100 mM NaCl 20 mM Tris pH 7,5
IB-buffer P:	6 M Guanidiniumhydrochloride 150 mM NaCl 50 mM NaH ₂ PO ₄ pH 7,5
IB-buffer pH:	6 M Guanidiniumhydrochloride 100 mM NaH ₂ PO ₄ 10 mM Tris pH 7,5 e.g. pH 4,5

2.10.3 Refolding GCP1 from inclusion bodies

In order to refold GCP1 from 6 M guanidinium hydrochloride solutions, 8 different buffer conditions were tested as listed in the table below. 0,5 ml from the eluted fraction (Chapter 2.9.3, Version 1) were rapidly diluted with 9,5 ml of refolding buffer in a 10 ml screw top tube. After centrifugation of the protein solution at 25000 x g for 20 minutes, the supernatant was adjusted to 12% TCA to denature and precipitate soluble protein. The precipitate from each approach was taken up in 20 µl of SDS-sample buffer and applied on a SDS-PAGE in order to determine if the supernatant contained soluble protein.

Buffer	Detergent	[NaCl]	pH	Buffer substance
1	0,05 % Dodecylmaltoside	100 mM	7,5	20 mM Tris
2	0,05 % Dodecylmaltoside	100 mM	8,3	20 mM Tris
3	0,0 5% Dodecylmaltoside	500 mM	7,5	20 mM Tris
4	0,05 % Dodecylmaltoside	500 mM	8,3	20 mM Tris
5	1% SDS	100 mM	7,5	20 mM Tris
6	1% SDS	100 mM	8,3	20 mM Tris
7	1% SDS	500 mM	7,5	20 mM Tris
8	1% SDS	500 mM	8,3	20 mM Tris

2.11 Comparison of growth of CWCM4 with and without arabinose

50 ml of LB medium containing 0,2 % arabinose were inoculated with the conditionally lethal *gcp1* mutant CWCM4 harboring pCW06 from a 5 ml preculture to $OD_{578nm} = 0,05$ and cultivated at 37°C (150 rpm) in a 500 ml conical flask until the culture reached $OD_{578nm} = 0,1$. The cells were washed twice with LB-medium and subsequently split into 2 independent cultures of which one was grown in LB-medium solely and the second in LB-medium containing 0,2 % arabinose. Approximately every 30 minutes the OD_{578nm} of the cultures was determined. As approximate control the parental strain of CWCM4 harboring pCW06, MG1655 (*E. coli* WT) was cultivated with the same parameters. LB-medium was chosen since it is a standard medium and no induction of the *gcp1* gene under control of the P_{BAD} -promoter was observed in LB.

2.12 Localization of overexpressed GCP1

The strain BL21(DE3) harboring pCW01 was cultivated in 250 ml NZA medium and GCP1 overexpression was induced as described above. Cells were pelleted and resuspended in 10 ml of prep-buffer (table below). Subsequently cells were disrupted in a “French Pressure Cell” (Aminco) and the extract was subjected to differential centrifugation (Osborn et al., 1972). During the differential centrifugation, in each step the supernatant of the previous centrifugation was applied to the following one. The table below lists the individual centrifugation steps of this experiment.

Fractionation:	Supernatant:	Pellet:
10 ml disrupted cells 1000 x g / 15 minutes	Cellular debris, membranes, soluble components	insoluble components, especially Inclusion Bodies
10 ml of the supernatant from the previous step 27000 x g / 30 minutes	Membranes, soluble components	Cellular debris
100 µl of the supernatant from the previous step 132000 x g / 2 minutes (Beckmann Airfuge)	Soluble components	Membranes

Two samples were taken from each centrifugation step (pellet and supernatant) and applied on a SDS-PAGE. The preparation of the samples is briefly described in the table below.

Fractionation:	Supernatant	Pellet
1000 x g 15 minutes	Sample 1: 300µl of 4x sample buffer were added to 100µl supernatant Sample 2: 90µl of 4x sample buffer were added to 10µl of supernatant	The pellet was resuspended in 10ml Prep. Buffer. Sample 1: 300µl of 4x sample buffer were added to 100µl of this suspension Sample 2: 90µl of 4x sample buffer were added to 10µl of the suspension
27000 x g 30 minutes	Sample 1: 300µl of 4x sample buffer were added to 100µl supernatant Sample 2: 90µl of 4x sample buffer were added to 10µl of supernatant	The pellet was resuspended in 1ml Prep. Buffer. Sample 1: 300µl of 4x sample buffer were added to 100µl of this suspension Sample 2: 90µl of 4x sample buffer were added to 10µl of the suspension
132000 x g 2 minutes	Sample 1: 300µl of 4x sample buffer were added to 100µl supernatant Sample 2: 90µl of 4x sample buffer were added to 10µl of supernatant	The resulting pellet was resuspended in 20 µl of 1x sample buffer

2.13 Expression studies in *E. coli* WT cells

A 500 ml MG1655 (*E. coli* WT) culture was inoculated from a fresh colony to an initial $OD_{578nm} = 0.02$ and grown in LB-medium at 37°C in a 5000 ml conical flask until it reached stationary phase. At the times when an aliquot of each culture was taken for measuring the growth curve, also an aliquot for SDS-Page was taken. Cells from each aliquot (equaling 10 µl of $OD_{578nm} = 5$) were boiled in equal amounts of SDS sample buffer and applied to SDS-PAGE and immunoblot analysis. Three different immunoblots were prepared using antibodies against GCP1, YeaZ and FtsZ.

2.13.1 Determination of the subcellular localization of GCP1 in WT *E. coli*

In order to extract the periplasmic fraction from *E. coli* cells a MG1655 culture from stationary phase was subjected to cold osmotic shock (Neu and Heppel 1965). Cells were pelleted by applying 6000 x g at 4°C. The collected cells (1g, wet weight) were suspended in 80 ml of 20 % sucrose – 30 mM Tris-HCL, pH 8.1. The suspension was treated with 3 mM Na₂EDTA and mixed in a 1 liter flask on a rotary shaker (180 rpm) for 10 minutes. Subsequently the mixture was centrifuged at 13000 x g at 4°C for 10 minutes. The supernatant was removed and the pellet was rapidly resuspended in 80 ml of cold water. The suspension was incubated in an ice bath on a rotary shaker for 10 minutes and subsequently centrifuged at 13000 x g for 10 minutes at 4°C. The supernatant resembles the periplasmic fraction while the pellet resembles spheroplasts and the outer membrane fraction.

Periplasmic and inner membrane fraction:

The outer membrane fraction and the inner membrane fraction were prepared as described by Sukumaran et al., 2001.

Cytoplasmic fraction

In order to separate into cytoplasmic and cytoplasmic membrane fraction, the spheroplasts yielded from the cold osmotic shock were resuspended in prep-buffer (table) and disrupted using the “French Pressure cell” as described above. The resulting extract was centrifuged at 130,000 x g for 1 hour at 4°C in a Beckman Coulter Optima LE-80K ultracentrifuge. The resulting supernatant (cytoplasmic fraction) and the pellet (inner membrane fraction) were collected solubilized in equal amounts of sample buffer and subjected to SDS-PAGE and immunoblotting as described above.

Total membrane fraction

To collect the total membrane fraction, an aliquot was collected from the MG1655 culture was taken at logarithmic and stationary phase. Cells were resuspended in 10ml prep-buffer to

OD_{578nm} = 5,0 and disrupted by French press and cellular debris was removed by centrifugation at 27,000 x g for 20 minutes at 4°C. The supernatant was collected and centrifuged at 130,000 x g for 1 hour at 4°C in a Beckman Coulter Optima LE-80K ultracentrifuge. The pellet (containing total membrane protein) was collected, solubilized in sample buffer and subjected to SDS-PAGE and immunoblotting as described above.

2.14 Microscopy

Two independent cultures (200 ml LB medium) of the conditionally lethal *gcp1* mutant strain CWCM5 harboring pCW06 were inoculated from a 5 ml preculture to OD_{578nm} = 0,05. One culture was supplemented with 0,2 % arabinose, the other with 0,2 % glucose. Approximately 90 min after the inoculation of the 200 ml cultures, *ftsZ-gfp* expression was induced by the addition of 10 µM IPTG and an aliquot of 1 ml was collected from both cultures after the growth deficit became apparent in the glucose-containing culture. Pelleted cells were then analyzed with an epifluorescence Axioplan2 microscope (Zeiss, Germany) equipped with AxioCam HPm camera system (Zeiss, Germany). Digital pictures were acquired with the Axio vision (Rel. 4.5) software (Zeiss, Germany).

2.15 Effects of long time GCP1-depletion

The conditionally lethal *gcp1* mutant strain CWCM4 harboring pCW06 was cultivated at 37°C in 5 ml LB-medium supplemented with 0,2 % arabinose inoculated from a fresh colony. When the culture reached OD_{578nm} = 1,0 the arabinose was washed out of the medium and the cells were cultivated further for additional 45 minutes. Two independent cultures were then inoculated to OD_{578nm} = 0,01 using cells from the 5 ml culture as inoculum. One of the cultures was grown in LB-medium supplemented with 0,2 % arabinose while the other contained LB-medium supplemented with 0,2 % glucose. Both cultures were grown until the arabinose-supplemented culture reached stationary phase. At each time the growth curve was measured an aliquot of each culture was taken. Cells from each aliquot (equaling 10 µl of OD_{578nm} = 5) were boiled in equal amounts of SDS sample buffer and applied to SDS-PAGE and immunoblot analysis. Three different immunoblots were prepared using antibodies against GCP1, YeaZ and FtsZ.

2.16 Testing cell viability

Viability of cells was tested using the “Cell Viability Kit” (Invitrogen) according to the manufacturers protocol. The strain CWCM4 harboring pCW06 was cultivated for 7 hours in the presence and absence of arabinose respectively as described above and cells stained with the kit. Stained cells were investigated under a fluorescence microscope: Epifluorescence Axioplan2 microscope (Zeiss, Germany) equipped with AxioCam HPm camera system (Zeiss, Germany). Digital pictures were acquired with the Axio vision (Rel. 4.5) software (Zeiss, Germany).

2.17 Complementation studies

In order to determine which domains and motifs of GCP1 are essential for the physiological function of GCP1, different constructs encoding truncated GCP1 were engineered (Figure 16) the cloning of these constructs is described above. The strain CWCM4 harboring pCW06 was cultured in the presence of arabinose and individually transformed with each of these constructs using TSS-transformation. Positive clones were subsequently plated on LB-agar plates containing or lacking arabinose respectively. Constructs that allowed the formation of colonies in the absence of arabinose were accounted as capable of complementing for the *gcp1* deletion.

2.18 Pulldown experiments

Two types of constructs for pull-down experiments were prepared using the pMalc2x vector. Both constructs contained the HSP70-actin fold domain of GCP1 (aa 147-337) fused to the maltose-binding protein (MalE-GCP1₁₄₇₋₃₃₇) but the C-terminal three aa SsrA-tag was either present (pCW50) or deleted (pCW51) in these constructs. The strain BL21(DE3) was independently transformed with each of the constructs using TSS transformation. The cells were cultivated in 200 ml LB medium and expression of the construct was induced by adjusting the medium to 200 μ M IPTG when the culture reached an $OD_{578nm} = 1,0$. Expression was carried out for 3 hours, cells were harvested by centrifugation at 4,000 x g at 4°C, resuspended in 10 ml prep-buffer and disrupted by French Press (SLM Aminco) treatment as described above. Following a centrifugation step at 30,000 x g for 20 min at 4°C, the supernatant was collected and applied on a 1 ml Biorad column packed with amylose resin (New England Biolabs) connected to a FPLC (Biorad Biologic Workstation). The column was washed with the

preparation buffer until no more protein was detectable in the flow through prior to the elution of bound proteins. Applying preparation buffer supplemented with 20 mM D-maltose to the column carried out elution. An alternative approach included an additional binding step of MG1655 cell extract followed by a wash before the elution. Eluted proteins were subjected to SDS-PAGE and immunoblotting. Bands of interest were excised from Coomassie-stained gels and analyzed by mass spectrometry (Proteome Factory, Berlin, Germany).

2.19 YeaZ overexpression

The strain BL21(DE3) was transformed with the plasmids pCW10 and pCW11 using TSS transformation. YeaZ-expression was carried out in 250 ml of NZA medium (100 μg kanamycin $\cdot \text{ml}^{-1}$) at 37°C with a rotation of 150 rpm in a 2 liter conical flask. Expression was induced by IPTG (final concentration 400 $\mu\text{g} \cdot \text{ml}^{-1}$). Induction was tested during different growth phases of the culture ($\text{OD}_{578\text{nm}} = 0,3$ and $\text{OD}_{578\text{nm}} = 1,0$) in order to identify the ideal time point of induction. Expression was carried out over night. For testing the expression, 20 μl of concentrated cell suspension ($\text{OD}_{578\text{nm}} = 5$) before and after induction respectively, were applied on an SDS-PAGE.

2.20 YeaZ purification

The strain BL21(DE3) transformed with pCW11 was cultivated in 250 ml NZA medium as described above. Expression was induced when the culture reached an $\text{OD}_{578\text{nm}} = 1,0$ by adjusting the medium to 0,2 mM IPTG. After 3 hours of expression cells were pelleted by application of 6000 x g at 4°C. The resulting pellet was resuspended in 10 ml prep-buffer and cells disrupted in a “French Pressure Cell” by applying 1200 psi according to the manufacturers protocol. Disrupted cells were centrifuged at 1000 x g for 15 minutes in an SS34 rotor. The resulting supernatant was applied on a NiNTA-agarose column connected to a FPLC (BioRad, “Bio-Logic Workstation”). Protein was loaded on the column in prep-buffer and the column was subsequently washed with prep buffer containing 10 mM imidazole until no more protein was detectable in the washing buffer that passed through the column. Elution was carried out using rising concentrations of imidazole: 120 mM, 140 mM, and 400 mM).

2.21 Bioinformatics

Similarity searches were done using the BLAST program. The transmembrane regions were predicted using the dense alignment surface method (DAS). Using sequence motif search and protein motif fingerprint databases performed protein pattern and motif predictions. The software programs used are accessible on the Web pages: <http://www.expasy.org/tools> and <http://www.genome.jp>.

3 Results

3.1 Overexpression and purification of GCP1 from *E. coli*

GCP1 from *E. coli* was to be overexpressed and purified in order to be able to perform further biochemical characterization of the protein.

3.1.1 GCP1 is overexpressed in substantial amounts

The IPTG inducible overexpression plasmids pCW01 (encoding WT GCP1) and pCW02 (encoding GCP1 with a C-terminal his₆-tag) were each transformed in the expression strain BL21λDE3 and expressed in the presence of IPTG. Expression was induced with 200 μM IPTG when the culture reached OD_{578nm} = 0,3 or 1,0 respectively and was carried out for 3 hours. A strong overexpression of both constructs was observed by SDS-PAGE prepared out of whole cells from the overexpression culture (Figure 7, Page 46).

Figure 7: A SDS-PAGE gel of the overexpressed GCP1 using the plasmids pCW01 and pCW02

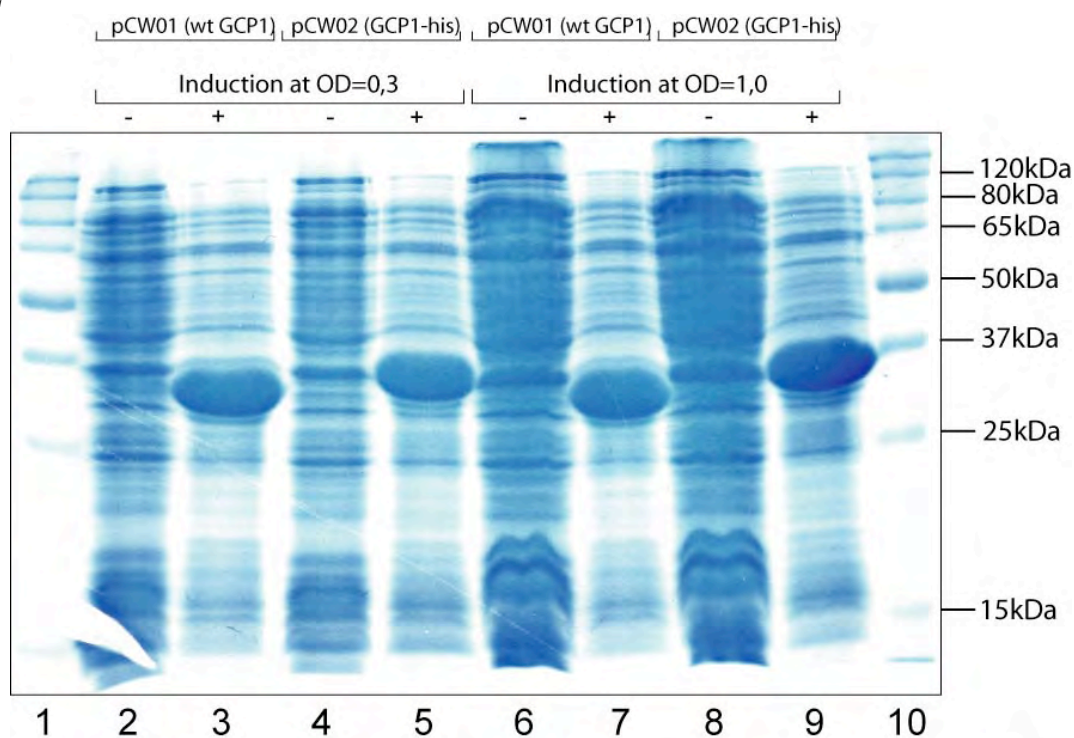


Figure 7 shows a SDS-PAGE of GCP1 overexpressed in the strain BL21(DE3). Lane 1 and 10 contain the protein standard as labeled in kDa, lanes 2, 4, 6 and 8 show total cell protein from cultures before induction of overexpression (-), Lanes 3, 5, 7 and 9 show total cell protein from the cultures after induction (+). The OD_{578nm} of the cultures when overexpression was induced is marked above the gel, as well as the respective plasmid encoding WT GCP1(pCW01) or C-terminally his₆-tagged GCP1(pCW02).

3.1.2 Small amounts of overexpressed GCP1 co-sediment with the membrane fraction of an *E. coli* cell lysate

Since no antibody against GCP1 was available at the beginning of this work, the first hint about the subcellular localization of GCP1 was obtained from overexpressed protein. *E. coli* cells from the overexpression experiment were mechanically disrupted applying french press treatment followed by fractionation of the obtained extract via differential centrifugation. The fractionation distinguished between insoluble constituents, large cell fragments, membrane fraction and soluble components (Chapter 2.12, Page 39). Resulting fractions were analyzed by SDS-PAGE for a band corresponding to the predicted molecular mass of GCP1. The majority of the protein, about 95 %, appeared as insoluble fraction (inclusion bodies) and in the pellet containing cellular debris. The soluble protein fraction contained no visible GCP1 band. A small part of the GCP1, about 5 %, cosedimented with the membrane fraction from the cell-lysate (data not shown). This suggests that GCP1 might be a membrane protein as predicted. Considering the thick GCP1 bands appearing on the gels from GCP1 overexpression (Figure 7, Page 46), We conclude that these inclusion bodies almost exclusively contain GCP1.

3.1.3 Purification of GCP1 from inclusion bodies

As the vast majority of the overexpressed protein was present as inclusion bodies, pelleted inclusion bodies were resuspended in IB-buffer (containing 6 M guanidinium hydrochloride) and subjected to purification in denatured form. Diverse approaches for purifying GCP1 from inclusion bodies failed (Chapter 2.10.2, Page 37 data not shown). Nevertheless, SDS-PAGE analysis from these approaches confirmed the assumption that the inclusion bodies prepared as described above (Chapter 3.1.2, Page 47) yielded almost exclusively GCP1. Therefore the formation of inclusion bodies was used as alternative method for purification. Inclusion bodies were separated from soluble constituents and cellular debris by means of centrifugation (Chapter 3.1.2) and dissolved in IB-buffer. For further experiments such inclusion bodies enriched in GCP1 were used.

3.1.4 Refolded GCP1 from inclusion bodies remains soluble in distinct buffers

Attempts to refold insoluble GCP1 from inclusion bodies into its native conformation were undertaken. For this reason solubilized protein in IB-buffer (contains guanidinium hydrochloride) was rapidly diluted with different buffers lacking the chaotropic agent guanidinium hydrochloride in a 1:20 protein to buffer ratio. All buffers contained 0,05 % dodecylmaltoside, but varied in respect to the concentration of NaCl and pH. Protein remaining soluble after rapid dilution was considered as refolded. For identifying the most efficient buffer for refolding, solutions of diluted protein were centrifuged and afterwards protein was precipitated (Page 38). The precipitate was solubilized in SDS-sample buffer and analyzed by SDS-PAGE (Figure 8, Page 48). The gel revealed that GCP1 remained soluble only in buffers containing 500 mM NaCl. Furthermore, a pH-dependent effect can be observed. Namely, refolding occurred more efficiently at pH 7,5 than at pH 8,3.

Figure 8: A SDS-PAGE from refolding experiments

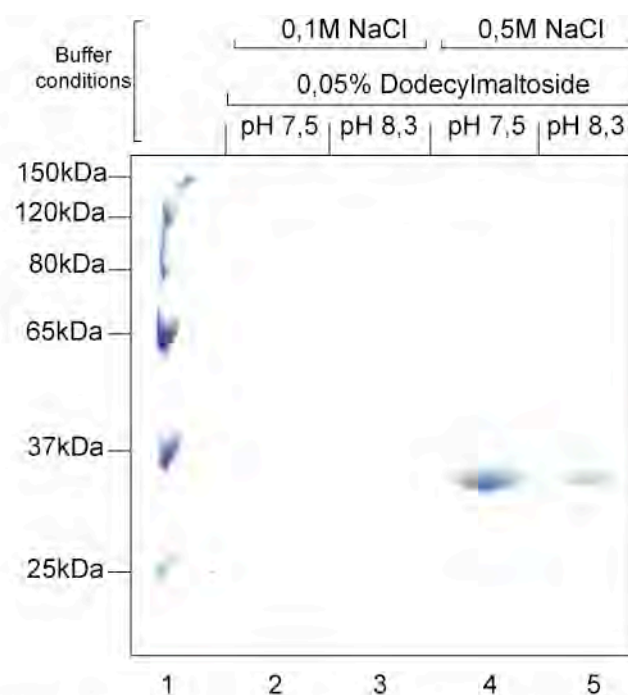


Figure 8: A SDS-PAGE from experiments for refolding GCP1 from inclusion bodies to a soluble fold (Chapter 1.4.). The gel compares different buffers used for refolding. Buffer conditions vary in respect of NaCl concentration and pH (as labeled). All buffers contained 0,05% dodecylmaltoside. Lane 1 contains the protein standard (as labeled in kDa). Lanes 2-5 represent the protein that stayed soluble after 500 μ l of inclusion bodies solubilized in guanidinium hydrochloride were rapidly diluted with the different buffers.

3.2 Characterization of the $\Delta gcp1$ mutant

For identifying the physiological role of GCP1, a deletion mutant in *gcp1* was constructed. Observing the phenotype of such deletion mutants may hint towards the function of the gene-product.

3.2.1 GCP1 is essential for growth of *E. coli* on LB medium

For investigating the $\Delta gcp1$ mutant phenotype, *gcp1* was replaced by a kanamycin resistance cassette (*neo*) via double homologous recombination by means of the Wanner technique in the strain DY330 ($\Delta lacU169 gal490 (\lambda c1 857 \Delta(cro-broA))$). This strain features an increased rate of genetic recombination events that is temperature dependently inducible. The recombination yielded in the strain CW1 (DY330, $\Delta gcp1::neo$ (kan^R)) and was proven by a control PCR shown in Figure 9, Page 50. For this PCR the primer pair KanF / rpsU_rev was used. These primers anneal within the kanamycin resistance cassette (KanF) and within the ORF downstream of the *gcp1* ORF (rpsU_rev). A colony PCR using this primer pair will only deliver a DNA fragment of a distinct length if the kanamycin cassette is inserted correctly into the chromosome, thereby replacing the *gcp1* ORF. For the recombination event that deletes the *gcp1* ORF, the expected DNA fragment size of 750 bp was obtained, thus verifying the deletion of *gcp1*. After the recombination event that led to *gcp1* deletion, it took 2 days of incubation at 20°C for tiny colonies to appear on LB (kan 25) plates (data not shown). These colonies ceased growth and could not be restreaked. Thus, we concluded that *gcp1* is essential for growth of *E. coli* on LB-medium.

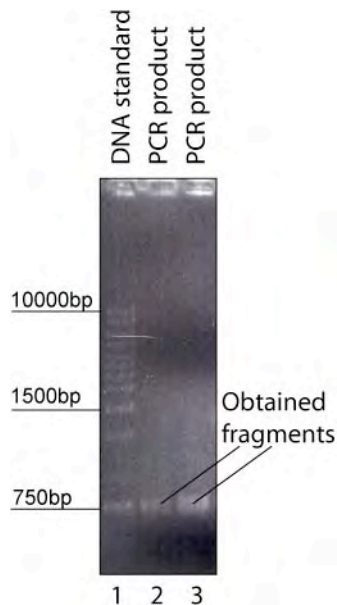
Figure 9: The test PCR confirms correct insertion of the kanamycin cassette

Figure 9 shows an agarose gel with the PCR-product of the PCR that verified the correct insertion of the kanamycin resistance cassette into the *gcp1* locus on the chromosome. Lane 1 contains the DNA standard, lanes 2 and 3 the yielded DNA fragments of the PCR reaction. The expected size of PCR products for correct insertion was 750bp. In lanes 2 and 3 a fragment of 750 bp is clearly visible. The primer pair 5'KanR / 3'rpsU_rev was used for amplification and colonies of CW1 ($\Delta gcp1::neo$ (kan^R)) were used as template.

3.2.2 A conditionally lethal mutant in *gcp1* was constructed using an arabinose-inducible plasmid system

Since the $\Delta gcp1$ mutation is lethal (Chapter 3.2.1, Page 49), further analysis of molecular effects on the bacterial cell that are caused by the depletion of GCP1 demands the construction of a conditionally lethal mutant in *gcp1*. In such a mutant, *gcp1* is deleted from the chromosome and the deletion is complemented by a version of *gcp1* that is exclusively expressed under the control of a specific induction system. Shutting off the expression in a conditional *gcp1* mutant thereby allows inducing the depletion of GCP1. The expression system must not exhibit any basal-expression of *gcp1* in order to achieve complete GCP1-depletion. For the construct complementing the $\Delta gcp1$ genotype, an induction system featuring linear induction was approached. First, the plasmid carrying an inducible version of *gcp1* was transformed in the strain DY330 ($\Delta lacU169 gal490 (\lambda c1 857 \Delta(cro-broA))$). Subsequently *gcp1* was deleted from

the chromosome as described above. All plasmids expressing *gcp1* under the control of such systems complemented for the $\Delta gcp1$ mutation, but when *gcp1* expression from the plasmid was not induced, cells did not cease growth. Thus, we concluded that already a low expression level of *gcp1* is sufficient for growth. Since the previous result suggested that already minor expression levels of *gcp1* result in a viable phenotype, an AraC controlled expression system (Dhiman and Schleif 2000; Johnson and Schleif 2000) was chosen for controlling *gcp1* expression from a complementing plasmid. AraC activates the P_{BAD} -promoter when arabinose is bound to the protein. Without arabinose bound, AraC inhibits this promoter, thereby ensuring tight repression of genes expressed under its control. The *gcp1* ORF was cloned in pBAD33 (expresses *araC* and contains a MCS under control of the P_{BAD} -promoter) resulting in the plasmid pCW06 (pBAD33, *araC*⁺, P_{BAD} -*gcp1*). On this plasmid, expression of *gcp1* exclusively occurs under the control of the P_{BAD} -promoter (AraC-arabinose inducible). The plasmid pCW06 was transformed in DY330 ($\Delta lacU169$ *gal490* (λ *c1* 857 $\Delta(cro-broA)$)) and *gcp1* was deleted from the chromosome as described before (Chapter 3.2.1). The resulting strain is CW1 (DY330- $\Delta gcp1::neo$) harboring pCW06. In order to be able to transduce the $\Delta gcp1::neo$ genotype into other strains, a P1 lysate was prepared using the strain CW1 as donor. Subsequently, a conditionally lethal *gcp1* mutant was constructed in the strain MC1061 ($\Delta araABC-leu$), a strain accumulating arabinose with high affinity but not utilizing it: MC1061 was transformed with pCW06. Chromosomal *gcp1* was deleted via P1-transduction under inducing conditions for plasmid-encoded *gcp1* (0,2 % w/v arabinose) using the P1 lysate prepared from CW1. The resulting strain from this transduction is CWCM1 (MC1061, $\Delta gcp1::neo$) harboring plasmid pCW06 (pBAD33, *araC*⁺, P_{BAD} -*gcp1*). This strain grows regularly on LB-agar plates supplemented with 0,2 % arabinose, but reveals no growth on agar plates containing only LB medium. The hereby constructed mutant allows abolishing *gcp1* expression, thereby depleting GCP1. Immunoblot analysis of a conditionally lethal *gcp1* mutant derived from CWCM1 (MC1061, $\Delta gcp1::neo$) harboring pCW06 (pBAD33, *araC*⁺, P_{BAD} -*gcp1*) using α -GCP1 antibodies confirmed GCP1-depletion when arabinose is removed from the culture medium (Figure 19, Page 76).

3.3 Characterization of the conditionally lethal *gcp1* mutant

3.3.1 The conditionally lethal mutant reverts with high frequency

When depleted in arabinose, the conditionally lethal mutant CWCM1 (MC1061, $\Delta gcp1::neo$) harboring pCW06 (pBAD33, *araC*⁺, P_{BAD-gcp1}) revealed the same phenotype as the $\Delta gcp1$ strain CW1 (DY330, $\Delta gcp1::neo$). Small colonies of a diameter of < 0,3 mm were formed when CWCM1 harboring pCW06 was streaked on LB-agar plates and incubated at 37°C for 24 hours. Interestingly some colonies did not cease growth, but reverted to a synthetic WT that formed regular colonies without induction of *gcp1* expression. Such revertants could be restreaked and reveal arabinose independent growth. When CW1 (DY330, $\Delta gcp1::neo$ (kan^R)) was plated on LB-agar plates after *gcp1* deletion, no such colonies appeared. A second conditionally lethal *gcp1* mutant was tested for the occurrence of revertants that can grow without induction of the AraC-system. In this mutant the kanamycin resistance cassette that served as selectable marker for the *gcp1* deletion (Chapter 3.2.1, Page 49), was looped out of the chromosome by the use of pCP20 (encoding the Flp-recombinase) as described by Wanner et al. (Datsenko and Wanner 2000). The resulting strain is CWCM2 (MC1061 ($\Delta gcp1$)) harboring pCW06 (pBAD33, *araC*⁺, P_{BAD-gcp1}). CWCM2 harboring pCW06 develops the same revertants as described for CWCM1 (MC1061, $\Delta gcp1::neo$) harboring pCW06 (pBAD33, *araC*⁺, P_{BAD-gcp1}). For a more accurate determination of the reversion frequency, 10⁶ cells were plated on LB-agar plates lacking arabinose. Occurring revertants were counted. An average rate of 2 suppressor mutants • 10⁵ cells was determined. Since this value is unusually high, it was tested whether a mutation on the plasmid pCW06, or a mutation on the chromosome of CWCM2 harboring pCW06 is responsible for the observed reversion. For this purpose CWCM2 harboring pCW06 was reconstructed as described in Chapter 3.2.2 Page 50, yet using the plasmid pCW06 prepared from the revertants described above. If the mutation responsible for reversion occurred on the plasmid pCW06, resulting clones should grow in an arabinose independent manner. If the mutation leading to reversion occurred on the chromosome, clones should grow arabinose dependently. CWCM2 harboring pCW06 was plated on LB-agar plates lacking arabinose. From revertants appearing on these plates, eight independent suppressor mutants were randomly chosen and cultured for preparing pCW06 plasmid from each suppressor mutant. Individual plasmid from each of the eight revertants was separately transformed in MC1061. Subsequently chromosomal *gcp1* was deleted by transducing the kanamycin resistance cassette ($\Delta gcp1::neo$) from CWCM1 via P1 transduction into the *gcp1* locus of MC1061. Theoretically the resulting clones from each

transduction are genetically identical with CWCM1 (MC1061 $\Delta gcp1::neo$) harboring pCW06 and will only grow in dependence of arabinose presence. However, only one out of the eight transductants tested was detained in growth when arabinose was absent. This result demonstrates that only one out of these eight mutations leading to reversion occurred on the chromosome, while the other seven occurred on the plasmid pCW06 (pBAD33, *araC*⁺, *P_{BAD}-gcp1*).

3.3.2 The reversion frequency of the conditionally lethal mutant can be reduced

It became apparent that most mutations that led to arabinose-independent growth of the conditionally lethal *gcp1* mutant CWCM2 (MC1061 $\Delta gcp1$) harboring pCW06 (pBAD33, *araC*⁺, *P_{BAD}-gcp1*) occurred on the plasmid pCW06 (Chapter 3.3.1, Page 52). For testing the assumption that a mutation in *araC* resulted in an AraC protein that constitutively activated the *P_{BAD}*-promoter without regard to arabinose bound (Reed et al. 2002), an AraC overexpression plasmid (pWR03) was transformed in the conditionally lethal strain CWCM2. Thereby a sufficient amount of AraC was to be provided to the cell, ensuring the *P_{BAD}*-promoter to be tightly shut down, allowing no more expression without the inducer arabinose. Comparison of the reversion frequency of CWCM2 harboring only pCW06 with the reversion frequency of CWCM2 harboring both plasmids pCW06 and pWR03 revealed, that the number of revertants emerging on plates lacking arabinose was significantly decreased (Figure 10, Page 55) when an *araC*-overexpressing plasmid is present in the cell. This indicates that suppressor mutations most likely occurred in *araC*, resulting in an AraC protein constitutively activating the *P_{BAD}*-promoter (Reed and Schleif 1999) (Dirla, Chien et al. 2009). The occurrence of revertants after prolonged incubation under GCP1-depleting conditions was also tested. CWCM2 harboring pCW06 and CWCM2 harboring pCW06 + pWR03 were again streaked on plates with and without arabinose as described above. In order to allow revertants to appear, the plates were incubated for 3 days at 37°C. CWCM2 harboring the two plasmids pCW06 and pWR03 reverted with a significantly lower rate than CWCM2 harboring only pCW06. CWCM2 harboring only pCW06 developed many suppressor mutants as observed before (Chapter 3.3.1. Page 52). However, the diameter of a few revertant colonies exceeded the size of most other revertant colonies by several fold (arrows in Figure 10B Page 55). Most presumably cells that formed these colonies were already reverted when the strain was streaked on the plate, while cells that reverted “on plate” formed the smaller colonies. Thus, we conclude that cells depleted in GCP1 are not dead, but can revert after prolonged incubation time on agar plates.

3.3.3 Lack of the inducer arabinose leads to a growth deficit of the conditionally lethal *gcp1* mutant

Growth of the conditionally lethal mutant strain CWCM4 (MG1655 $\Delta gcp1::neo$) harboring pCW06 (pBAD33, *araC*⁺, $P_{BAD-gcp1}$) was ceased or induced by the lack or presence of arabinose and compared to its parental strain MG1655 (WT *E. coli*). These strains transport and metabolize arabinose. A growth curve of both strains grown in LB medium supplemented with 0,2 % arabinose was measured. In order to investigate the effects of GCP1-depletion on growth, the cultures were washed with LB medium at $OD_{578nm} \approx 0,1$ and cultivated further in LB medium without arabinose. In LB medium solely, as well as in LB medium supplemented with 0,2 % arabinose CWCM4 harboring pCW06 revealed almost identical growth rates for the first three hours after washing out the arabinose (arrows in figure 11). The MG1655 (WT *E. coli*) culture generally exhibited a higher growth rate than the strain CWCM4 harboring pCW06 in LB medium with and without arabinose. This finding demonstrates that the non-physiological expression level of *gcp1* from the plasmid pCW06 also impairs the growth of the CWCM4 cells harboring pCW06 culture.

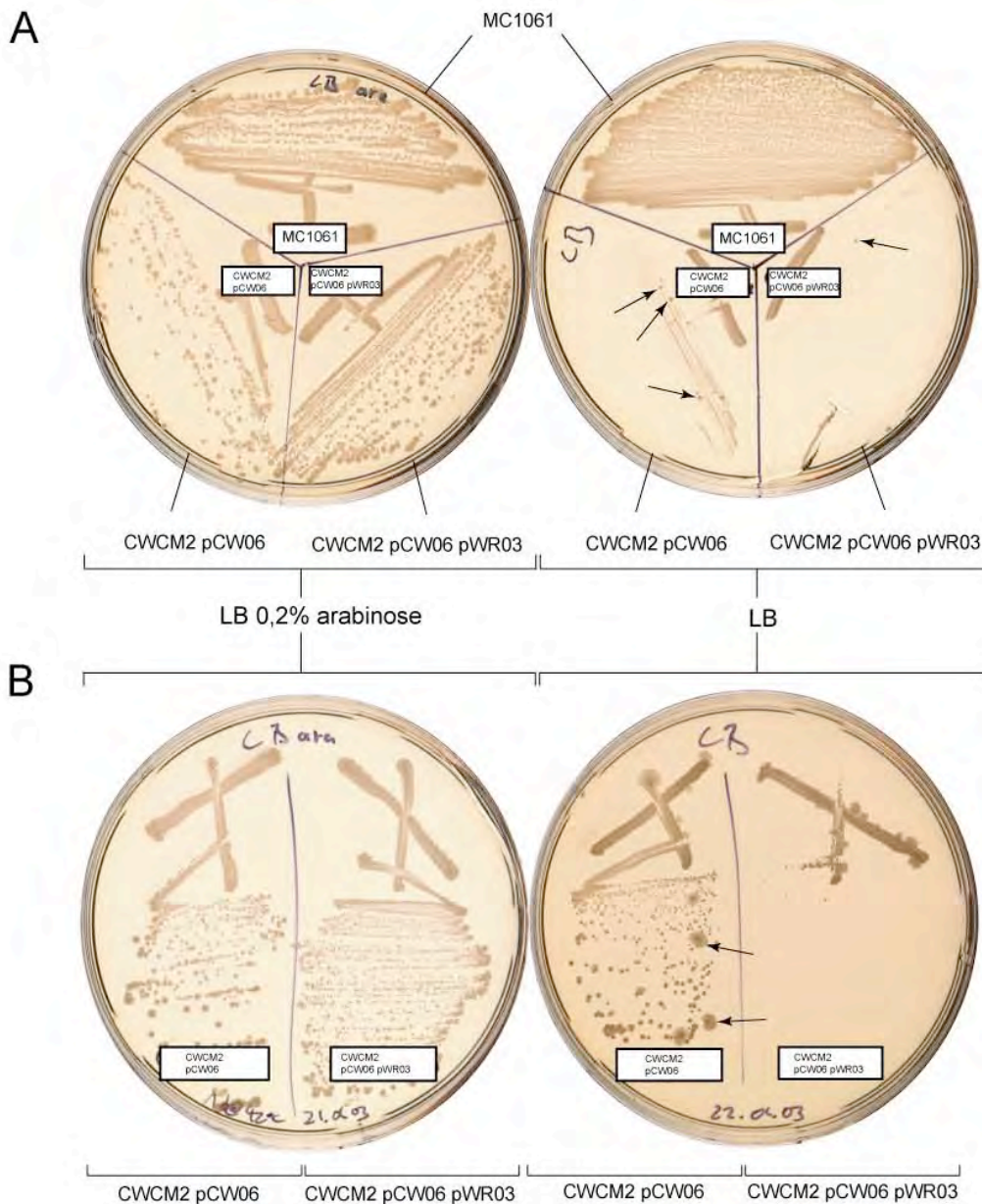
Figure 10: Suppressor mutants appear with a high frequency in the conditionally lethal mutant

Figure 10 compares the growth of different conditional *gcp* mutants on LB-agar plates with the growth of these mutants on LB-agar plates supplemented with 0.2% arabinose. In **A** CWCM2 (MC1061 Δgcp) harboring plasmid pCW06 (pBAD33, *araC*, $P_{BAD-gcp}$) and CWCM2 harboring plasmids pCW06 and pWR03 (*araC*⁺) are compared in their capability of growth with and without the inducer of *gcp* expression arabinose. The genetic background of this strain, MC1061 ($\Delta araABC-leu$) is also streaked on the plates. The plate on the left contains LB supplemented with 0.2% w/v arabinose while the plate on the right contains solely LB medium. Both plates were incubated 24 hours at 37°C. Both conditional *gcp* mutants reveal a clear arabinose dependent growth. CWCM2 (MC1061 Δgcp) harboring plasmids pCW06 (pBAD33, *araC*, $P_{BAD-gcp}$) and pWR03 (*araC*⁺) forms significantly less revertants than CWCM2 (MC1061 Δgcp) harboring plasmid pCW06 (pBAD33, *araC*, $P_{BAD-gcp}$). Revertants growing independently of arabinose are marked with an arrow. As expected, MC1061 grows independently of arabinose presence. **B**: The same conditional mutants as shown in Figure 4A are compared: CWCM2 (MC1061 Δgcp) harboring plasmid pCW06 (pBAD33, *araC*, $P_{BAD-gcp}$) and CWCM2 harboring plasmids pCW06 and pWR03 (*araC*⁺). The plate on the left contains LB 0.2% arabinose, while the plate on the right contains solely LB medium. Here both plates were incubated for 3 days at 37°C. CWCM2 carrying the two plasmids pCW06 and pWR03 reverts with a significantly lower rate as CWCM2 harboring only pCW06. Arrows mark larger revertant colonies that most presumably emerged from cells that were already reverted when the strain was streaked on the plate.

Figure 11: CWCM4 mutant strain cultured under GCP1-depleting and non-depleting conditions

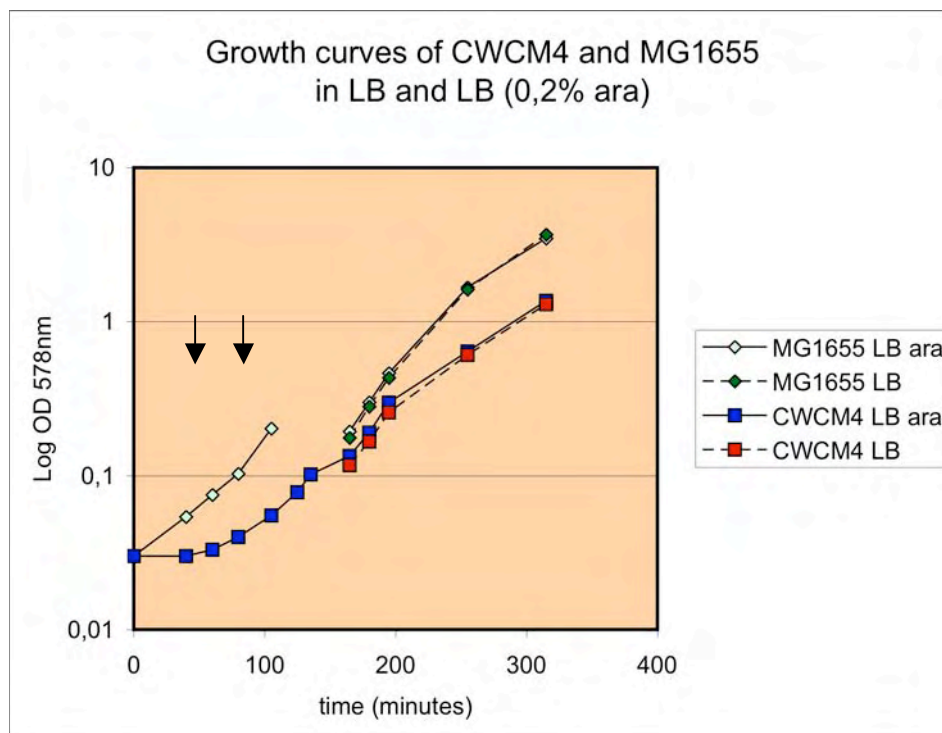


Figure 11 shows a growth curve describing the growth of cultures of MG1655 (*E. coli* WT) and CWCM4 (MG1655 $\Delta gcp1::neo$ harboring pCW06 (pBAD33, *araC*, $P_{BAD-gcp1}$)) in LB medium containing 0,2% arabinose. At $OD_{578nm} \approx 0,1$ cultures were each washed twice with LB medium and subsequently split into two independent subcultures (one containing 0,2% arabinose, the other lacking arabinose). The wash is marked with arrows.

As shown in Figure 11 the conditionally lethal mutant CWCM4 harboring pCW06 exhibits no growth deficit for the first 3 hours being cultivated in LB medium lacking the inducer arabinose. After preparing a subculture inoculated with cells from the cultures shown in the growth curve above (cells from $T = 320$ minutes), a considerable growth deficit became apparent in the arabinose free medium for the conditionally lethal mutant CWCM4 harboring pCW06. The resulting growth curve for this strain is shown in Figure 12, Page 57 (data only shown for the conditionally lethal mutant CWCM4 (MG1655 $\Delta gcp1::neo$) harboring pCW06 (pBAD33, $araC^+$, $P_{BAD-gcp1}$)).

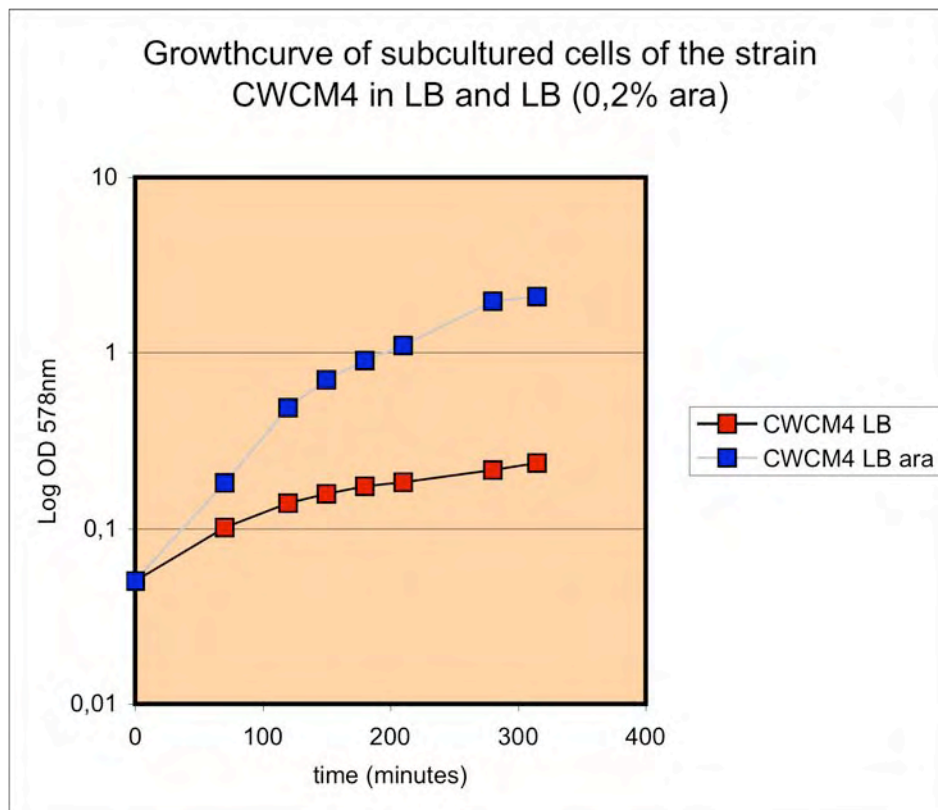
Figure 12: CWCM4 mutant strain subcultured from GCP1-depleted and non-depleted cultures

Figure 12: Since the growth curve in Figure 5 revealed no growth deficit of cells cultivated in LB medium lacking arabinose, a second growth curve was measured. Inoculum for this curve were cells from the previously shown growth curve at time = 320 minutes (Figure 11)

When no arabinose was present in the medium, the subcultured mutant CWCM4 harboring pCW06 ceased growth after about 120 minutes ($OD_{578nm} = 0,14$) and reached a final $OD_{578nm} = 0,23$. In contrast, the CWCM4 culture supplemented with 0,2 % arabinose revealed a clearly higher growth rate. These cells reached an $OD_{578nm} = 0,49$ after 120 minutes (when the culture lacking arabinose was impaired in growth) and a final $OD_{578nm} = 2,09$ after 315 minutes, a final value 9-fold higher than the one from the culture grown in LB only. However, the arabinose induced expression of *gcp1* did not enable the culture to grow as far as the WT. MG1655 cultures reached a final $OD_{578nm} = 5$ in this experiment and clearly exhibited a higher growth rate (as observed before in Figure 11). Thus, we conclude that the elevated non-physiological expression of *gcp1* in CWCM4 harboring pCW06 reduces the growth rate of the culture. In addition, comparing the growth of cultures that already reached a relatively high cell density before *gcp1* expression was depleted with the growth of a culture where *gcp1* expression was already depleted at low cell density (Figure 19, Page 76, Chapter 3.6.1, Page 75) demonstrates

that the duration of the period between depletion of *gcp1* expression and development of the $\Delta gcp1$ phenotype of CWCM4 harboring pCW06 is depending on the number of generations. Thus, we conclude that the amount of GCP1 already synthesized at the start of GCP1-depletion is high in the cell and has to be diluted by several cell divisions until cessation of growth is caused by GCP1-depletion. Because of the obvious delay between depletion of *gcp1* expression and GCP1-depletion below the level required for growth, in further experiments depletion was exclusively carried out at low cell density of investigated cultures.

3.3.4 2D-PAGE gel analysis of protein patterns from WT *E. coli* and the conditionally lethal *gcp1* mutant strain CWCM4

The conditionally lethal *gcp1* mutant CWCM4 (MG1655 $\Delta gcp1::neo$) harboring pCW06 (pBAD33, *araC*⁺, *P*_{BAD}-*gcp1*) was cultured in LB (0,2 % ara) to a low OD_{578nm}, washed with LB medium and the culture split into GCP1 induced (+ arabinose) and non-induced (- arabinose) subcultures. Both subcultures were compared in regard to differences in the proteome. In order to enhance GCP1-depletion 0,2 % glucose was added to the medium of the GCP1-depleted subculture, thereby making use of inducer exclusion and catabolite repression. Samples were prepared when the growth deficit became apparent in the growth curve. Total cell protein of each culture was mapped by means of 2D-PAGE applying the NEPHGE method (Chapter 2.8.2, Page 33) followed by coomassie staining of the gels. For comparison, the strain MG1655 (WT *E. coli*) was cultivated in parallel under identical conditions concerning medium, culture flasks, temperature, rotation and cell density of the inoculum. Samples from this culture were taken simultaneously with the occurrence of growth cessation in the GCP1-depleted culture of CWCM4 (MG1655 $\Delta gcp1::neo$) harboring pCW06 (pBAD33, *araC*⁺, *P*_{BAD}-*gcp1*). In order to load equal amounts of protein onto the gels, cells from each culture were pelleted in a 1.5ml reaction tube until the pellet equaled the volume of 50 μ l. Cells were then disrupted by the freeze-thaw method and subsequently subjected to preparation according to the protocol for 2D-PAGE. The first dimension isoelectric focusing was performed using ampholytes in the range between pH 3 and pH 10. Second dimension separation of proteins was carried out on 12 % gels by SDS-PAGE.

3.3.5 2D-PAGE gels of the conditionally lethal *gcp1* mutant CWCM4 show consistent and significant differences in protein patterns in comparison to the WT strain

All gels resulting from both strains CWCM4 (MG1655 $\Delta gcp1::neo$) harboring pCW06 (pBAD33, *araC*⁺, *P*_{BAD}-*gcp1*) and MG1655 (WT *E. coli*) grown under GCP1-depleting (- arabinose) and non-depleting (+ arabinose) conditions show an overall consistent protein pattern, thus confirming the comparability of the gels. Yet, a closer inspection of the gels revealed quite a number of distinct differences. The protein patterns of the strain CWCM4 harboring pCW06 cultured under *gcp1*-depleting and non-depleting conditions exhibited several differences in protein signals that occurred in response to GCP1-depletion. However, the presence of glucose or arabinose will also result in induction or repression of arabinose and glucose specific proteins. Therefore, in order to exclude these proteins from the effects of GCP1-depletion, 2D-gels from the WT strain MG1655 were analyzed for protein signals that are specifically caused by the presence of glucose or arabinose respectively in the culture medium.

3.3.5.1 The presence of arabinose or glucose is responsible for differential protein patterns on 2D-gels prepared from total cell protein of *E. coli* WT cells

In order to determine differential protein abundance caused by effects of either glucose or arabinose in the culture medium, the strain MG1655 (*E. coli* WT) was cultivated in LB medium containing either 0,2 % arabinose or 0,2 % glucose. 2D-gels of these cultures were prepared (as described in Chapter 3.3.4) and the protein patterns on the gels were compared (Figure 13, Page 60). Ten proteins are induced when glucose is present in the medium and other two are missing. For the culture grown in the presence of arabinose, the complementary result is obtained: The two proteins missing in response to glucose are induced by arabinose (red circle in Figure 13) while the other ten are missing or reduced in strength (black circle in Figure 13). Proteins induced by glucose are most likely involved in glucose metabolism as for example components of the phosphotransferase system (PTS) or are at least affected by glucose metabolism. Such arabinose or glucose specific proteins that were identified for the WT strain MG1655 can be transferred to CWCM4 (MG1655 $\Delta gcp1::neo$) harboring pCW06 (pBAD33, *araC*⁺, *P*_{BAD}-*gcp1*), since this strain was constructed in the genetic background of MG1655. With this knowledge of specifically arabinose and glucose induced or repressed proteins, the conditionally lethal *gcp1* mutant could now be tested. However, if GCP1-depletion affects genes that are also influenced by arabinose or glucose, the respective proteins will not be depicted by this experiment.

Figure 13: 2D-gels of the MG1655 culture grown in LB medium containing arabinose or glucose stain consistently and reveal specific effect of the sugars on protein expression

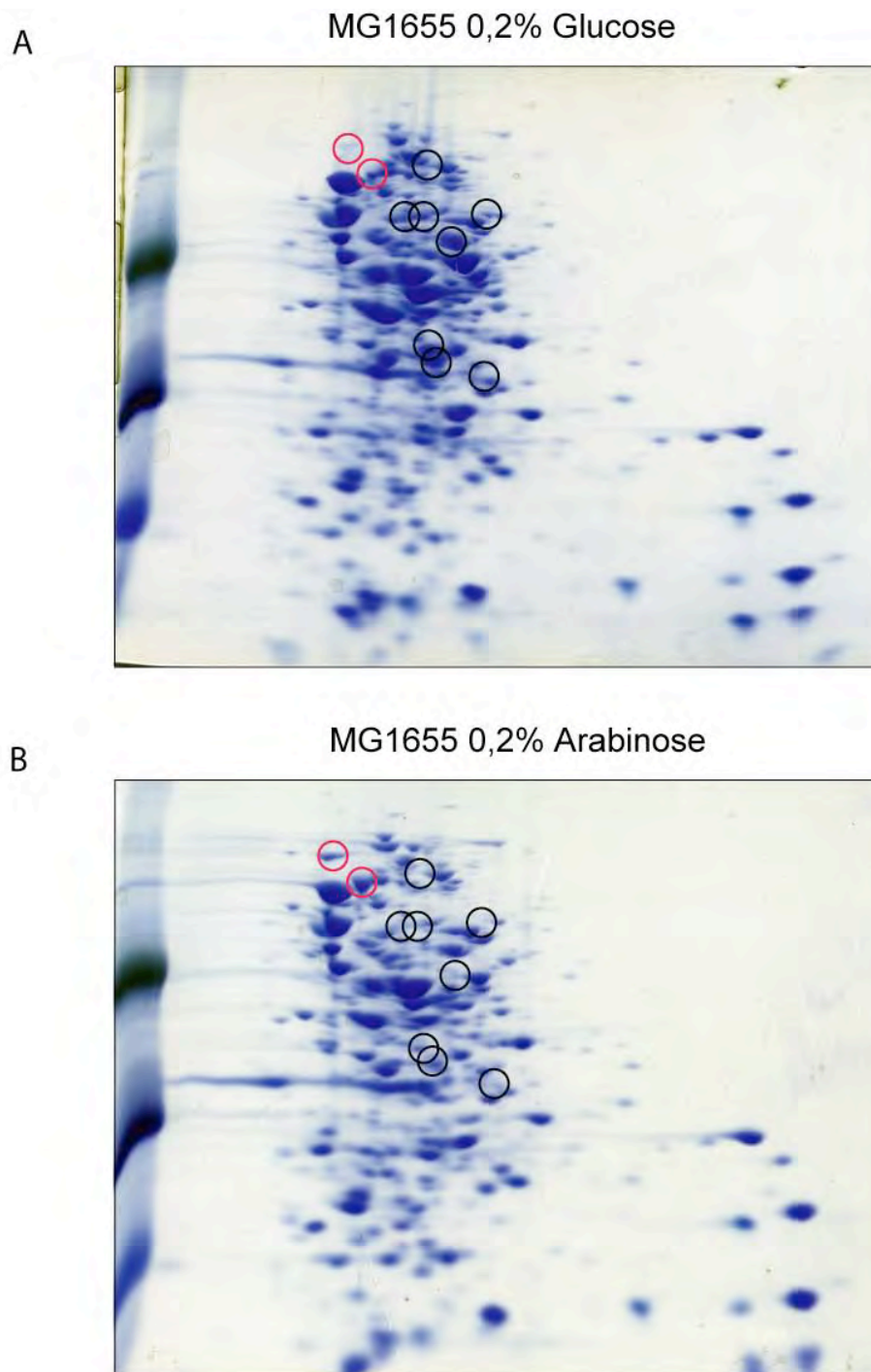


Figure 13 shows 2D-gels prepared from total cell protein of *E. coli* WT cells (MG1655) cultivated in LB medium supplemented with 0,2% arabinose (**B**) or 0,2% glucose (**A**) respectively. First dimension isoelectric focusing was performed using ampholytes in the range between pH 3 and pH 10. The marker covers the molecular weight from 20kDa to 60kDa as labeled. Other growth parameters of the cultures compared on these gels, besides the sugars arabinose or glucose in the medium, were identical for both cultures. Protein signals emerging due to glucose presence (A) are marked with a black circle, proteins fading in response to glucose are shown in a red circle. The complementary applies to these protein signals on the gel prepared from the culture supplemented with arabinose (B).

3.3.5.2 Comparison of CWCM4 cultures depleted and non-depleted in GCP1 reveals several proteins affected by GCP1-depletion

After having identified the protein signals that are specifically correlated to the presence of arabinose or glucose in the medium (Chapter 3.3.5.1, Page 59), proteins specifically induced or repressed by the depletion of GCP1 could be determined by comparing these gels (Figure 14, Page 62). Altogether ten proteins differently expressed under both conditions were chosen and subjected to mass spectrometry. Great care was taken not to contaminate excised protein spots with other proteins. These protein signals are marked with numbered arrows in Figure 14 and the identified proteins are listed in Table 1. The expression of four of these proteins was repressed under GCP1 depleting conditions (Figure 14A), while 6 were induced (Figure 14B). Despite the cessation in growth, the rise of protein signals after GCP1-depletion indicated that the cells obviously still perform protein biosynthesis. One has to mention here, that 2D-gels prepared from cultures of the strain CWCM4 harboring pCW06 obviously contain less protein than such gels prepared from cultures of the strain MG1655. Since intensive care was taken to load equal amounts of cells on the gels (Chapter 3.3.4, Page 58), this is most presumably an effect caused by GCP1-depletion.

Figure 14: 2D-gels from CWCM4 mutant cultures grown under GCP1-depleting and non-depleting conditions reveal differences in the protein pattern

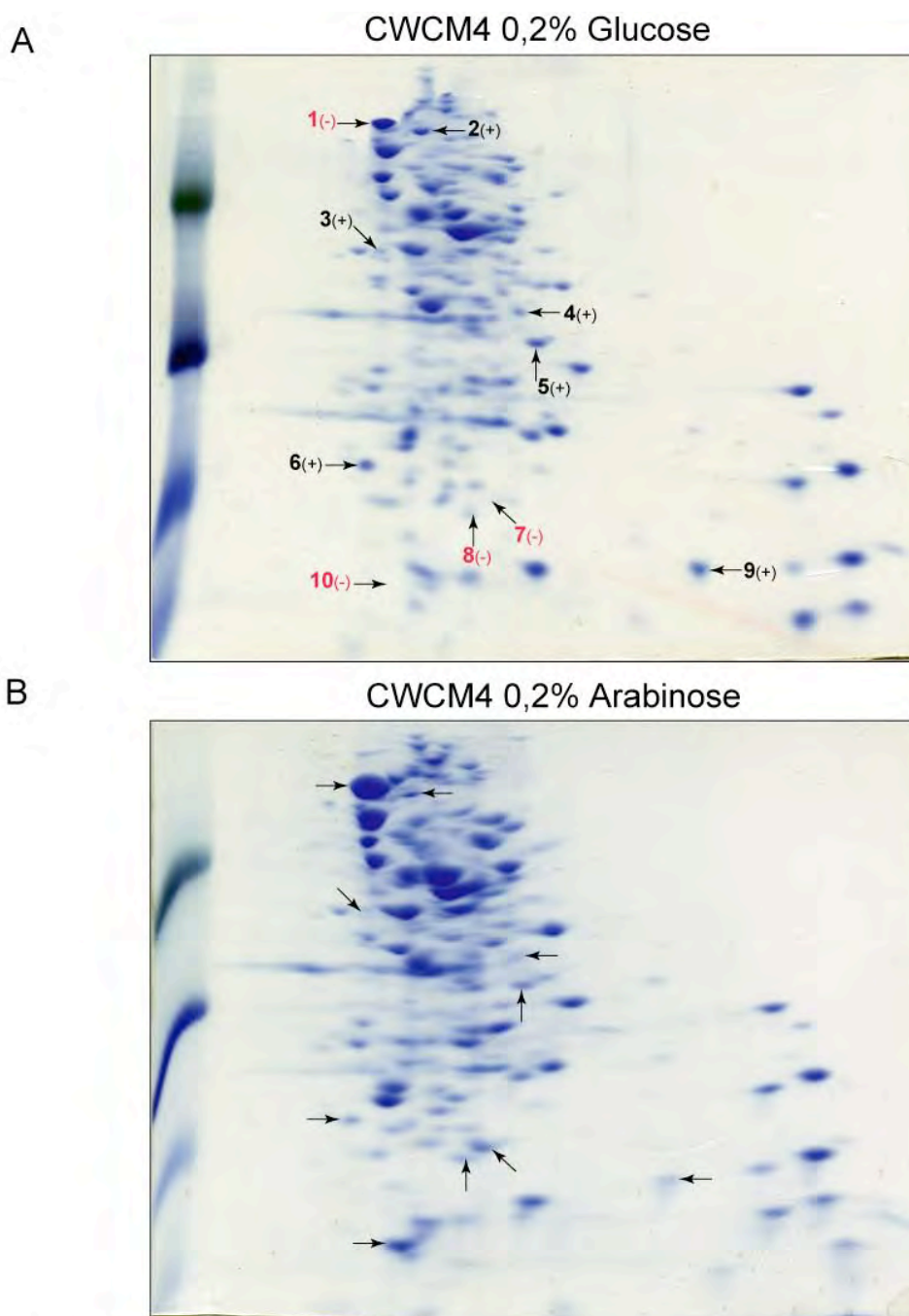


Figure 14 shows 2D-gels prepared from total cell protein of the conditionally lethal *gcp1* mutant strain CWCM4 (MG1655 $\Delta gcp1::neo$ harboring pCW06 (pBAD33, *araC*, P_{BAD} -*gcp1*)) grown under GCP1-depleting (**A**) and non-depleting (**B**) conditions respectively. The protein standard marks regions of 20, 50 and 60 kDa as labeled. Since effects of glucose or arabinose on differential protein patterns of the genetic background (MG1655) of the strain CWCM4 were previously determined (Figure 7), any differences in protein signal between the gels shown here, that are not observed in Figure 7, must be caused by GCP1 depletion. Ten such proteins emerging on one of the gels and disappearing on the other (depleted and non-depleted) were identified. Each spot responding to GCP1-depletion is marked with an arrow and has a number assigned. For a better overview, numbers were only noted on the gel resulting from the glucose supplemented (GCP1 depleted) culture. Red numbers correspond to proteins disappearing when GCP1 is depleted, black numbers correspond to proteins emerging in response to GCP1 depletion.

3.3.6 Proteins affected by GCP1-depletion are related to protein biosynthesis and cell division

The protein spots corresponding to GCP1-depletion were excised from the gels and subjected to a tryptic digest. Intensive care was taken not to contaminate excised protein spots with foreign protein. Mass spectrometry identified the proteins of interest. For means of assigning these fragments to a specific protein sequence, “MASCOT search” (<http://www.matrixscience.com>) was deployed. Since some of the peptide fragments resulting from the tryptic digest can match more than one protein sequence, more than one hit for protein identification can be obtained by MASCOT search. Proteins that were identified in this experiment were only considered as relevant if several peptides covered the sequence of the identified protein. Furthermore *E. coli* can synthesize over 4000 proteins of which only the most abundant are visible on the 2D-gels. Therefore, it is expected that one protein spot might contain different proteins migrating to the same position in the gel. Since mass spectrometry is an extremely sensitive method for the identification of proteins but provides no information about the quantities of proteins in a sample, contaminations of other proteins will yield a misleading result. For this reason, the molecular weight of identified proteins was compared with the protein standard on each gel. Identified proteins whose molecular mass clearly contradicted the corresponding mass of the excised protein spot were considered as not relevant. Among the proteins that were up- or down regulated by GCP1-depletion were ribosomal subunits, t-RNA synthetases and enzymes involved in amino acid synthesis. Table 1 lists the identified proteins including the response to GCP1-depletion, the function of the protein, the responsible gene, and the molecular weight. Numbers in the table correspond to the number that was assigned to each protein in Figure 14, Chapter 3.3.5.2.

Table 1: Protein-identifications from the 2D-gels

Number in Figure 14	Effect of GCP1-depletion	Identified Protein	Function	Gene	Molecular weight in kDa
1	-	DnaK	HSP-70-type molecular chaperone, stress-related heat-shock DNA biosynthesis	<i>dnaK</i>	69
2	+	Prolyl-tRNA synthetase	tRNA synthesis	<i>proS/drpA</i>	63
3	+	GalM	Sugar metabolism	<i>galM</i>	38
4	+	DapA	Diaminopimelate synthesis (cell wall)	<i>dapA</i>	31,1
		MraW	Methylates membrane proteins	<i>mraW</i>	53,3
5	+	Fkpa	Controls periplasmic folding	<i>fkpa</i>	28,7
			Peptidylprolyl cis,trans-Isomerase		
6	+	50S ribosomal protein L10	Protein biosynthesis	<i>rplJ</i>	17,56
7	-	Slp	outer membrane lipoprotein	<i>Slp</i>	20,8
8	-	Dps	Stress response DNA-binding protein + starvation	<i>pexB/dps</i>	18,5
9	+	Hpr	Phosphocarrier protein for glucose of the PTS	<i>crr</i>	18,1
10	-	UspA	Global regulatory gene for stress response	<i>uspA</i>	15,92

3.4 Characterization of *gcp1* expression in WT cells

The conditionally lethal *gcp1* mutant is a suitable tool for analyzing effects of GCP1-depletion on the bacterial cell. However, *gcp1* expression in such cells is constitutive and exclusively controlled by the arabinose-system (Chapter 3.2.2, Page 50). In order to explore physiological *gcp1* expression in the genetic WT background, the strain MG1655 (WT *E. coli*) was chosen for further investigation. Collecting samples of MG1655 cultures from different growth phases, various growth curves were prepared and the expression of *gcp1* was investigated by SDS-PAGE and immunoblotting using antibodies against GCP1.

3.4.1 GCP1 accumulates during the early logarithmic phase of *E. coli* growth

In order to determine growth phase dependent alterations in GCP1 levels, a growth curve was prepared from stationary phase inoculum (to $OD_{578nm} = 0,02$) (Figure 15, Page 67). Total cell protein was monitored by SDS-PAGE during growth of the culture up to the stationary phase (Figure 15B) and immunoblots using antibodies against GCP1, YeaZ and FtsZ were prepared (Figure 15C). YeaZ is a protein of unknown function that was reported to interact with GCP1 (Butland, Peregrin-Alvarez et al. 2005). FtsZ is a cytoskeletal protein that is essential for cell division in *E. coli* (Bramhill 1997). Later findings in this work demonstrate that GCP1 interacts with FtsZ (Chapter 3.6, Page 73). For each sample, whole cells from the MG1655 culture were disrupted by boiling in SDS-sample buffer and applied on the SDS-PAGE gel, taking care to apply identical amounts of protein. The amount of GCP1 was low in the freshly inoculated culture, its level increased 5-7-fold during early logarithmic growth and decreased thereafter reaching the plateau during the stationary phase. In contrast, amounts of YeaZ protein were high upon inoculation decreasing during logarithmic growth and rising again when stationary phase was reached. The level of FtsZ increased almost linearly until the late logarithmic phase and decreased again during the stationary phase (Figure 15C, Page 67). Thus, in WT *E. coli* cells *gcp1* is expressed in a growth phase dependent manner during early logarithmic growth.

3.4.2 GCP1 is distributed between soluble and membrane fractions

For localization studies WT *E. coli* cells (MG1655) from the stationary phase were mechanically disrupted by french press treatment and the extract was differentially centrifuged, resulting in total membrane and soluble fraction. SDS-PAGE of proteins from each fraction (Figure 15D) and immunoblots (Figure 15E, Page 67) with α -MalY (a soluble protein marker) and α -EIICBGlc component of the phosphotransferase (PTS) system (a membrane marker) confirmed the purity of the separation. The results revealed that GCP1 was distributed between the soluble and the membrane fraction with the slightly higher amount detected in the soluble fraction. A similar distribution was found for FtsZ (Figure 15E, Page 67).

3.4.3 GCP1 is recruited to the membrane during logarithmic growth

To test whether the membrane association of GCP1 changes during the bacterial growth, immunoblot analysis was performed using membrane fractions isolated from various time points of logarithmic and stationary phases (Figure 15F, Page 67). A 5-fold higher level of GCP1 was detected in the membrane fraction during logarithmic growth as compared to the stationary phase or early logarithmic growth.

3.4.4 GCP1 is not detectable in the periplasm, nor is it secreted to the medium

Since the homologue of GCP1 from the bovine pathogen *M. haemolytica* is reported as being secreted outside of the cell, a potential secretion of GCP1 into the periplasm or culture medium was tested. For preparing of cell sub fractions, the harvested MG1655 (*E. coli* WT) cells were pelleted and the collected supernatant representing growth medium with potential secreted proteins was collected. Pellets were subjected to cold osmotic shock after (Neu and Heppel 1965). Periplasmic and cytoplasmatic fractions were analyzed by SDS-PAGE and immunoblotting using antibodies against GCP1 and FtsZ. In order to demonstrate the purity of the preparations the following antibodies were used as markers for each compartment: α -TreA for the periplasm, α -MalY for the cytoplasm, α -PTS (EIICBGlu) for the inner membrane and α -OmpA for the outer membrane. As demonstrated in Figure 15, a clean preparation was achieved. A single prominent protein was present in the culture medium. This protein was identified by G. Krämer (Heidelberg) as “Antigen 43” (fluffing protein), which is an outer membrane protein that causes auto-aggregation of *E. coli* cells in stationary phase. No signal for GCP1 is detectable in

the periplasmic fraction or in the medium in contrast to the cytoplasmic fraction. This indicates that GCP1 is not secreted into the periplasm, neither out of the cell as suggested in the past (Abdullah, Lo et al. 1991).

Figure 15: Characterization of *gcp1* expression in WT cells

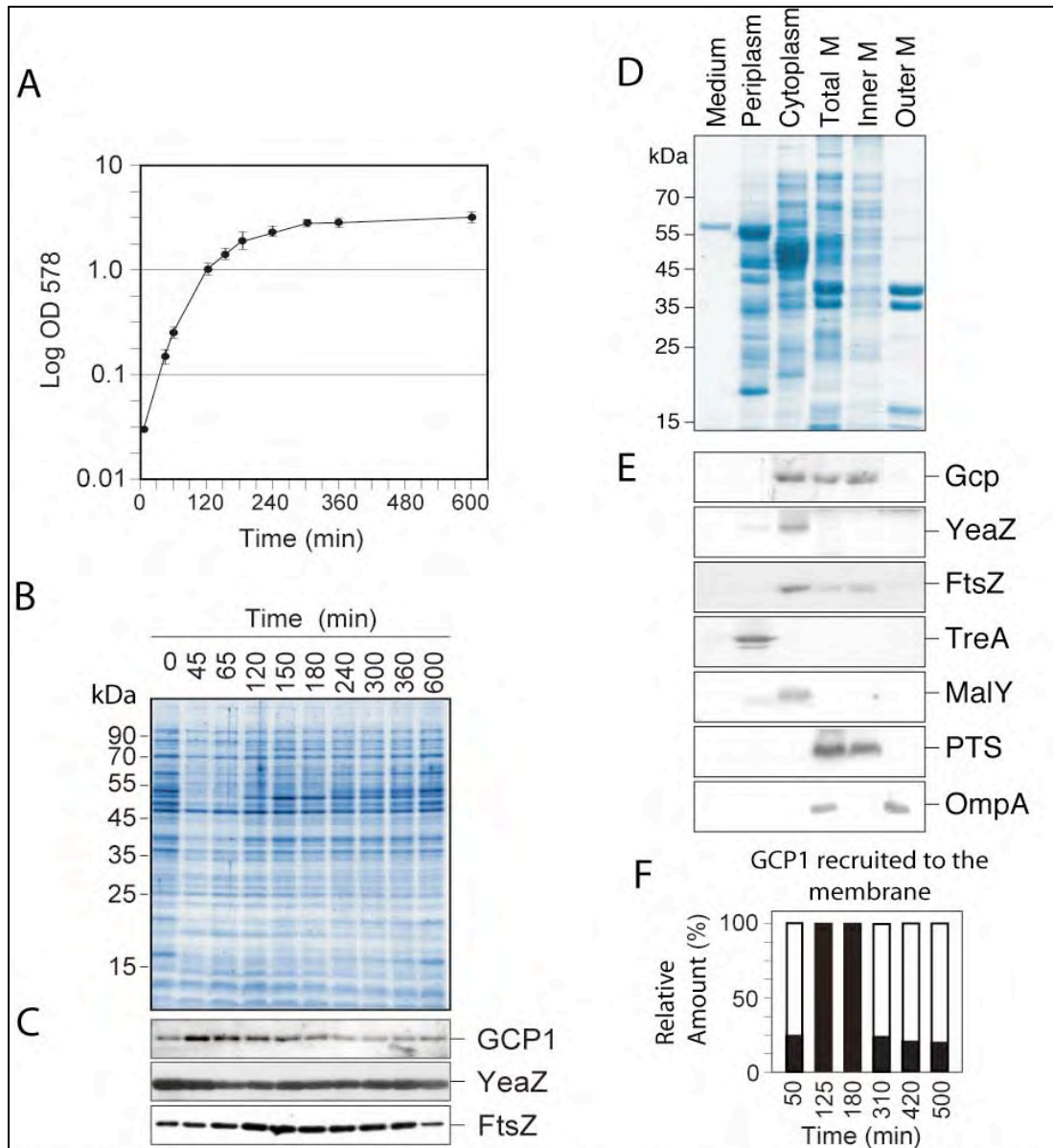


Figure 15 shows the results from the characterization of *gcp1* expression in WT *E. coli* cells from the strain MG1655. Expression studies and localization studies were performed. **(A)** Growth curve of the investigated MG1655 (*E. coli* WT) culture in LB medium at 37°C. **(B)** SDS-PAGE and Coomassie staining of proteins collected at various time points of bacterial growth. For each time point in **(A)** equal amounts of cells from the growth curve were applied to the SDS-PAGE gel. **(C)** Immunoblot analysis with α -GCP1, α -YeaZ and α -FtsZ antibodies using samples collected for **(B)**. Equal amounts of cells were loaded in each gel line. **(D)** SDS-PAGE and Coomassie staining of the culture in the stationary phase. Cells extract after French press and centrifugation at 30,000 x g (Total), total membrane and soluble fractions collected after centrifugation at 130,000 x g. **(E)** Immunoblot analysis with α -GCP1, α -YeaZ and α -FtsZ. Distribution of TreA served as marker for periplasmic localization, MalY for the cytoplasm, the EII_{CB}Glu subunit of the phosphotransferase system (PTS) for the inner membrane and OmpA for the outer membrane. All fractions were solubilized in equal amounts of sample buffer and loaded on equal volume basis back-calculated to the initial extract (Total). **(F)** Relative localization of GCP1 in the membrane fraction assayed during the logarithmic and the stationary phase (Time in correspondence to the growth phase in **A**). Results showed **F** represent the average of three (localization studies) to seven (expression studies) independent experiments.

3.5 Biochemical characterization of GCP1

3.5.1 GCP1 contains a C-terminal protease recognition sequence sharing similarity with the *ssrA*-tag

The last three C-terminal amino acids in the GCP1 sequence, P₃₃₆, A₃₃₇ and A₃₃₈, share similarities with the *ssrA*-tag that are known to be a recognition motif for the ClpXP protease (Flynn et al., 2003). Amongst other substrates, ClpXP degrades proteins modified by addition of the *ssrA* tag, an 11 residue sequence added cotranslationally to the C-terminus of nascent polypeptides on stalled ribosomes (Keiler, Waller et al. 1996) (Gottesman, Roche et al. 1998). The *ssrA* tag is not exclusively recognized by ClpXP, but also by several other proteases such as ClpAP, Tsp (PrC) and FtsH (Silber and Sauer 1994) (Karzai, Roche et al. 2000). Difficulties in purifying different GCP1 constructs containing this sequence (Chapter 3.6, Page 73) could possibly be explained by the presence of this C-terminal recognition site. Hereafter this *ssrA*-like tag will be called PAA-tag. Two strategies were applied for answering the question whether or not ClpXP is responsible for degradation of GCP1. First, constructs for which the purification of the expressed polypeptide (containing the PAA-tag) failed, were transformed in the strain KM568 ($\Delta clpX::neo$) lacking the subunit ClpX that recognizes substrates and activates the proteolytical subunit ClpP. No purification of the overexpressed protein could be achieved. This suggests that either ClpXP is not responsible for GCP1 degradation, that other proteases complemented for the ClpXP function in *E. coli* cells or that overexpressed GCP1 is degraded during the purification procedure after cell disruption. SDS-PAGE analysis and immunoblots revealed that overexpressed GCP1 was present in intact cells boiled in SDS-sample buffer prior to gel electrophoresis but a strong degradation of this protein was observed in cellular extracts (Figure 18, Page 74). Thus, in the second approach, the PAA-tag was deleted from the C-terminus of GCP1. When such constructs were overexpressed no degradation of GCP1 after disrupting the cells was observed. Since degradation of protein constructs containing the PAA-tag was not observed prior to cell disruption, the responsible protease is probably located in the periplasm or the outer membrane.

3.5.2 The evolutionary invariant histidines are essential for the function of GCP1

Sequence alignments of GCP1 homologues from diverse species of all kingdoms of life revealed the presence of two highly conserved (invariant) histidines in all genomes (*E. coli* H₁₁₁ and H₁₁₅). As mentioned in the introduction, these histidines may coordinate Zn²⁺ ions to form a catalytic center. In order to prove the assumption that these invariant histidines are essential for the function of GCP1, the conditionally lethal *gcp1* mutant CWCM4 (MG1655 $\Delta gcp1::neo$) harboring pCW06 (pBAD33, *araC*⁺, P_{BAD-gcp1}) was complemented with a constitutively expressed construct in which the two potential catalytic histidines were replaced by alanines (pGCP1_{H111A/H115A}, Figure 16, Page 71). The conditionally lethal *gcp1* mutant complemented with pGCP1_{H111A/H115A} was viable only in the presence but not in the absence of arabinose suggesting that H₁₁₁ and/or H₁₁₅ are essential for cell viability. Since the result of this experiment is not conclusive, expression of the construct lacking the histidines was to be demonstrated. When the expression of pGCP1_{H111A/H115A} was induced, the overexpression culture ceased growth. This result suggests that the product of this construct is dominantly negative.

3.5.3 The HSP70-actin-fold of GCP1 is not essential for cell viability

The GCP1 sequence contains an HSP70-actin-fold on its C-terminus, described in the introduction. To test whether this domain is essential for the function of GCP1, the protein was truncated from the C-terminus resulting in three different constructs, Figure 16 Page 71). Each construct was cloned in a constitutive expression vector, resulting in plasmids pGCP1_{N291}, pGCP1_{N243} and pGCP1_{N195}. When the conditionally lethal *gcp1* mutant CWCM4 (MG1655 $\Delta gcp1::neo$) harboring pCW06 (pBAD33, *araC*⁺, P_{BAD-gcp1}) was complemented with these deletion constructs, each construct was capable of complementing for the lack of GCP1 when the conditionally lethal mutant was cultured under GCP1 depleting conditions. Thus, we conclude that the C-terminus of GCP1 is not essential for cell viability.

3.5.4 The N-terminus of GCP1 is essential for cell viability

In order to determine whether or not the N-terminus of GCP1 is essential for cell viability, three N-terminally truncated constructs (Figure 16, Page 71) were engineered and cloned into a constitutive expression vector. As described for the C-terminally truncated constructs, the resulting plasmids pGCP1₂₀₋₃₃₈, pGCP1₄₀₋₃₃₈ and pGCP1₆₀₋₃₃₈ were used to complement for the $\Delta gcp1$ mutation in the conditionally lethal mutant CWCM4 (MG1655 $\Delta gcp1::neo$) harboring pCW06 (pBAD33, *araC*⁺, P_{BAD}-*gcp1*) cultured under GCP1-depleting conditions. Even though expression of these constructs was confirmed (Figure 17, Page 72), none of these constructs was capable of complementing for the $\Delta gcp1$ mutation. Obviously the N-terminus of GCP1 is essential for the protein to sustain cell viability.

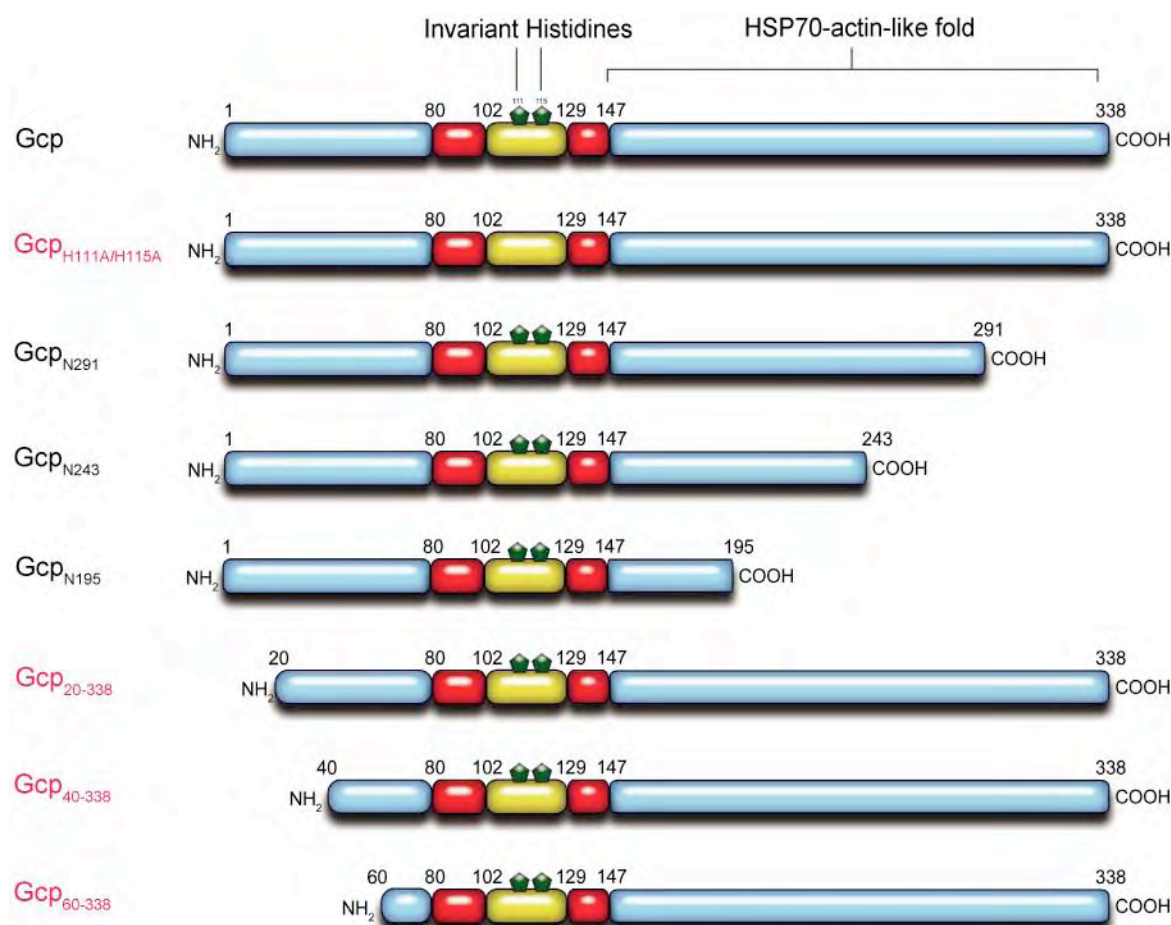
Figure 16: Truncated GCP1-constructs tested for the ability to complement for the $\Delta gcp1$ mutation

Figure 16 shows a model of WT GCP1 (on top) and the different truncated constructs that were designed for complementation studies. Hydrophilic regions are marked in blue or yellow, hydrophobic regions in red. The invariant histidines are represented by green pentagons. Numbers above each model indicate the position of the last aminoacid bordering each region in WT GCP1. Numbers above the terminui of each model indicate the aminoacid to which each truncated construct was shortened. Each construct was transformed into the conditionally lethal Δgcp background of CWCM4 (MG1655 $\Delta gcp::neo$) harboring pCW06 (pBAD33, *araC*, PBAD-*gcp*). Expression of WT *gcp1* from pCW06 was abolished to test the ability of each construct to complement for the loss of wild type Gcp. All C-terminally truncated constructs (Gcp_{N291} , Gcp_{N243} and Gcp_{N195}) led to viable cells. The construct lacking the invariant histidines ($Gcp_{H111A/H115A}$) as well as the N-terminally truncated constructs (Gcp_{20-338} , Gcp_{40-338} and Gcp_{60-338}) were not able to complement the deletion mutant. The names of constructs that were not capable of complementing for the *gcp1* deletion are marked in red.

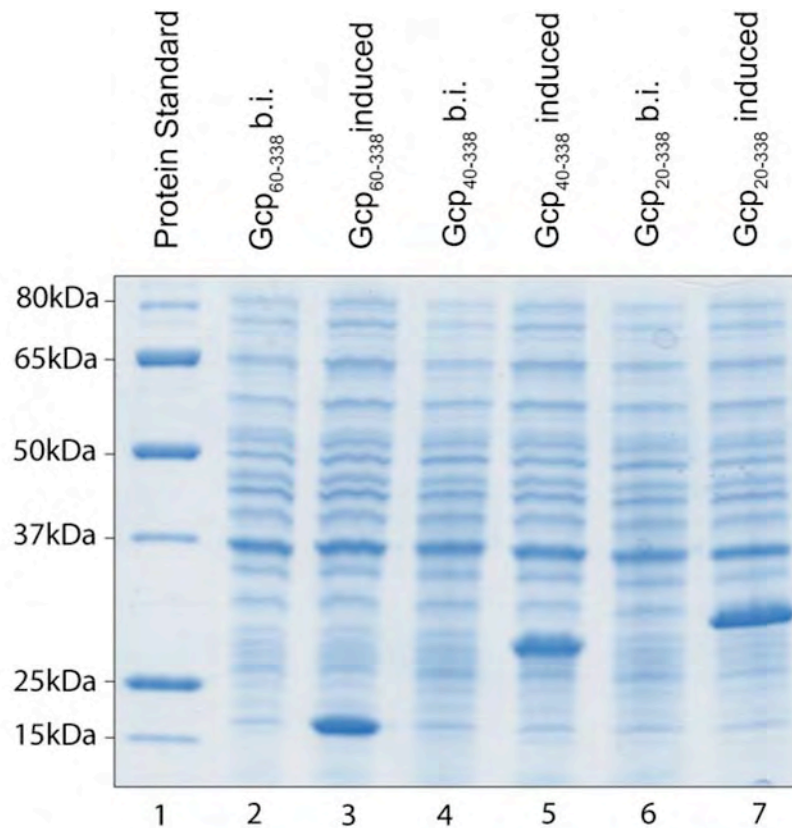
Figure 17: Expression of the N-terminally truncated *gcpI*-constructs is confirmed by SDS-PAGE

Figure 17 shows a SDS-PAGE from expression trials of the N-terminally truncated GCP1-constructs drafted in Figure 16. Lane 1 contains the protein standard as labeled in kDa. Lanes 2, 4 and 6 contain cells from the overexpression cultures of these constructs before induction, lanes 2, 5 and 7 contain such cells after induction. On lanes 2-7 5 μ l culture equaling OD_{578nm} = 10 were applied.

3.6 The HSP70-actin-fold domain interacts with FtsZ protein

For identifying potential protein-protein interactions of GCP1, a global pull down assay was performed. As HSP70-fold domains are often involved in protein-protein interactions, the C-terminal HSP70-actin-fold of GCP1 (amino acids 148-338) described in chapter 1.1, page 5, was C-terminally fused to maltose binding protein (MBP, MalE). The resulting construct was overexpressed from pCW50 in BL21(DE3) and purified under native conditions using an affinity column. Eluted MalE-HSP70_(gcp1) fusion protein was analyzed for proteins bound to the HSP70-actin fold by comparing protein patterns after SDS-PAGE with immunoblots using a α -MalE antibody. Initial pull down experiments failed due to proteolytical degradation of the MalE-HSP70_(gcp1) fusion-protein caused by the presence of the PAA-tag at the C-terminus of the fusion-protein. However, when cells overexpressing MalE-HSP70_(gcp1) fusion-protein were boiled in SDS-sample buffer directly after overexpression, overexpressed protein with the expected molecular weight of approximately 63 kDa (MalE \approx 43 kDa, GCP1_{HSP70-actin} \approx 20 kDa) was visible on α -MalE immunoblots. Constructing the fusion-protein lacking the last three C-terminal amino acids PAA, resulting in the overexpression plasmid pCW51. The experiment was repeated and the fusion-protein without the PAA-tag was expressed from pCW51 in the overexpression strain BL21(DE3). Again cellular extract and eluted MalE-HSP70_(gcp1) fusion-protein were analyzed by comparing SDS-PAGE analysis with α -MalE immunoblots prepared from these samples. The intact fusion-protein localizes correctly according to its molecular mass of approximately 63 kDa. However, also smaller proteins were detected by SDS-PAGE and α -MalE immunoblots (Figure 18, Page 74). Especially in the range of around 40 kDa, prominent signals were obtained for MalE on the blots. Since MalE has a molecular mass of 43 kDa, most likely the HSP70_(gcp1) domain is degraded, but to a significantly lower extent than compared to the degradation that was observed when the fusion-protein contained the PAA-tag. One band with the apparent molecular mass of approximately 40 kDa was visible in the eluted fraction by Coomassie staining (Figure 18, Page 74) and this band did not cross-react with the α -MalE antibody. Since this band might represent the GCP1 interaction partner its identity was analyzed by means of mass spectrometry. Eight peptides of the mass spectrometry result covered 20.6 % of the FtsZ protein sequence. The MASCOT score of 417 provided unequivocal protein identification. No interacting proteins were detected when the pull down was performed with MalE fused to the N-terminal part (amino acids M1-D74) of GCP1 (data not shown).

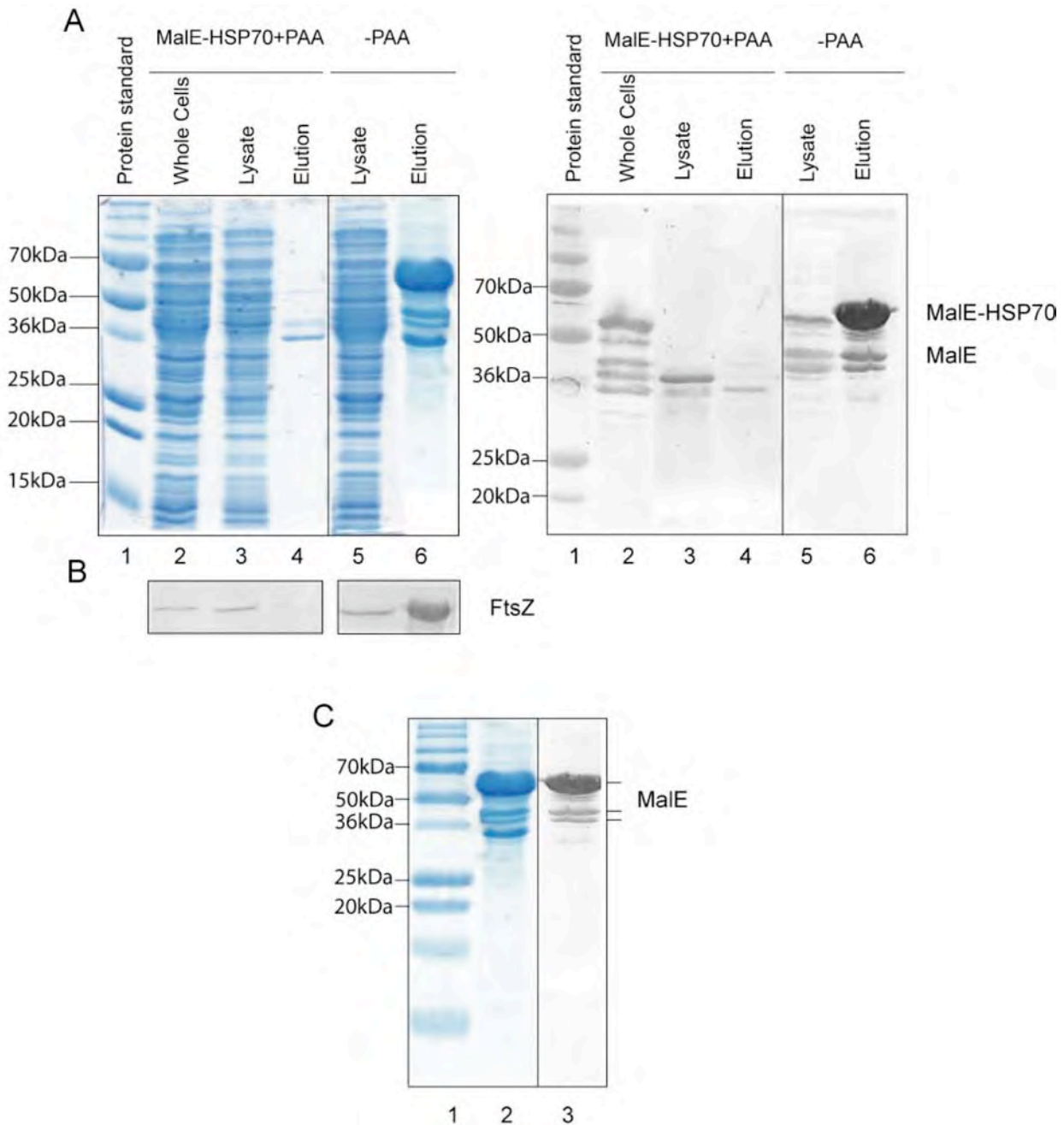
Figure 18: A protein interacting with GCP1 was coeluted with the MalE-HSP70-actin-like fold fused to MalE

Figure 18 shows the results from the pull down experiments with the HSP70-actin fold of Gcp fused to MalE. HSP70-actin fold without the C-terminal SsrA-tag (amino acids G147-L334) was overexpressed as a fusion protein with maltose-binding protein (MalE) and purified by affinity chromatography on amylose resin column. Bound proteins were eluted with 20 mM maltose and analyzed by SDS-PAGE, immunoblotting and mass spectrometry. **(A)** On the left, a Coomassie Stained SDS-PAGE from approaches using the fusion-protein including the PAA-tag (left panel, lanes 2-4) and approaches using fusion-protein lacking the PAA-tag (left panel, lanes 5+6) is shown. On the right, immunoblots with α -MalE antibodies using fusion-protein including the PAA-tag (right panel, lanes 2-4) and fusion-protein lacking the PAA-tag (lanes 5+6) are shown. Total *E. coli* cells from the overexpression, the lysate and eluted fractions are labeled. **(B)** Immunoblots of fractions from (A) using Antibodies against FtsZ show the presence of FtsZ protein in the samples. **(C)** The eluted fraction yielded with pull-down approaches using MalE-HSP70_(GCP) fusion-protein lacking the PAA-tag is compared by SDS-PAGE and an immunoblot against MalE. The band in lane 2 that is not recognized by antibodies against MalE was identified as FtsZ.

To exclude the possibility that FtsZ unspecifically binds to the column matrix or to MalE, pull down experiments were performed as described above, using lysates from *E. coli* cell cultures transformed with pMalc2x, the parental plasmid of pCW51 (encodes MalE-HSP70_(gcp1)) an vector expressing MalE without the HSP70_(gcp1)-like domain. Yielded fractions were then tested for their crossreactivity with antibodies against FtsZ. Obtained blots revealed no FtsZ protein in the eluted fractions, in contrast to the soluble extract and whole cells. Thus, we conclude that FtsZ specifically interacts with the HSP70_(GCP1)-like domain. In addition, fractions in which the HSP70_(GCP1)-actin fold of the fusion-protein was endogenously degraded (Chapters 3.5.1 and 3.6) did not show crossreactivity with the FtsZ antibody in immunoblots (Figure 18, Page 74), thus confirming the specificity of the interaction between FtsZ and the HSP70-like C-terminus of GCP1.

3.6.1 Depletion of GCP1 is lethal due to impaired cell division

Growth curves of the strain CWCM4 (MG1655 $\Delta gcp1::neo$) harboring pCW06 (pBAD33, *araC*⁺, *P_{BAD}-gcp1*) confirmed that almost no growth of cells occurred after long time GCP1-depletion (Figure 19B, Page 76). Samples from CWCM4 harboring pCW06 cultures grown under GCP1-depleting and non-depleting conditions were taken logarithmic phase, intersection of logarithmic phase to stationary phase and stationary phase. SDS-PAGE analysis and immunoblots using antibodies against GCP1 revealed different protein patterns from cultures grown under depleting and non-depleting conditions. Care was taken to load identical amounts of protein on the gels (OD_{578nm}). In contrast to the culture that expressed *gcp1*, where the protein pattern changed with the time of growth, the protein pattern in the GCP1-depleted culture remained relatively constant. The exception was an unknown 21 kDa protein, which accumulated in GCP1-depleted cultures (Figure 19C, Page 76 marked by an asterisk). A slight decrease in overall protein content was found in cultures after prolonged GCP1-depletion. As expected GCP1 accumulated in the conditionally lethal *gcp1* mutant strain CWCM4 harboring pCW06 in the presence of arabinose but no detectable amounts of this protein were present after the arabinose depletion (Figure 19D, Page 76). Decreasing amounts of FtsZ and YeaZ were assayed in GCP1-depleted cells, while constant or increased amounts of these proteins, respectively, were detected in the arabinose-supplemented culture. To prove whether depletion of GCP1 leads to cell death, a vital staining of CWCM4 cells harboring pCW06 cultivated for 7

hours in the presence and in the absence of 0,2 % arabinose was performed. The applied stain indicates the integrity of membranes by fluorescence when cells are examined under a fluorescence microscope. Living cells with intact membranes will exhibit green fluorescence when a GFP-filter is applied. Dead cells with defective membranes show fluorescence when an RFP-filter is used. Analyzing 5000 cells from each culture revealed that 160 (3,2 %) and 30 (0,6 %) cells were dead in the presence and the absence of arabinose, respectively. The remaining cells were viable. The accumulation of 21 kDa protein in the conditional *gcp1* mutant after arabinose depletion (Figure 19C, Page 76) and the up-regulated proteins displayed on 2D-gels (Figure 14, Page 62) confirm the findings of Chapter 3.3.5.2 and Chapter 3.3.2 that the general ability of cells for transcription and translation was not abolished in the absence of GCP1. Thus, we conclude that the cells are still viable but cell division in these cells is impaired.

Figure 19: Prolonged GCP1-depletion does not lead to cell death

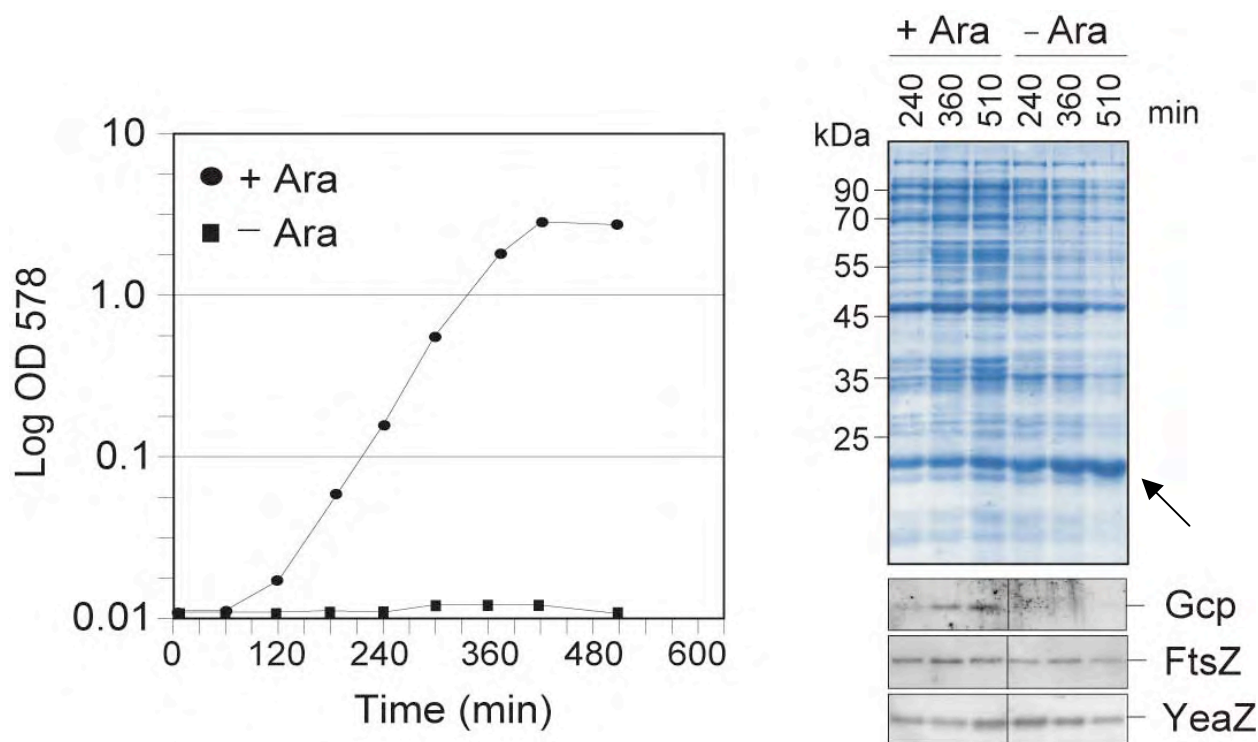


Figure 19 shows a growth curve measured from a CWCM4 culture harboring pCW06. Cells were cultivated under GCP1-depleting and non-depleting conditions and a SDS-PAGE resulting from total cells taken from the cultures at times indicated. Below the SDS-PAGE, immunoblots prepared from the regarding samples are shown. The arrow marks the protein that accumulates during GCP1-depletion.

3.6.2 Depletion of GCP1 abolishes FtsZ ring formation

Formation of the FtsZ ring at the cytoplasmic membrane is the first step during *E. coli* cell division (reviewed by (Margolin 2000) (Wissel and Weiss 2004) (Vicente and Rico 2006) (Lutkenhaus 2007)). To test whether this step is arrested in the absence of GCP1, an IPTG inducible *ftsZ-gfp* fusion construct was transduced via P1 transduction into the conditionally lethal *gcp1* mutant background CWCM4 (MG1655 $\Delta gcp1::neo$) harboring pCW06 (pBAD33, *araC*⁺, P_{BAD}-*gcp1*). The resulting strain CWCM5 (MG1655 $\Delta gcp1::neo \Delta(\lambda att-lom)::bla lacI^q$ P₂₀₄-*ftsZ-gfp*) harboring pCW06 (pBAD33, *araC*⁺, P_{BAD}-*gcp1*) was cultured under GCP1-depleting and non-depleting conditions and a growth curve was prepared (data not shown). The strain CWCM5 still possesses the endogenous allele of *ftsZ*, leading to a merodiploid situation in regard to this gene. Expression of *ftsZ-gfp* was induced with 10 μ M IPTG approximately 45 minutes after *gcp1*-expression was depleted. Thereby potential artificial effects of expressing *ftsZ-gfp* were reduced to a minimum. Cells were examined by light and fluorescence microscopy when the growth deficiency of the GCP1-depleted culture became apparent in the growth curve. When grown in medium supplemented with arabinose, CWCM5 showed a normal FtsZ ring formation during cell division as observed under a fluorescence microscope (Figure 20, Page 78). This excludes that the expression of *ftsZ-gfp* affects cell division. In contrast, in GCP1-depleted cultures no FtsZ ring was detected by fluorescence microscopy (Figure 20, Page 78). Instead, fairly strong GFP-fluorescence was observed at the cell poles of the GCP1-depleted cells (Figure 20C, Page 78). Furthermore, such cells exhibited an additional GFP-fluorescence unevenly distributed throughout the cell (Figure 20C, Page 78) that was weaker than the signal on the cell poles. Apparently FtsZ-GFP forms aggregates or polymers on the cell poles and smaller aggregates unevenly distributed across the cell. These aggregates seem to be associated with the cytoplasmic membrane of GCP1-depleted cells. No irregular FtsZ-GFP aggregates across the cell or aggregates on the cell poles are observed in the non-depleted cells, FtsZ-GFP exclusively located along the division ring of dividing cells (Figure 20C, Page 78). The SDS-PAGE and immunoblot analysis of both cultures confirmed that FtsZ-GFP is expressed in both cultures and the expression of *gcp1* is arrested in the absence of arabinose (Figure 20B, Page 78). Much higher levels of the recombinant FtsZ-GFP and the endogenous FtsZ were detected in the absence of arabinose (Figure 20B, Page 78). Thus, we conclude that GCP1 is involved in controlling cell division in *E. coli* and influences the amount and localization of FtsZ in the cell.

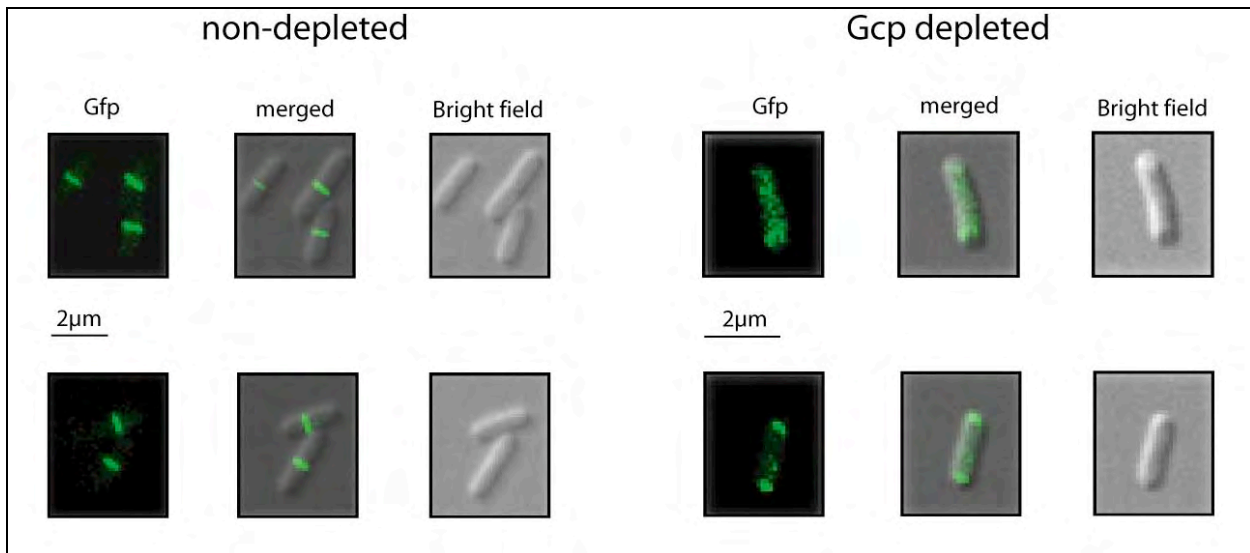
Figure 20: Depletion of GCP1 abolishes FtsZ ring formation

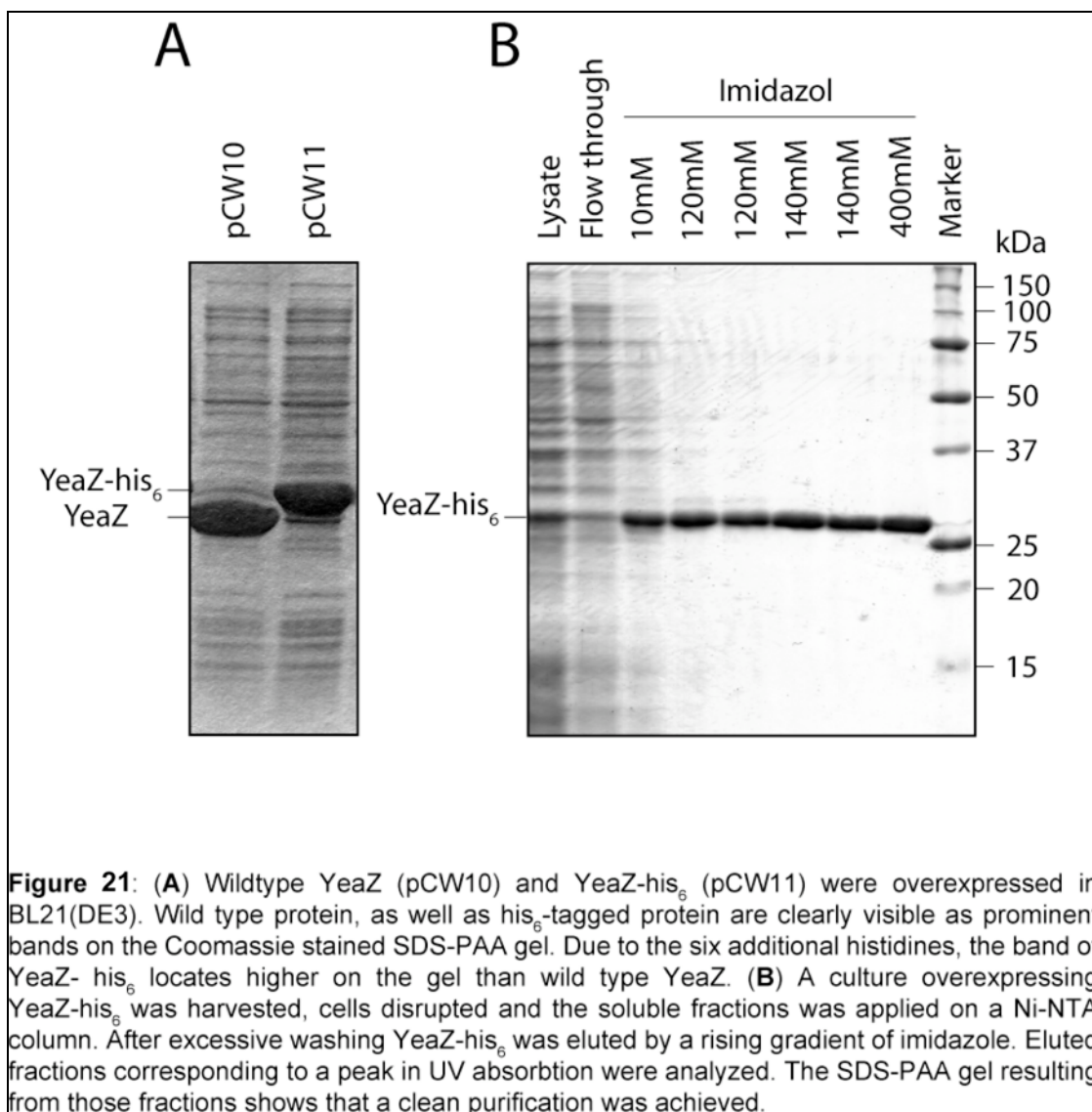
Figure 20 shows fluorescence microscope images of CWCM5 cells harboring pCW06 cultivated under GCP1-depleting and non-depleting conditions. FtsZ-Gfp expression was induced by 10µM IPTG. Images show cells from the non-depleted culture and the depleted culture as indicated.

3.7 Characterization of YeaZ

Since YeaZ is reported to interact with GCP1 in *E. coli* (Butland, Peregrin-Alvarez et al. 2005), overexpression and purification of YeaZ was approached in order to be able to raise antibodies against this protein. Furthermore the localization of YeaZ was determined.

3.7.1 YeaZ is easily overexpressed and purified

The *yeaZ* ORF was cloned into two different IPTG inducible expression vectors, one expressing wild type YeaZ (pCW10) the other provides a his₆-tag on the C-terminus of YeaZ (pCW11). Both constructs were expressed in the strain BL21(DE3) and expression levels of YeaZ for different conditions of induction were monitored by SDS-PAGE. Strong overexpression was observed for all OD_{678nm} tested for induction and for all concentrations of the inducer IPTG. WT protein (from pCW10), as well as his₆-tagged protein (from pCW11) is clearly visible as prominent bands on the gel when expression is induced with 200 μM IPTG for 3 hours. Overexpressed his₆-tagged protein was purified by the use of a NiNTA-column. Eluted fractions were collected and fractions containing protein (corresponding to peaks in UV absorption during elution) were analyzed by SDS-PAGE. Such gels showed that a good purification of YeaZ was achieved (Figure 21, Page 80). A protein concentration of approximately 0.8 mg • ml⁻¹ was determined for the merged YeaZ-containing fractions.

Figure 21: YeaZ is easily overexpressed and purified

3.7.2 A polyclonal antibody against YeaZ was raised

Purified YeaZ-his₆ protein was collected in large yields (Chapter 3.7.1) and imidazole was removed from the protein solution by means of dialysis. Subsequently the protein concentration was determined and adjusted to approximately 1mg • ml⁻¹. The protein was used for repeated immunization of a rabbit against the protein. The received serum tested in immunoblots was applied in a 1:2000 dilution and revealed a strict specificity for the YeaZ antigen (see Figure 15C, Page 67 and Figure 19, Page 76).

3.7.3 YeaZ is a soluble protein

To determine the subcellular localization of overexpressed YeaZ, mechanically disrupted *E. coli* cells were fractionated using differential centrifugation as described for GCP1. The fractionation distinguished between insoluble constituents, large cell fragments, membrane fraction and soluble components. SDS-PAGE analysis revealed that YeaZ is exclusively located in the soluble fraction as shown in Figure 15E, Page 67. No YeaZ signal was obtained for the membrane fraction.

4 Discussion

This study aimed at the functional characterization of *gcp1*, a gene of unknown function from *E. coli*. The main approach for identifying the molecular function of the gene-product was the analysis of the *gcp1* deletion mutants and the detection of protein-protein interactions and their further characterization. Furthermore, the subcellular localization and endogenous GCP1 expression were investigated.

4.1 Structural and functional conservation of GCPs across kingdoms

As already described during the introduction, the members of the M22 peptidase family (GCP1, GCP2 and YeaZ) share highly conserved similarities in their amino acid sequence, but differ in their secondary and tertiary structure. While GCP2 from some species and YeaZ in all cases represent soluble proteins, GCP1 is either an integral membrane protein (*A. thaliana*) or is distributed between the soluble fraction and the membrane fraction (*E. coli*). Archaea GCP2 resembles a DNA-binding protein responsible for chromosome replication and maintaining transcription (Hecker, Leulliot et al. 2007; Hecker, Lopreiato et al. 2008; Hecker, Graille et al. 2009). Our data demonstrated that transcription and translation occurred also in the absence of GCP1 – thus excluding this function for GCP1 in *E. coli*. Preliminary data demonstrated that GCP1 from other species were not capable of complementing for the function of GCP1 from *E. coli*, thus confirming that the observed similarities in the amino acid sequence do not necessarily represent identical modes of action.

4.2 GCP1 localization in *E. coli*

Our data demonstrated that GCP1 from *E. coli* is present as soluble protein, but can be recruited to the membrane under certain conditions. This is no unusual behavior, especially when the direct physical interaction of GCP1 with FtsZ is considered. FtsZ is also present as soluble protein and only recruited to the membrane by other proteins (ZipA) when cell division occurs. Even though GCP1 from *M. haemolytica* is annotated as being secreted to the medium, this finding does not apply to GCP1 from *E. coli* and most probably the described localization of *M. haemolytica* GCP1 might result from non-specific observations like bacterial lysis rather than

active secretion. The given fact that GCP1 is essential for cell viability throughout all kingdoms of life, the secretion of GCP1 to the medium would make *M. haemolytica* the only organism that could dispense this protein and still remain viability, making the described secretion very improbable. However, the secretion of proteins outside the cell is a very common phenomenon among pathogenic bacteria.

4.3 Is GCP1 an active protease?

Although GCP1 accomplishes all theoretical requirements for being an active protease there is still no direct evidence to support such a function. Unfortunately, in our study overexpressed GCP1 accumulated in inclusion bodies and the attempt to refold denatured GCP1 in the presence of various detergents and to obtain a proteolytical active form failed (data not shown). No proteolytical activity of GCP1 was assayed *in vitro* against general protease substrates, such as β -casein, bovine milk κ -casein gelatin, hemoglobin, azocoll or albumin (data not shown). This suggests that GCP1 might not be correctly folded in our system, may have very narrow substrate specificity, or may require specific cofactors or posttranslational modifications for its activity, or finally, has another enzymatic/non-enzymatic function. Against the later possibility speaks the fact that GCP1 with mutated potential catalytic histidines was not able to rescue the lethal conditional *gcp1* mutant phenotype (Figure 16, Page 71) suggesting that these two amino acids are essential for cell viability. However, the accumulation of certain proteins in the 2D-gels could also be due to a potential proteolytical activity of GCP1 as proposed in the past.

However, as already mentioned in the introduction, a recent publication suggested that during the preparation of the GCP1 from *M. haemolytica*, at least one additional protease was co-purified together with GCP1 and this protease might be responsible for the specific cleavage of the O-sialoglycosylated substrate (Jiang 2004).

4.4 YeaZ in bacteria

The member of the M22 protease family YeaZ is exclusively found in bacteria, but not in eukaryotes and was reported to be indispensable for cell viability and to directly interact with GCP1 from *E. coli* (Butland, Peregrin-Alvarez et al. 2005). Because YeaZ is lacking the invariant histidines described for the other members of the M22 peptidase family it most probably does not exhibit the proteolytical activity proposed for GCP1 and GCP2. We report

here, that YeaZ is exclusively located as soluble protein in the cytoplasmic fraction of *E. coli* and thus conclude that the described interaction between GCP1 and YeaZ only occurs when GCP1 is not recruited to the membrane. Possibly YeaZ triggers the dissociation of GCP1 from the cytoplasmic membrane and thereby inhibits a potential activity of GCP1 in this compartment of the bacterial cell. Considering the given essentiality of YeaZ, the protein could also form a complex with GCP1 in order to exhibit a specific function, similar to the interaction of GCP2 (Kae1) from archaea with the Bud32-kinase, briefly described in the introduction. Preliminary data demonstrated regions of high homology between the N-termini of GCP1 and YeaZ, thus suggesting this terminus to resemble an interaction domain between both proteins. In our pulldown experiment no YeaZ was detected. This is most probably due to the fact that YeaZ is one of the most abundant proteins in *E. coli* and will compete with YeaZ for interaction. Furthermore our pulldown was performed with the C-terminus of the protein.

4.5 Low amounts of GCP1 are sufficient to facilitate cellular growth

The deletion of *gcp1* is lethal. However, deletion mutants in *gcp1* can form small colonies that cannot be restreaked (Chapter 3.2.1, Page 49). Obviously such cells were able to divide several times after the deletion of *gcp1*. In these cells, each division cycle halves the amount of GCP1. After the GCP1-amount sinks below the critical level, cells can no longer perform cell division. This also explains why colonies yielded from the deletion experiment could not be restreaked. Furthermore, this finding suggests that already a small amount of GCP1 is sufficient for the cell to divide. Since each colony resulted from a single cell that was deleted in *gcp1* and thereby could not synthesize new GCP1, the physiological GCP1 concentration in the parental cell must have been sufficient for several divisions. In addition, one can conclude from these findings that GCP1 is relatively stable in the cell and is not rapidly degraded.

The results from constructing a conditionally lethal *gcp1* mutant indicate that GCP1 is a low abundant protein in the cell. For complementation of the $\Delta gcp1$ genotype, a linear induction of this protein was chosen. However, all plasmids expressing *gcp1* under the control of such systems were capable of complementing the $\Delta gcp1$ mutation, but cells also exhibited growth when *gcp1* expression from the plasmid was not induced. This is contributed to a low basal GCP1 expression level of the induction system that was sufficient to complement the $\Delta gcp1$ mutation. After using an AraC controlled expression system, that ensures tight repression of

genes under its control, the conditionally lethal mutant revealed no more growth without inducer. Thus, we conclude that already low expression levels of *gcp1* are sufficient for growth. When the conditionally lethal mutant CWCM4 (MG1655 $\Delta gcp1::neo$) harboring pCW06 (pBAD33, *araC*⁺, *P*_{BAD}-*gcp1*) is cultured under inducing conditions and the inducer arabinose is washed out from the culture (Chapter 3.3.3, Page 54), the growth deficit develops with a delay of several generations. Comparing the growth of cultures that already reached a relatively high cell density before *gcp1* expression was depleted (Figure 12, Page 57) with the growth of a culture where *gcp1* expression was depleted at low cell density (Figure 15, Page 67) demonstrates that the duration of the period between depletion of *gcp1* expression and development of the $\Delta gcp1$ phenotype of CWCM4 (MG1655 $\Delta gcp1::neo$) harboring pCW06 (pBAD33, *araC*⁺, *P*_{BAD}-*gcp1*) is depending on the generation time of the culture. These findings lead to the conclusion that GCP1 synthesized before removal of the inducer stays relatively stable in the cell and has to be diluted by several cell divisions until cessation of growth occurs. One has to mention here, that the elevated, non-physiological expression level of GCP1 from the plasmid pCW06 (pBAD33, *araC*⁺, *P*_{BAD}-*gcp1*) also negatively affects the growth of CWCM4 cultures.

4.6 The reversion frequency of the conditionally lethal mutant suggest a “loss-of-function” mutation in a second gene

The determination of the reversion frequency of a null-mutant allows to determine whether the mutation leading to reversion is a „loss-of-function“ mutation or a „gain-of-function“ mutation (Beckwith 1991). A reversion frequency in the range of 10^7 suggests that a “loss-of-function” mutation occurred within the genome and led to reversion, while a low reversion frequency in the range of 10^9 suggests a “gain-of-function” mutation.

After excluding revertants whose mutation occurred on the complementing plasmid pCW06 (pBAD33, *araC*⁺, *P*_{BAD}-*gcp1*), the chromosomal reversion frequency of the *gcp1*-deletion mutant was determined to approximately 10^6 (Chapter 3.3.1, Page 52). This result suggests that a “loss-of-function” mutation in a second gene is responsible for the reversion. An example of an essential cell division protein (FtsK) whose deletion mutant could be rescued by the loss-of-function mutation in a second gene is described in chapter 4.10. among many more striking similarities between the results obtained for GCP1 in this study and results obtained when FtsK was characterized.

4.7 Cells remain viable after the depletion of *gcp1*

The results from different experiments indicate that the deletion of *gcp1* leads to cessation of growth, but not to cell death. When constructing the conditionally lethal *gcp1* mutant, reverted cells formed colonies that grew independent of the presence of arabinose – the inducer of *gcp1* expression. Such colonies did not appear instantaneously, but after prolonged incubation of 3 days (Chapter 3.3.2). Interestingly, the size of such revertant colonies differed in diameter (Figure 10, Page 55). Most likely the larger colonies resulted from cells that were already reverted at the time plated, while the smaller colonies reverted “on plate”. Thus, we conclude that cells deleted in *gcp1* are not dead, but can revert after prolonged incubation.

When CWCM4 (MG1655 $\Delta gcp1::neo$) harboring pCW06 (pBAD33, *araC*⁺, *P*_{BAD}-*gcp1*) cells were depleted in *gcp1* for a prolonged period of time and the protein content was monitored on SDS-PAGE gels (Figure 19, Page 76), an overall decrease in protein content was observed, but one protein of the size of about 21 kDa was accumulating in the depleted cells. Again, the result demonstrates that the general ability of cells for transcription and translation was not abolished in the absence of GCP1.

By comparing the protein patterns of 2D-gels that were prepared from the conditionally lethal *gcp1* mutant strain CWCM4 harboring pCW06, grown under GCP1 depleting and non-depleting conditions, it was observed that some proteins were elevated when *gcp1* expression was abolished. Among these proteins were the prolyl-tRNA-synthetase (ProS) and the 50S ribosomal protein L10, both polypeptides involved in protein biosynthesis. The increase of some proteins indicates a general ability for protein-biosynthesis in GCP1-depleted cells. The accumulation of ProS and L10 in conditionally lethal GCP1 mutant under GCP1-depleting conditions is in accordance with this view. Nevertheless, one has to mention here, that the L10 protein is a structural component of the ribosome (de Narvaez and Schaup 1979). In addition L10 protein is regulated on the post-transcriptional level. L10 protein alone is subject to rapid proteolytic decay (half life of 1.5 minutes), but is stable if it is in a complex (Petersen 1990). Contradictory to the post-transcriptional regulation of L10 protein, ProS protein is reported being regulated on the transcriptional level. Synthesis of ProRS complex is derepressed by starvation for proline (Archibold and Williams 1972). The results from the 2D-gels indicate, that the rise of some specific proteins after *gcp1*-depletion may be caused by an increase synthesis of these proteins or their lower degradation rate. However, if this assumption is true, one has to presume that GCP1-depletion primarily leads to a loss of proteolytic activity and with some delay to abolishment of protein-biosynthesis. If protein biosynthesis would be aborted simultaneously with the protease

activity, no proteins could accumulate. The observation of the accumulation of a 21 kDa protein contradicts this theory. For a final explanation, cells were tested for viability by the use of a vital staining (Chapter 3.6.1, Page 75). CWCM4 cells harboring pCW06 that were depleted in GCP1 for 7 hours were compared to a control culture that was grown under non-depleting conditions in parallel. Analyzing 5000 cells from each culture revealed that 160 (3.2%) and 30 (0.6%) cells were dead in the presence and the absence of arabinose, respectively. The remaining cells were viable. Thus, we conclude that the depletion of *gcp1* results in viable cells in which cell division and growth is impaired.

4.8 Correct divisome assembly is dependent on GCP1

The sequence of GCP1 contains an HSP70-actin-like fold on its C-terminus. Since HSP70 domains are often involved in protein-protein interactions, the C-terminus of GCP1 was fused to MalE in order to perform a global pulldown assay. One protein specifically interacting with the HSP70-actin-like fold of GCP1 was coeluted with the fusion-protein and identified as FtsZ (Chapter 3.6, Page 73).

The finding of the direct physical interaction of GCP1 with the cell division protein FtsZ is supported by the results from characterizing *gcp1* expression in wild type cells (Chapter 3.4.1, Page 65). First, GCP1 accumulates in early logarithmic phase. Second, GCP1 is distributed between the plasma membrane and the cytoplasm in the stationary phase but the vast of this protein is bound to the membrane during logarithmic growth (Chapter 3.4.3, Page 66). A similar distribution was found for FtsZ, which is consistent with the previous (Stricker, Maddox et al. 2002) that only one-third of the cellular FtsZ pool is present in the Z-ring. Thus, similarly to FtsZ, GCP1 could also be recruited to the membrane during cell division and dissociate to the cytoplasm for storage. This is supported by the finding that GCP1 is present in the cell in excess, since the removal of arabinose from the medium of the conditional *gcp1* mutant did not lead to an immediate cessation of cell growth.

When expressing an FtsZ-Gfp fusion in the conditionally lethal *gcp1* mutant strain CWCM4 harboring pCW06 under GCP1-depleting conditions, Z-ring assembly was impaired (Chapter 3.6.2, Page 77).

How might GCP1 influence FtsZ ring formation? To stabilize the FtsZ ring, at least one membrane anchor, provided either by the C-terminal amphipathic helix of the cytosolic protein FtsA (Pichoff and Lutkenhaus 2005) or by the transmembrane domain of ZipA (Hale and de

Boer 1997), is required. Inactivation of both ZipA and FtsA as well as overproduction of these proteins abolishes Z-ring formation (Pichoff and Lutkenhaus 2002; Geissler, Elraheb et al. 2003)). Since the ratio of FtsZ to FtsA or ZipA is critical for cell division, the loss of GCP1 might lead to the depletion/enhancement in ZipA and FtsA amounts due to changes of their synthesis or degradation rates. In contrast, cell division is relatively insensitive to increase/decrease in levels of downstream division proteins with the exception of FtsN (reviewed by (Lutkenhaus 2007).

Another possibility is that the proteolytic activity discussed to be dependent on GCP1 is directed towards inhibitors of cell division that accumulate in the absence of GCP1 and arrest Z-ring formation. It was reported that the cell division inhibitor Sula, induced after any perturbation of DNA replication, is degraded by ATP-dependent Lon and HslVU proteases in *E. coli* (Canceill, Dervyn et al. 1990) (Kanemori, Yanagi et al. 1999). Deletion of both proteases led to the growth defect without DNA-damaging treatment due to the accumulation of excess Sula (Kanemori, Yanagi et al. 1999).

The GCP1 could be also involved in the degradation of two other cell division inhibitors, DicB or SlmA. It was reported that in addition to the MinCDE inhibition system, preventing Z-ring formation near the cell poles, MinC alone can be activated by DicB and that the MinC-DicB complex is target directly to the Z-ring destabilizing it regardless of cellular location (de Boer, Crossley et al. 1990) reviewed by (Lutkenhaus 2007). Overproduction of SlmA, a protein responsible for nucleoid occlusion in *E. coli* recruits FtsZ to the nucleoid and prevents Z-ring formation (Bernhardt and de Boer 2005). Whether GCP1 is involved in one of these processes awaits further investigation.

4.9 2D-gel analysis of GCP1-depleted cells sustains the involvement of GCP1 in cell division

The protein patterns of GCP1-depleted and non-depleted cells on 2D-gels were compared. Significant alterations in the proteome caused by GCP1-depletion were visible (Chapter 3.3.5.2, Page 61). The amount of several proteins increases in response to GCP1-deletion, while others decrease. As discussed above, cells are not dying after GCP1-depletion, but remain viable and can still perform protein-biosynthesis (Chapter 3.6.1, Page 75).

Interestingly, almost all proteins that were identified to increase in response to GCP1-depletion are either involved in protein biosynthesis (ProS and RplJ) or in cell envelope synthesis (FkpA,

MraW and DapA). (This is mentioned above) DapA is the dihydropicolinate synthetase, involved in lysine biosynthesis and diaminopimelate (cell wall building block) synthesis (Laber, Gomis-Ruth et al. 1992) (Acord and Masters 2004). MraW is an essential protein that methylates proteins at the cytoplasmic membrane and the gene encoding the protein is located in the *mra*-cluster, also known as “cell envelope biosynthesis and cell division cluster” (Carrion, Gomez et al. 1999) (Arifuzzaman, Maeda et al. 2006)). FkpA is a periplasmic protein that enhances the correct folding of proteins by cis-trans isomerization of prolyl residues within the polypeptide binding (Saul, Arie et al. 2004)

On the other hand, all proteins that decrease after GCP1-depletion are related to stress conditions, starvation and stationary phase. DnaK is a heat shock protein that acts as chaperone and also binds DNA during stress situations (Genevaux, Georgopoulos et al. 2007). Dps is induced by starvation stress and upregulated in stationary phase (Almiron, Link et al. 1992). It binds to DNA and protects it by forming a condensed protein-DNA complex (Wolf, Frenkiel et al. 1999),(Martinez and Kolter 1997)). Slp is a starvation and stationary phase induced lipoprotein and reported to be induced in response to slow growth (Shimada, Makinoshima et al. 2004) (Alexander and St John 1994). UspA is a global stress response regulator induced during various stress conditions (Nystrom and Neidhardt 1992). Mutants in the corresponding gene *uspA* exhibit a defect in survival during prolonged periods of growth inhibition (Nystrom and Neidhardt 1994)

One has to ask why stress and stationary phase regulated proteins are reduced after GCP1-depletion and on the other hand, protein-biosynthesis related and cell envelope synthesis related genes are upregulated. After abolished cell division, one would expect the converse alteration in protein abundance. Obviously GCP1-depletion leads to aborted cell division, but not to a classical stress-situation for the cell. This assumption is confirmed by the finding that cells are not dying after GCP1-depletion and the survival rate of cells after prolonged depletion is even higher in the GCP1-depleted culture than in the non-depleted culture (Chapter 3.6.1, Page 75). Especially UspA is reported to be induced immediately after the growth rate decrease (Nystrom and Neidhardt 1994). If cells would cease growth for any other reason than the incorrect divisome assembly, one would expect that UspA should be upregulated. Probably the cells are “in the starting blocks” for cell division, but divisome assembly and constriction of the cell is blocked for structural reasons, hence these proteins are not used for divisome assembly and accumulate in the cell. This assumption would explain why protein-biosynthesis and cell envelope-synthesis related proteins are accumulating in such cells.

4.10 GCP1 could control the correct time point for initiation of cell division

There is some controversy concerning a possible function of GCP1. Since the *gcp1* gene in *E. coli* is located in front, but transcribed in opposite direction, to the *rpsU-dnaG-rpoD* operon (encoding ribosomal protein S21, DNA primase and sigma subunit of RNA polymerase, respectively) it was proposed that the *gcp1* gene might be a functional part of this gene cluster (Nesin, Lupski et al. 1987). Our data demonstrated that transcription and translation occurred in the absence of GCP1 thus excluding the essential role of GCP1 in these processes (Hecker, Graille et al. 2009) (Hecker, Lopreiato et al. 2008) (Hecker, Leulliot et al. 2007).

A role in the cell wall peptidoglycane biosynthesis pathway was proposed for GCP1 in *S. aureus* (Zheng, Yu et al. 2007). Cultures of the *gcp1* antisense mutant displayed reduced activity of murein hydrolases that are important for targeting cell wall peptidoglycane during cell division. Based on our data we suggest that the described phenotype might be linked primarily to Z-ring formation. Several lines of evidence were provided demonstrating that FtsZ is able to initiate the process of cell division by facilitating the switch from lateral to polar peptidoglycane synthesis (Varma and Young 2004) (Aarsman, Piette et al. 2005). However, the upregulation of cell envelope-biosynthesis related proteins observed on 2D-gels also hints into this direction.

Intriguing parallels to findings in this work were observed during the characterization of FtsK. FtsK is an essential protein that is involved in divisome-assembly and couples segregation of the chromosome terminus, the *ter* region, with cell division (Bigot, Sivanathan et al. 2007). FtsK colocalizes with FtsZ to the septal ring structure and this localization is dependent on FtsZ, FtsA and ZipA, but not on FtsI and FtsQ (Yu, Tran et al. 1998) (Wang, Khattar et al. 1998) (Pichoff and Lutkenhaus 2002). Conversely, FtsQ, FtsL and FtsI require FtsK for localization to the Z-ring (Chen and Beckwith 2001). FtsK inserts into the cytoplasmic membrane with its C-terminus facing the periplasm and the N-terminus facing the cytoplasm. The N-terminal domain of FtsK is sufficient for targeting FtsK to the septum (Yu, Tran et al. 1998) and for its function in cell division (Draper, McLennan et al. 1998) (Wang, Khattar et al. 1998). It contains four transmembrane helices linking two periplasmic loops, one of which contains a zinc metalloprotease consensus sequence that is essential for function of FtsK (Dorazi and Dewar 2000). The C-terminal domain of FtsK is required for chromosome segregation, activating the recombinase and actively positioning the *dif* sites (Aussel, Barre et al. 2002; Capiiaux, Lesterlin et al. 2002) (Massey, Aussel et al. 2004). The deletion of *ftsK* can be rescued by overexpression of *ftsN* or deletion of *dacA*, which encodes PBP5 (modifying-modifying D-alanine:D-alanine carboxypeptidase) (Begg, Dewar et al. 1995) (Draper, McLennan et al. 1998). The C-terminus of

FtsK, which obviously plays a role in murein biosynthesis, is not essential for FtsK function, while the N-terminus that facilitates chromosome segregation during cell division, is essential for (Goehring, Robichon et al. 2007). Finally, similar to the findings for depleting GCP1 and monitoring induced or repressed proteins (Chapter 3.3.5), depletion of FtsK reduces UspA levels in the cell (Diez, Farewell et al. 1997).

All these findings are analogs to the results obtained for GCP1 during this study. Both genes *gcp1* and *ftsK* are essential, but the deletion mutant can be rescued by a loss of function mutation in a second gene. The proteins both contain a Zn²⁺ binding site and localize to the membrane. For both proteins, the N-terminus is essential for the essential function, while the C-terminus is dispensable (Chapter 3.5.4 Page 70 and Chapter 3.5.3, Page 69).

Due to these parallels, we conclude that GCP1 might play a similar role in cell division as FtsK. Cells depleted in FtsK still perform vegetative growth and form filamentous cells while no increase in cell size is observed after GCP1 depletion. As FtsK assembles to the divisome after FtsZ forms the Z-ring, GCP1 must influence cell division at an earlier stage. For these reasons we suggest that GCP1 might be involved in an earlier process that determines the correct time point of cell division.

For *Bacillus subtilis* an example of a regulatory system that controls divisome assembly at an earlier stage was recently reported. A metabolic sensor governing cell size was discovered (Weart, Lee et al. 2007). The proteins UgtP, GtaB and PgcA act as a sensing system that couples growth rate to cell size and determines the appropriate time for cell division in regard to the growth phase. UgtP, as key component, localizes to the division site and inhibits FtsZ polymerization into the Z-ring until the appropriate cell size for division is reached.

GCP1 could be involved in a similar regulatory pathway governing cell division in *E. coli*. However, the definite role of GCP1 in regulating cell division is awaiting further investigation.

5 Literature

- Aarsman, M. E., A. Piette, et al. (2005). "Maturation of the *Escherichia coli* divisome occurs in two steps." Mol Microbiol **55**(6): 1631-45.
- Abdullah, K. M., R. Y. Lo, et al. (1991). "Cloning, nucleotide sequence, and expression of the *Pasteurella haemolytica* A1 glycoprotease gene." J Bacteriol **173**(18): 5597-603.
- Acord, J. and M. Masters (2004). "Expression from the *Escherichia coli* *dapA* promoter is regulated by intracellular levels of diaminopimelic acid." FEMS Microbiol Lett **235**(1): 131-7.
- Alexander, D. M. and A. C. St John (1994). "Characterization of the carbon starvation-inducible and stationary phase-inducible gene *slp* encoding an outer membrane lipoprotein in *Escherichia coli*." Mol Microbiol **11**(6): 1059-71.
- Almiron, M., A. J. Link, et al. (1992). "A novel DNA-binding protein with regulatory and protective roles in starved *Escherichia coli*." Genes Dev **6**(12B): 2646-54.
- Aravind, L. and E. V. Koonin (1999). "Gleaning non-trivial structural, functional and evolutionary information about proteins by iterative database searches." J Mol Biol **287**(5): 1023-40.
- Archibold, E. R. and L. S. Williams (1972). "Regulation of synthesis of methionyl-, prolyl-, and threonyl-transfer ribonucleic acid synthetases of *Escherichia coli*." J Bacteriol **109**(3): 1020-6.
- Arifuzzaman, M., M. Maeda, et al. (2006). "Large-scale identification of protein-protein interaction of *Escherichia coli* K-12." Genome Res **16**(5): 686-91.
- Aussel, L., F. X. Barre, et al. (2002). "FtsK Is a DNA motor protein that activates chromosome dimer resolution by switching the catalytic state of the XerC and XerD recombinases." Cell **108**(2): 195-205.
- Beckwith, J. (1991). "Strategies for finding mutants." Methods Enzymol **204**: 3-18.
- Begg, K. J., S. J. Dewar, et al. (1995). "A new *Escherichia coli* cell division gene, *ftsK*." J Bacteriol **177**(21): 6211-22.
- Bernhardt, T. G. and P. A. de Boer (2005). "SlmA, a nucleoid-associated, FtsZ binding protein required for blocking septal ring assembly over Chromosomes in *E. coli*." Mol Cell **18**(5): 555-64.
- Bigot, S., V. Sivanathan, et al. (2007). "FtsK, a literate chromosome segregation machine." Mol Microbiol **64**(6): 1434-41.

- Bramhill, D. (1997). "Bacterial cell division." Annu Rev Cell Dev Biol **13**: 395-424.
- Buddelmeijer, N. and J. Beckwith (2002). "Assembly of cell division proteins at the *E. coli* cell center." Curr Opin Microbiol **5**(6): 553-7.
- Buddelmeijer, N., N. Judson, et al. (2002). "YgbQ, a cell division protein in *Escherichia coli* and *Vibrio cholerae*, localizes in codependent fashion with FtsL to the division site." Proc Natl Acad Sci U S A **99**(9): 6316-21.
- Butland, G., J. M. Peregrin-Alvarez, et al. (2005). "Interaction network containing conserved and essential protein complexes in *Escherichia coli*." Nature **433**(7025): 531-7.
- Canceill, D., E. Dervyn, et al. (1990). "Proteolysis and modulation of the activity of the cell division inhibitor Sula in *Escherichia coli* lon mutants." J Bacteriol **172**(12): 7297-300.
- Capiaux, H., C. Lesterlin, et al. (2002). "A dual role for the FtsK protein in *Escherichia coli* chromosome segregation." EMBO Rep **3**(6): 532-6.
- Carrion, M., M. J. Gomez, et al. (1999). "mraW, an essential gene at the dcw cluster of *Escherichia coli* codes for a cytoplasmic protein with methyltransferase activity." Biochimie **81**(8-9): 879-88.
- Chen, J. C. and J. Beckwith (2001). "FtsQ, FtsL and FtsI require FtsK, but not FtsN, for colocalization with FtsZ during *Escherichia coli* cell division." Mol Microbiol **42**(2): 395-413.
- Cordell, S. C., E. J. Robinson, et al. (2003). "Crystal structure of the SOS cell division inhibitor Sula and in complex with FtsZ." Proc Natl Acad Sci U S A **100**(13): 7889-94.
- Datsenko, K. A. and B. L. Wanner (2000). "One-step inactivation of chromosomal genes in *Escherichia coli* K-12 using PCR products." Proc Natl Acad Sci U S A **97**(12): 6640-5.
- de Boer, P. A., R. E. Crossley, et al. (1990). "Central role for the *Escherichia coli* minC gene product in two different cell division-inhibition systems." Proc Natl Acad Sci U S A **87**(3): 1129-33.
- de Narvaez, C. C. and H. W. Schaup (1979). "In vivo transcriptionally coupled assembly of *Escherichia coli* ribosomal subunits." J Mol Biol **134**(1): 1-22.
- Dhiman, A. and R. Schleif (2000). "Recognition of overlapping nucleotides by AraC and the sigma subunit of RNA polymerase." J Bacteriol **182**(18): 5076-81.
- Diez, A. A., A. Farewell, et al. (1997). "A mutation in the ftsK gene of *Escherichia coli* affects cell-cell separation, stationary-phase survival, stress adaptation, and expression of the gene encoding the stress protein UspA." J Bacteriol **179**(18): 5878-83.
- Dirla, S., J. Y. Chien, et al. (2009). "Constitutive mutations in the *Escherichia coli* AraC protein." J Bacteriol **191**(8): 2668-74.

- Dorazi, R. and S. J. Dewar (2000). "Membrane topology of the N-terminus of the *Escherichia coli* FtsK division protein." FEBS Lett **478**(1-2): 13-8.
- Draper, G. C., N. McLennan, et al. (1998). "Only the N-terminal domain of FtsK functions in cell division." J Bacteriol **180**(17): 4621-7.
- Errington, J., R. A. Daniel, et al. (2003). "Cytokinesis in bacteria." Microbiol Mol Biol Rev **67**(1): 52-65, table of contents.
- Geissler, B., D. Elraheb, et al. (2003). "A gain-of-function mutation in *ftsA* bypasses the requirement for the essential cell division gene *zipA* in *Escherichia coli*." Proc Natl Acad Sci U S A **100**(7): 4197-202.
- Genevaux, P., C. Georgopoulos, et al. (2007). "The Hsp70 chaperone machines of *Escherichia coli*: a paradigm for the repartition of chaperone functions." Mol Microbiol **66**(4): 840-57.
- Goehring, N. W., C. Robichon, et al. (2007). "Role for the nonessential N terminus of FtsN in divisome assembly." J Bacteriol **189**(2): 646-9.
- Gottesman, S., E. Roche, et al. (1998). "The ClpXP and ClpAP proteases degrade proteins with carboxy-terminal peptide tails added by the SsrA-tagging system." Genes Dev **12**(9): 1338-47.
- Hale, C. A. and P. A. de Boer (1997). "Direct binding of FtsZ to ZipA, an essential component of the septal ring structure that mediates cell division in *E. coli*." Cell **88**(2): 175-85.
- Hanahan, D., J. Jessee, et al. (1991). "Plasmid transformation of *Escherichia coli* and other bacteria." Methods Enzymol **204**: 63-113.
- Hecker, A., M. Graille, et al. (2009). "The universal Kae1 protein and the associated Bud32 kinase (PRPK), a mysterious protein couple probably essential for genome maintenance in Archaea and Eukarya." Biochem Soc Trans **37**(Pt 1): 29-35.
- Hecker, A., N. Leulliot, et al. (2007). "An archaeal orthologue of the universal protein Kae1 is an iron metalloprotein which exhibits atypical DNA-binding properties and apurinic-endonuclease activity in vitro." Nucleic Acids Res **35**(18): 6042-51.
- Hecker, A., R. Lopreiato, et al. (2008). "Structure of the archaeal Kae1/Bud32 fusion-protein MJ1130: a model for the eukaryotic EKC/KEOPS subcomplex." EMBO J.
- Hecker, A., R. Lopreiato, et al. (2008). "Structure of the archaeal Kae1/Bud32 fusion-protein MJ1130: a model for the eukaryotic EKC/KEOPS subcomplex." EMBO J **27**(17): 2340-51.
- Hu, Z., A. Mukherjee, et al. (1999). "The MinC component of the division site selection system in *Escherichia coli* interacts with FtsZ to prevent polymerization." Proc Natl Acad Sci U S A **96**(26): 14819-24.

- Huesgen, P. F. (2007). "Functional genomics of Deg and GCP in photosynthetic organisms." Universität Konstanz.
- Jiang, P. M., A. (2004). "O-Sialoglycoprotein endopeptidase." Handbook of Proteolytic Enzymes, 2 edn (Barrett, A.J., Rawlings, N.D. & Woessner, J.F. eds), Elsevier.
- Johnson, C. M. and R. F. Schleif (2000). "Cooperative action of the catabolite activator protein and AraC in vitro at the araFGH promoter." J Bacteriol **182**(7): 1995-2000.
- Kabsch, W. and K. C. Holmes (1995). "The actin fold." FASEB J **9**(2): 167-74.
- Kanemori, M., H. Yanagi, et al. (1999). "The ATP-dependent HslVU/ClpQY protease participates in turnover of cell division inhibitor SulA in *Escherichia coli*." J Bacteriol **181**(12): 3674-80.
- Karzai, A. W., E. D. Roche, et al. (2000). "The SsrA-SmpB system for protein tagging, directed degradation and ribosome rescue." Nat Struct Biol **7**(6): 449-55.
- Keiler, K. C., P. R. Waller, et al. (1996). "Role of a peptide tagging system in degradation of proteins synthesized from damaged messenger RNA." Science **271**(5251): 990-3.
- Laber, B., F. X. Gomis-Ruth, et al. (1992). "*Escherichia coli* dihydrodipicolinate synthase. Identification of the active site and crystallization." Biochem J **288** (Pt 2): 691-5.
- Laemmli, U. K. (1970). "Cleavage of structural proteins during the assembly of the head of bacteriophage T4." Nature **227**(5259): 680-5.
- Lutkenhaus, J. (2007). "Assembly dynamics of the bacterial MinCDE system and spatial regulation of the Z ring." Annu Rev Biochem **76**: 539-62.
- Mao, D. Y., D. Neculai, et al. (2008). "Atomic structure of the KEOPS complex: an ancient protein kinase-containing molecular machine." Mol Cell **32**(2): 259-75.
- Margolin, W. (2000). "Themes and variations in prokaryotic cell division." FEMS Microbiol Rev **24**(4): 531-48.
- Martinez, A. and R. Kolter (1997). "Protection of DNA during oxidative stress by the nonspecific DNA-binding protein Dps." J Bacteriol **179**(16): 5188-94.
- Massey, T. H., L. Aussel, et al. (2004). "Asymmetric activation of Xer site-specific recombination by FtsK." EMBO Rep **5**(4): 399-404.
- Mellors, A. and R. Y. Lo (1995). "O-sialoglycoprotease from *Pasteurella haemolytica*." Methods Enzymol **248**: 728-40.
- Mellors, A. and D. R. Sutherland (1994). "Tools to cleave glycoproteins." Trends Biotechnol **12**(1): 15-8.

- Nesin, M., J. R. Lupski, et al. (1987). "Possible new genes as revealed by molecular analysis of a 5-kb *Escherichia coli* chromosomal region 5' to the rpsU-dnaG-rpoD macromolecular-synthesis operon." Gene **51**(2-3): 149-61.
- Neu, H. C. and L. A. Heppel (1965). "The release of enzymes from *Escherichia coli* by osmotic shock and during the formation of spheroplasts." J Biol Chem **240**(9): 3685-92.
- Nystrom, T. and F. C. Neidhardt (1992). "Cloning, mapping and nucleotide sequencing of a gene encoding a universal stress protein in *Escherichia coli*." Mol Microbiol **6**(21): 3187-98.
- Nystrom, T. and F. C. Neidhardt (1994). "Expression and role of the universal stress protein, UspA, of *Escherichia coli* during growth arrest." Mol Microbiol **11**(3): 537-44.
- O'Farrell, P. Z., H. M. Goodman, et al. (1977). "High resolution two-dimensional electrophoresis of basic as well as acidic proteins." Cell **12**(4): 1133-41.
- Petersen, C. (1990). "*Escherichia coli* ribosomal protein L10 is rapidly degraded when synthesized in excess of ribosomal protein L7/L12." J Bacteriol **172**(1): 431-6.
- Pichoff, S. and J. Lutkenhaus (2002). "Unique and overlapping roles for ZipA and FtsA in septal ring assembly in *Escherichia coli*." EMBO J **21**(4): 685-93.
- Pichoff, S. and J. Lutkenhaus (2005). "Tethering the Z ring to the membrane through a conserved membrane targeting sequence in FtsA." Mol Microbiol **55**(6): 1722-34.
- Reed, W. L. and R. F. Schleif (1999). "Hemiplegic mutations in AraC protein." J Mol Biol **294**(2): 417-25.
- Saul, F. A., J. P. Arie, et al. (2004). "Structural and functional studies of FkpA from *Escherichia coli*, a cis/trans peptidyl-prolyl isomerase with chaperone activity." J Mol Biol **335**(2): 595-608.
- Shimada, T., H. Makinoshima, et al. (2004). "Classification and strength measurement of stationary-phase promoters by use of a newly developed promoter cloning vector." J Bacteriol **186**(21): 7112-22.
- Silber, K. R. and R. T. Sauer (1994). "Deletion of the prc (tsp) gene provides evidence for additional tail-specific proteolytic activity in *Escherichia coli* K-12." Mol Gen Genet **242**(2): 237-40.
- Stricker, J., P. Maddox, et al. (2002). "Rapid assembly dynamics of the *Escherichia coli* FtsZ-ring demonstrated by fluorescence recovery after photobleaching." Proc Natl Acad Sci U S A **99**(5): 3171-5.
- Sutherland, D. R., K. M. Abdullah, et al. (1992). "Cleavage of the cell-surface O-sialoglycoproteins CD34, CD43, CD44, and CD45 by a novel glycoprotease from *Pasteurella haemolytica*." J Immunol **148**(5): 1458-64.

- Sukumaran, S., Krishnan Sankaran et al. (2001). "Cytopathic effects of outer-membrane preparations of enteropathogenic *Escherichia coli* and coexpression of maltoporin with secretory virulence factor, EspB" *J. Med. Microbiol.* **50**: 602-612
- Varma, A. and K. D. Young (2004). "FtsZ collaborates with penicillin binding proteins to generate bacterial cell shape in *Escherichia coli*." *J Bacteriol* **186**(20): 6768-74.
- Vicente, M. and A. I. Rico (2006). "The order of the ring: assembly of *Escherichia coli* cell division components." *Mol Microbiol* **61**(1): 5-8.
- Wang, L., M. K. Khattar, et al. (1998). "FtsI and FtsW are localized to the septum in *Escherichia coli*." *J Bacteriol* **180**(11): 2810-6.
- Weart, R. B., A. H. Lee, et al. (2007). "A metabolic sensor governing cell size in bacteria." *Cell* **130**(2): 335-47.
- Wissel, M. C. and D. S. Weiss (2004). "Genetic analysis of the cell division protein FtsI (PBP3): amino acid substitutions that impair septal localization of FtsI and recruitment of FtsN." *J Bacteriol* **186**(2): 490-502.
- Wolf, S. G., D. Frenkiel, et al. (1999). "DNA protection by stress-induced biocrystallization." *Nature* **400**(6739): 83-5.
- Yu, X. C., A. H. Tran, et al. (1998). "Localization of cell division protein FtsK to the *Escherichia coli* septum and identification of a potential N-terminal targeting domain." *J Bacteriol* **180**(5): 1296-304.
- Zalacain, M., S. Biswas, et al. (2003). "A global approach to identify novel broad-spectrum antibacterial targets among proteins of unknown function." *J Mol Microbiol Biotechnol* **6**(2): 109-26.
- Zheng, L., C. Yu, et al. (2007). "Conditional mutation of an essential putative glycoprotease eliminates autolysis in *Staphylococcus aureus*." *J Bacteriol* **189**(7): 2734-42.

6 Acknowledgements

I owe gratitude to many people for supporting my way through this work. Above all, I am obliged to profound gratefulness towards **Prof. Dr. Iwona Adamska**: For being such a great group leader, supervisor and friend. For giving me fresh enthusiasm whenever the project went through tough times, for inspiration with new ideas and in particular for the freedom to follow my own strategies. Not least, for entrusting me with this extraordinarily interesting project.

Special gratitude is also due to **Prof Dr. Winfried Boos** in whose lab I completed a big share of this work. There was not a single day that I would have found his door closed for discussing the latest findings. There was always a proper portion of “infective” curiosity in these discussions, no matter how puzzling a result appeared at first sight. I am truly thankful for learning “microbial-classics” first hand from an “old stager”. Finally, many of the findings in this work became only possible by making use of his excellent international network.

I want to thank the technical staff of both groups for their fantastic work and collegueship. I particular: Roswitha Miller-Sulger for her patience and diligence while preparing dozens and dozens of 2D-Gels; Regina Grimm for her work, for being great company and for a lot of cleaning after me.

All members of both labs I want to thank for collegueship and help whenever I needed it. Also for the great atmosphere and working conditions that I experienced. In especial Dr. Jens Steinbrenner for always finding the right moment to have a conversation offside the daily science business, Dr. Dietmar Funck for his helpfulness in lab, for well dosed sarcasm whenever needed and for being a reliable “firewood-collector” during the red wine sessions of the Adamska group in the botanical garden.

Special thanks goes to Dr. Marcel Kremer, who strongly supported my work by teaching me the 2D-NEPHGE method, even more by reading over this work again and again, and most important I want to thank him for being a true friend.

Further I want to thank Dr. Nathan Goehring from John Beckwith’s lab for providing me with FtsZ-Gfp constructs.

There were many highs and lows during this work, and I want to convey my deepest gratefulness to my own family: My wife Dagmar for believing in me all the years, for lifting me up when I was down and for understanding the sometimes unconventional working hours and schedule. My parents for their believe in me and my way, for many times of stepping back in personal demands to enable me to attend university and to complete this education. For being the best family I can imagine.